RUPARELIA, PRIYANKA S., Ph.D. Synthesis and Characterization of Bacterial Cellulose Towards Osteogenic Differentiation of Stem Cells. (2019)
Directed by Dr. Dennis LaJeunesse 162 pp.

The extracellular matrix provides physical support and functional microenvironment in which cells exist for healthy tissue formation and maintenance. This dynamic interplay between the extracellular matrix and cells have significant effect on cellular functions like cell adhesion, cell proliferation and cell differentiation. To mimic this multimolecular three-dimension network during tissue damage, like disease, trauma or functional failure, tissue engineering introduces us to apply the principles of material science and life science for developing biocompatible materials.

According to 2019 United Network for Organ Sharing report 3,180 transplants were performed with 113,839 people still on the waiting list. The sole reliance on transplantation has not only created a waiting list but also a rise in the health care cost. Current strategies involve the use of donated organs or tissues either from one patient to another or from one part of the patient's body to another part of the body in the same patient. These practices have limitations like immunogenic rejection, risk of disease transmission, costly immunosuppression therapies and difficult and time-consuming surgical procedures. Therefore, there is a growing need for modifying factors like biomaterials that act as scaffold matrices and serve as a platform for the cells to grow and form tissues upon transplantation. In this study, we have utilized a biomimetic approach to produce a material that acts as a bioscaffold while examining its properties for its application in the field of bone tissue engineering.

Bacterial cellulose is a polysaccharide material that is synthesized by specific types of bacteria like *Acetobacter, Azotobacter, Gluconacetobacter, Pseudomonas, Salmonella and Sarcina ventriculi.* Among them the most effective are *Gluconacetobacter xylinum, Gluconacetobacter hansenii, and Gluconacetobacter pasteurianus.* These bacteria polymerize glucose residues into linear β-1,4-glucan chains that assemble and crystallize cellulose ribbons. These ribbons form a three-dimensional network of cellulose nanofibers with ideal properties like hydrophilicity, high surface area, excellent mechanical property, moldability and high purity as compared to plant cellulose. In this work, we have fermented bacterial cellulose using *Gluconacetobacter Hansenii* that produces a pellicle of cellulose with similar properties. Human-derived placental mesenchymal stem cells were cultured on bacterial cellulose to study its osteogenic differentiation potential to function as a cell-scaffold construct for bone regeneration.

Our study found novel advances that enable bacterial cellulose to support the growth and differentiation of human-derived placental mesenchymal stem cell *in vitro*. Material characterization showed that bacterial cellulose has a fiber diameter of 40-60nm with twisted and interwoven cellulose fibrils caused due to the rotation of bacteria during fermentation. In its never-dried state the material is flexible and has a high stiffness while being brittle upon drying. The nanoscale feature of bacterial cellulose supported the growth of placental stem cells and showed no toxicity upon culturing for long hours. Further, the hydrophilic nature of bacterial cellulose enabled the differentiation of placental stem cells with high expression of early osteogenic marker like alkaline

phosphatase and an increase in mineralized matrix by the end of 28 days. We have established the importance of hydrophilicity, nanotopography and material structure that showed improved biomineralization during osteogenic differentiation. This study provides a strong basis that material properties play a vital role in supporting the growth of the cells and its ability to deposit tissue-specific extracellular matrix. In this study, Bacterial cellulose showed as a promising biomaterial for bone tissue engineering applications.

SYNTHESIS AND CHARACTERIZATION OF BACTERIAL CELLULOSE TOWARDS OSTEOGENIC DIFFERENTIATION OF STEM CELLS

by

Priyanka S. Ruparelia

A Dissertation Submitted to
the Faculty of The Graduate School at
The University of North Carolina at Greensboro
in Partial Fulfillment
of the Requirements for the Degree
Doctor of Philosophy

Greensboro
2019

Approved by

_____
Committee Chair

To my mother Sheetal Ruparelia, father Sumit Ruparelia, brother Ravi Ruparelia and my best friend and partner Yash Sangani

APPROVAL PAGE

This dissertation written by PRIYANKA S. RUPARELIA has been approved by the following committee of the Faculty of the Graduate School at The University of North Carolina at Greensboro.

Committee Chair _____

Committee Members _____

_____

_____

_____
Date of Acceptance by Committee

_____
Date of Final Oral Examination

ACKNOWLEDGEMENTS

I would like to start by sincerely thanking my advisor, Dr. Dennis LaJeunesse for his continuous support during my PhD study, for his motivation and immense knowledge that served as a foundation for my research. Under his tutelage I was able to not only excel at my work but also perform artfully in various extracurricular activities in my city as well as at conferences around the nation.

Besides my advisor, I would like to thank my co-advisor, Dr. Sang Jin Lee and the Wake Forest Institute for Regenerative Medicine. This collaboration shaped my research while offering me with remarkable expertise in the field of tissue engineering. My sincere thanks also extend my committee members Dr. Christopher Kepley and Dr. Eric Josephs for their insightful comments and competitive questions that have encouraged me to widen my research.

I would also like to thank Dr. Shyam Aravamudhan for his constant support and guidance during my research. The opportunity to join their team during my early research years and to my training conducted by Steven Crawford inspired me to pursue my career in the field of tissue engineering and regenerative medicine technology.

I thank my fellow colleagues for the stimulating discussions and for all the amazing moments that we had in the past five years.

I would also like to thank my school: The Joint School of Nanoscience and Nanoengineering for providing me with a platform to pursue my dream career in the field of nanotechnology and to my university: The University for North Carolina Greensboro for providing access to all my research laboratories and on-campus facilities.

Lastly, I would like to thank my family: my parents and my brother for being my backbone throughout my life as well as during my PhD journey. I would also like to thank my best friend and partner: Yash Sangani for all his love, support and for his presence that has made this a smoother path to walk on and to all my friends for being my family away from home.

TABLE OF CONTENTS

Page

LIST OF TABLES

Page

LIST OF FIGURES

Page

CHAPTER I

TISSUE ENGINEERING AND BIOMATERIALS

1.1. Introduction

The growing tendency of age-related diseases that causes tissue damage or failure introduces us to the field of tissue engineering and regenerative medicine technology [1]. In general, autografts have been considered as the gold standard for treating tissue defects yet possesses limitations like risk of donor-site morbidity and the need of a second surgery [2]. The other traditional strategies like allograft, xenograft and metal implants have added disadvantages like rejection by the patient's body, risk of pathogen transmitted to the recipient's body, non-degradability and lack of integration into the host tissue [3]. To overcome the complications caused by the traditional methods, the field of tissue engineering has been growing continuously for the past ten years by combining research using stem cells, nanotechnology and biofunctional scaffold materials [4]. In this review, we will discuss the basic principles of tissue engineering that combines cell therapy and the application of different types of biomaterials for tissue repair and regeneration.

1.2. Cell Therapies

Stem cells have been widely used for the continual maintenance of the tissues because of their unique properties like self-renewal and ability to differentiate into

different cell types [5]. Stem cells mediates diverse roles in the process of tissue repair and treat disease progression and development [6]. Stem cells can be classified into different types like embryonic stem cells (ESCs), tissue specific progenitor stem cells (TSPSCs), mesenchymal stem cells (MSCs), umbilical cord stem cells (UCSCs), bone marrow stem cells (BMSCs), and induced pluripotent stem cells (iPSCs). The applications of each stem cells in the field of tissue engineering and regenerative medicine technology are listed in the table (TABLE 1) below [6] [1] :

Table 1. Stem Cell Therapies

Stem Cell Types	Promising Applications
Embryonic stem cells	• Cartilage lesion treatment • Heal heart defects • Treating spinal cord injury • Cartilage tissue engineering
Tissue specific progenitor stem cells	• Muscle regeneration • Neurodental applications • Cancer treatment
Mesenchymal stem cells	• Wound healing • Treating muscle injuries • Treating orthopedic injuries • Cardiovascular diseases • Cartilage tissue engineering
Umbilical cord stem cells	• Treating autoimmune disease • Nervous system diseases
Bone marrow stem cells	• Nerve tissue engineering • Alveolar bone regeneration • Regeneration of diaphragm tissue
Induced pluripotent stem cells	• Treating placental defects • Treating lung and liver disease

Among the different types of stem cells listed above, mesenchymal stem cells have been used for its properties to differentiate into osteoblasts for this study. In general, mesenchymal stem cells have shown to demonstrate immunoregulatory role due to specific surface markers that separate them from other undifferentiated cell and encourage them for its utilization for transplantation studies [7, 8].

1.3. Mesenchymal Stem Cells

The isolation of human mesenchymal stem cells was first performed using bone marrow with continuous progress achieved in insolating from various tissues like adipose tissue, peripheral blood, umbilical cord blood, amniotic cord membrane, etc. [7]. Mesenchymal stem cells are self-renewal and can be differentiated to multiple lineages like bone, cartilage, neuronal, adipose and stromal cells[8]. Mesenchymal stem cells are undifferentiated non-hematopoietic multipotent stromal cells that can regenerate injured or inflamed tissues in the body [9, 10]. They are described as multipotent because of their ability to act as a reservoir of reparative cells that lack tissue specific features [9]. Interesting properties of mesenchymal stem cells are that they can transdifferentiate (process by which cells differentiating to a specific lineage change their course and differentiate to other cell types due to genetic reprogramming) as well as dedifferentiate to its primitive stem-cell like stage when subjected to the right culture conditions [11]. The developing regenerative technologies have widely used mesenchymal stem cells for tissue repair as well as for therapeutic therapies. Maged et al., used mesenchymal stem cells for wound healing using chitosan scaffolds loaded with rosuvastatin and proved the potential of using stem-cell loaded scaffold in skin healing and regeneration [12]. Z.lei et

al., bone-marrow derived mesenchymal stem cells for its multi-directional differentiation potential and low immunogenicity. The study showed mesenchymal stem cells-thermosensitive hydrogel improvement in wound closure of adult mouse model, epithelial cell proliferation and encouraged tissue remodeling after wound healing[13]. To treat degeneration of articular cartilage leading to osteoarthritis F.Li et al., used mesenchymal stem cells for its promising role in cartilage regeneration and chondrogenic differentiation potential. The injectable microgels loaded with human bone marrow-derived mesenchymal stem cells tested positive for cartilage features using Alcian blue and Safranin O while showing distribution of type-II collagen and higher expression of early chondrogenic transcription factor Sox-9 confirming the differentiation of mesenchymal stem cells [14]. Schwann cells (SC) have been the promising seed cells for nerve tissue engineering, but due to expensive extraction method and inefficient cell production, M.Pan et al., explored the potential of induced peripheral-blood derived MSCs (iPBMSCs) to Schwann cells to repair injured peripheral nerves. The study showed that the iPBMSCs could be induced towards Schwann cells and survive into crushed injured sciatic nerve after transplantation in a rat model. They also found that the iPBMSCs served as a novel potential for nerve tissue engineering when seeded intro artificial nerve conduit in the sciatic nerve defect model [15]. For the application towards bone tissue engineering, Zhang et el., studied bone marrow-derived mesenchymal stem cells for osteogenic differentiation. While, the focus was on the 3D scaffold for bone regeneration, the study also showed that mesenchymal stem cells differentiated into

osteogenic lineage from alkaline phosphatase activity and gene expression studies with and without bone morphogenetic protein 2 (BMP-2) [16].

While stem cells alone have been widely used to treat an injury or disease by direct transplantation at the site of repair, it is important to make an artificial extracellular matrix (ECM) environment for the cells using biomaterials. This not only increases the chances of survival of the cells but also helps in supplying essential components to the cells during the process of tissue regeneration [1].

1.4. Biomaterials in Tissue Engineering

With the increasing limitation in the availability of human donors, risk of rejection by the patient's body, risk of infection due to organ transplant and poor long-term outcome due to synthetic implants the advent of biomaterials in the tissue engineering has been considered as an innovative solution for promoting structural and functional regeneration to restore the affected tissue [7].

Biomaterials are an integral component of tissue engineering that integrate well with the adjacent host tissue with an aim to replace damaged or missing tissue [17]. The growing tendency of increased life expectancy has created the need to apply the principles of cell transplantation and biomaterial to create constructs that can mimic the ECM, thereby guiding the formation of new tissues [18]. While the earlier need of biomaterial to match the mechanical and material properties with the native tissue was important [17], the current parameters have widely changed to focus on regeneration capabilities of the tissue.

An ideal biomaterial should have the following characteristics [19]:

- Possess biomimetic structure that covers multiple hierarchical regimes (from the nanoscale to the macroscale) thus resembling tissue structure.
- Control and regulate basic cellular functions such as adhesion and proliferation.
- Workable, having the ability to alter its form to fabricate desirable shapes and
- Controllable mechanical stability i.e. maintains its shape during new tissue formation but can if necessary be removed or degraded.
- The material should be cost-effective,
- Non-toxic for its translation to clinical setting
- The material should be easily produced without addressing material complexity

There are several types of biomaterials used in tissue engineering like natural materials and synthetic materials. The TABLE 2 AND 3 summarizes the application of different biomaterials to serve as a template for regeneration of varied tissue types that have been currently studied in the literature.

Table 2. Applications of Synthetic Biomaterials in Tissue Engineering

Synthetic Materials	Description	Advantages	Disadvantages	Applications	References
Ceramics	Hydroxy-apatite: Main organic component of bone and teeth	High compressive strength Mostly used for hard tissue engineering High mechanical strength as compared to other ceramics	Brittleness Difficult to shape Low restorability Difficult to replace by new regenerated bone	Bone Dental	[20-25]
Poly(lactide-*co*-glycolide)	Formed by copolymerization of lactic and glycolic acid monomers.	Tunable degradation rate	Acidic by-products upon degradation Lack of surface bioactivities such as cell adhesion Poor mechanical properties of porous structures	Bone Vascular	[26-29]
Poly-caprolactones	It is a hydrophobic synthetic polyester	Good bio-compatibility Excellent mechanical property Biodegradable with low melting point Improves structural stability when blended	Acidic by-products upon degradation Hydrophobic nature influences cell adhesion, thereby affecting cell proliferation and differentiation	Dental Skin Vascular Cartilage Bone	[25, 26, 30-32]

		with other materials			
Polyurethane	Produced by the reaction between molecules containing two or more hydroxyl groups and two or more isocyanate groups	Restoration of living tissues due to presence of urethane The surface can be modified to improve blood compatibility	Acidic by-products upon degradation	In the field of bone when fabricated as a composite with hydroxyapatite	[21, 26]

Table 3. Applications of Natural Biomaterials in Tissue Engineering

Natural Materials	Description	Advantages	Dis-advantages	Tissue Engineering Applications	References
Silk Fibroin	Fibrous protein produced by silkworms and spiders	Different species produces different forms of silk in terms of molecular and structural properties which can affect cell attachment. Biocompatible material as can easily be absorbed by the human skin.	Glue-like protein sericin which coats fibroin in combination is prone to cause allergic reactions. Hence, the cocoons should be processed appropriately. Slow degradation rate due to its β-sheet structure.	Bone Musculoskeletal injuries Cartilage Nerve	[26, 33-36]
Collagen	A type of protein which is found in all hard and soft tissues Maintains structural and biological functions of ECM	Aid in targeted delivery of small molecules, stem cell differentiation Biocompatible, mimic ECM Highly biodegradable	High cost of pure collagen Lack of mechanical strength and stability post hydration Difficult to fabricate using heat and cross-linking; disrupts native structure	Bone Musculo-skeleton and pancreatic applications Cartilage Vascular tissues	[20, 23, 37-41]
Chitosan	natural amino polysaccharide extracted from crustaceans	Structurally like extracellular proteoglycans Supports tridimensional cell growth	Lacks mechanical strength, but can be improved by additives like silicone Weak solubility	Cartilage Skin lesions	[20, 32, 35, 37]

Natural Materials	Description	Advantages	Dis-advantages	Tissue Engineering Applications	References
		Anti-bacterial effect	Low structural stability Low cell adhesion		
Alginate	Polymer composed of guluronic acid and mannuronic acid and extracted from brown seaweed	Low cost Highly abundant in nature Low toxicity Able to absorb large amount of aqueous biological fluids	Needs to be blended with other polymers or ceramics for improved mechanical strength	Wound healing Drug delivery Soft tissues	[20, 38, 40, 42]
Hyaluronic Acid	Polysaccharide with residues of D-glucuronicacid and N-acetyl glucosamine Found mostly in connective tissue and joints.	Biocompatible Elastic Ability to form composites with both natural and synthetic polymers Non-immunogenicity	Absorbed rapidly in human body	Wound healing Vocal fold Cartilage Adipose	[20, 43-46]
Cellulose	A renewable material extracted from plant fiber, wood and certain species of bacteria	Moderate degradation Can improve surface area when used as composites Excellent mechanical property	Highly ordered structure which makes it insoluble in water and most solvents.	Bone Skin Vascular	[23, 47-53]

Natural Materials	Description	Advantages	Dis-advantages	Tissue Engineering Applications	References
		Ability to be chemically modified due to presence of free hydroxyl groups Resemblance to ECM of human biology			

1.4.1. The Right Choice of Biomaterials

Extracellular matrix (ECM) is a natural template found in living organism. They are composed of structural proteins, cell adhesion proteins and glycans [17]. The functions supported by the ECM include [54, 55]:

First, structural and functional support to the cells: Extracellular matrix consists of fibers and ground substances. The ground substance is composed of glycosaminoglycans (long and unbranched polysaccharide units), proteoglycans (possess high degree of viscosity and has binding sites for signaling molecules) and glycoproteins (helps cells to adhere to extracellular matrix). These components help provide the support to the cells. For example, membrane-proteoglycans help bind cells to fibronectin (helps in blood clotting) and collagen fibers (structural support to cells) and glycoproteins that helps in regulating cells to adhere to the extracellular matrix.

Second, maintain Cellular Acitivity: The extracellular matrix is composed of two types of fibers, structural and adhesive fibers. For example, laminin, an adhesive fiber helps in cell adhesion and is involved in cellular migration and differentiation. Heparan sulphate, a glycosaminoglycan that is found on the surface of fibroblasts and epithelial cells helps mediate cell adhesion and angiogenesis (development of new blood vessels).

Third, regulate mechano-chemical properties: For example, keratan sulphate, a glycosaminoglycan, helps provide mechanical strength to the tissues and acts as a shock-absorbed in joints and chondronectin, an adhesive glycoprotein present in cartilage tissues imparts structural strength.

Fourth, involved in tissue remodeling and regeneration: For example, tenascin, an adhesive glycoprotein that is only expressed in embryonic tissues helps in cellular and tissue development. Another example of an adhesive glycoprotein is thrombospondin present in blood plasma and platelets is secreted during tissue injury to induce blood clotting while fibronectin, an adhesive fiber helps in the process of wound healing.

The right choice of material is a motivating factor for improving the living standards and be able to meet the high demands of the healthcare industry [56]. Given the ultrafine structure of ECM and the complexity [17], the structural/functional relationship it has with the cell growth and function, the questions that needs to be addressed for developing new biomimetic scaffold materials are:

1. What aspects of the extracellular matrix are critical for mimicking a specific tissue engineering application? For example, mechanics of native extracellular matrix ranges from 0.1kPa in terms of elasticity for brain tissues to 80kPa for pre-calcified bone tissues or to achieve water-swollen networks like found in native extracellular matrix, hydrogels have been investigated which enables efficient diffusion of nutrients and soluble signals [57].
2. How to achieve fidelity towards native ECM? For example, small pores present in biomaterials like hydrogels can impede cell infiltration while biomaterials that can be produced with fiber diameter between 50-500nm can mimic the length-scale of natural extracellular matrix [57]

3. What is the best possible approach needed while designing a biomaterial that not only supports the cell growth *in vitro* but also is subject to extensive remodeling *in vivo*?

   For example, fibers in connective tissues support surrounding tissues and are involved in transport of nutrients or waste [58]. To mimic the architecture and function of connective tissues, it may be necessary for the biomaterial to be flexible with characteristic strength like collagen fibers in ligaments or tendons or have properties like stretching and compressing to mimic elastic fibers in skin or fabricate biomaterials with random fiber orientation to impart strength like dense irregular connective tissue in bone and the dermis of the skin [58].

While bio-based materials integrate well with host-tissue, improve healing process and are non-toxic [7] they lack the necessary mechanical strength. While synthetic materials can be manufactured with the ability to control shape, structure and reproducibility [17] they lack structural and functional molecules that resemble the native ECM.

Thus, it is not necessary that a given biomaterials should provide positive outcomes for multiple applications, but it is very important to understand the human biology, host response to the biomaterial and how great a fit it is for clinical applications!

1.5. Tissue Engineering: Basic Principle

Tissue damage or end stage organ loss is generally treated by transplantation which is very challenging. According to organdonor.gov, US department of health and human, 34,770 transplants were performed in the year 2017 with 114,000 still on the transplant list as of August 2017 [59]. With this increase in number since 1991, the need

for alternate strategies and technologies is very crucial. This introduces us to the field of tissue engineering. Tissue engineering is a highly multidisciplinary approach utilizes the field of life sciences and engineering to restore, maintain and improve the functions of native tissues. The basic principle of tissue engineering is demonstrated in FIGURE1.

Briefly, the cells from donor patients or donor cells from the same species are extracted and cultured in the laboratory in tissue culture flasks. Second, the cells are then seeded on the biomaterial/scaffold of interest. These cell-scaffold constructs are engineered to support three-dimensional tissue function that should be biocompatible, non-toxic and support cellular functions like cellular adhesion, proliferation, differentiation and new tissue formation. The aim is developing a cell-scaffold construct that can support three-dimensional tissue formation. Finally, once the cell-scaffold construct is ready, it is implanted at the site of tissue damage or defect in the patient.

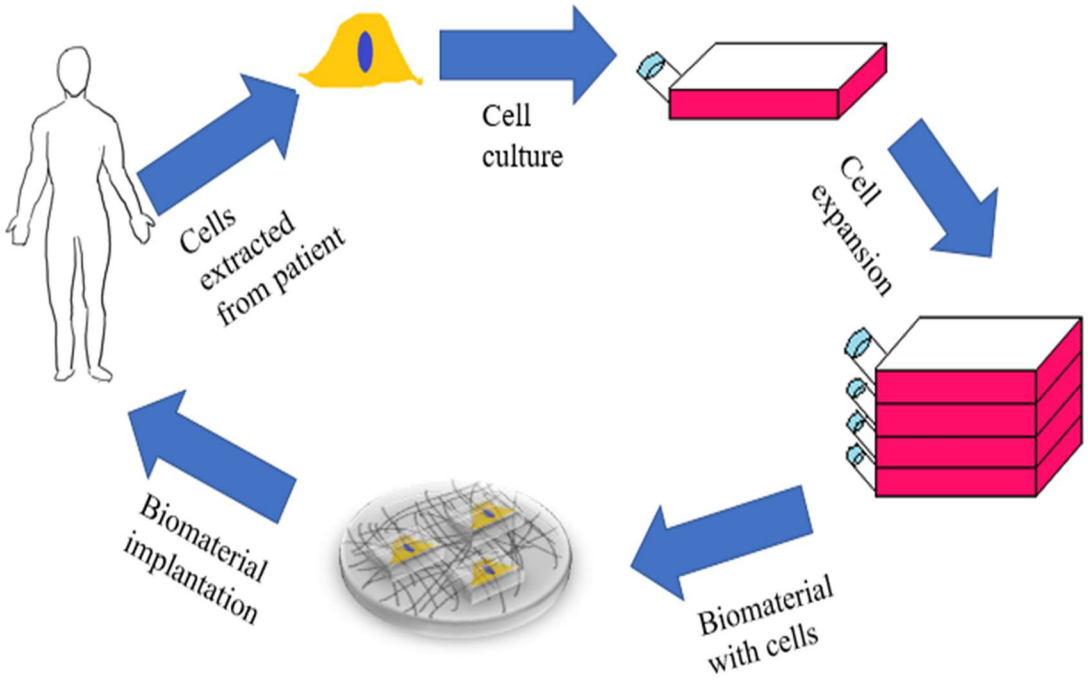

Figure 1. Basic Principle of Tissue Engineering

1.6. Study Goals

The main aim of this study is to define the properties of polysaccharide-based biomaterials for the facilitation of bone regeneration. In this study, we use *Gluconacetobacter hansenii* as a source of nanoscale crystalline cellulose to mimic the three-dimensional architect of the extracellular matrix. The nanoscale dimensions of bacterial cellulose and its unique properties forms an ideal biomaterial for applications in the field of tissue engineering. A comprehensive knowledge of material properties of bacterial cellulose and the interaction of stem cells on bacterial cellulose towards osteogenic differentiation has been explained.

<u>The aims and objectives of this study are to:</u>

1. Define conditions for the use of **Bacterial Cellulose (BC)** as a biomaterial for tissue engineering applications
    - Optimize the process parameters to obtain a homogenous pellicle of cellulose from *Gluconacetobacter Hansenii* bacteria with uniform diameter of fibers, and thickness and weight of the BC pellicle.
    - Characterize the material properties of the synthesized biomaterial cellulose.
    - Determine cellular responses to BC, specifically cell adhesion, proliferation, and viability of **human placental-derived mesenchymal stem cells (hPMSCs)**

2. Characterize the biomineralization property of BC to be used as a bone biomaterial
    - To investigate the extent of mineralization using hydroxyapatite as a model material on BC.
    - To study the material properties of the synthesized biomaterial.
3. Characterize the osteogenic differentiation of hPMSCs on BC biomaterial
    - Validate stem cell differentiation of stem cells by developing bioanalytical methods to quantitatively analyze the expression of biochemical markers of bone formation on BC biomaterial.
    - Define the cellular response of hPMSCs towards osteogenic differentiation on BC biomaterial.
4. Develop a three-dimensional bacterial cellulose foam using túngara frog (*Engystomops pustulosus*) foam protein
    - To transform expression plasmid Ranaspumin-2 (RSN-2; a surfactant protein) into BL21 (DE3) bacteria.
    - To perform recombinant protein purification and characterization to demonstrate the foaming nature of RSN-2.
    - To demonstrate BC foam formation using RSN-2 as a template to fabricate 3-dimensional structure of BC.

1.7. Dissertation Overview

This dissertation is divided into five chapters. Chapter 1 provides a detailed understanding of the background and discusses the aims and objectives of this study. Chapter 2 provides a brief understanding of polysaccharides and its different types while highlighting its application in the field of tissue engineering. Chapter 3 provides with detailed information on producing bacterial cellulose and the properties of bacterial cellulose that enable cellular responses of human-derived placental mesenchymal stems cells. Chapter 4 explains the application of bacterial cellulose in the field of bone tissue engineering, thereby highlighting on its mineralization property. The differentiation of human placental stem cells on bacterial cellulose biomaterial along with various biological assays and quantitative studies are a part of this chapter. Chapter 5 demonstrates a novel idea of making bacterial cellulose biomaterial into a 3-dimensional structure by controlling its growth on the air-liquid interface by using the properties of surfactants. Here, the use of ranaspumin-2, a surfactant protein which is found in túngara frog's foam nest has been described to be used as a template for producing bacterial cellulose foam structure followed by summarizing the study in this dissertation along with the future work.

CHAPTER II

POLYSACCHARIDES FOR TISSUE ENGINEERING

2.1. Introduction

Nature has provided great inspiration to prepare materials that displays complex hierarchy and organization which promise to a wide a range of applications and meet the desired goal [60]. In the context of tissue engineering scaffolds that effectively mimic the morphology and functions of the extracellular matrix (ECM) native to the cellular environment are being designed [49]. These biomimetic materials will be critically-important in the regenerative process with the need to grow and regenerate complex organs and tissues. The ECM is primarily composed of proteoglycans, glycosaminoglycans, glycoproteins and glycolipids [49]. The ECM is a complex heterogenous material that is as diverse as the types and number of cells in the human body; the ECM provides a dynamic and controlled environment that directs cell migration, adhesion, proliferation and differentiation, while being remodeled as needed [49].

Polysaccharides have gained much interest in the recent years as they provide excellent functional and mechanical cues that resemble the innate state of the native tissues, and are biocompatible, non-toxic, renewable and available in abundance [49].

They have a range of mechanical properties that which have encourage a wide range of applications in the biomedical field.

2.2. Definition of Polysaccharides

Polysaccharides are natural polymers that are composed of long chains of monosaccharide units which are covalently connected by glycosidic linkages as shown in FIGURE 2. The general formula of polysaccharides is (CnH2nOn). They are materials that are derived from natural sources like plants and bacteria and are present in most living organisms. They are further classified as linear or branched chain depending upon the type of monosaccharide unit [61]. Their chemical structure further possesses many reactive functional groups like hydroxyl and carboxylic acid groups that feature the possibility for chemical modifications and formation of new composite materials. The need for polysaccharides has an emerging interest as it is helping replace the use of conventional non-biodegradable and non-disposable petroleum-based materials that causes environmental problems like landfill disposals, air-borne particulates and greenhouse gas emissions [62, 63].

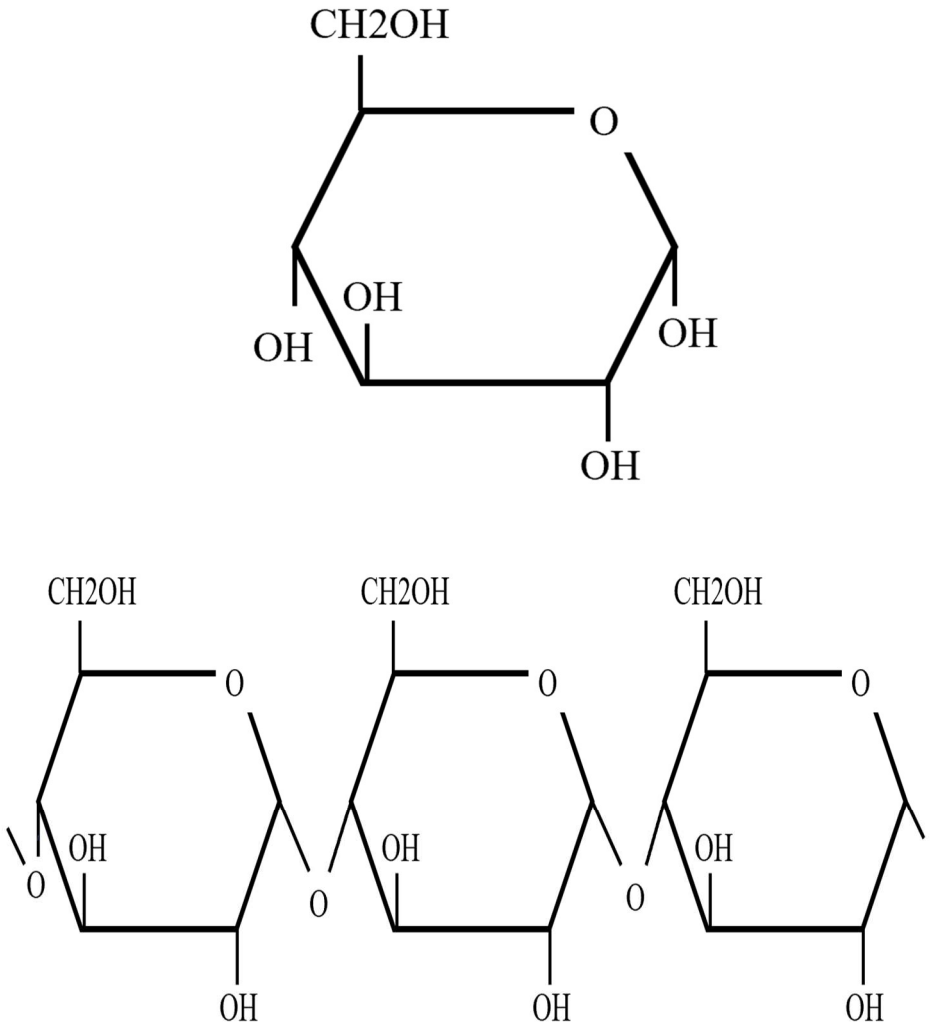

Figure 2. Chemical Structure of (top) Monosaccharide (example: glucose);

(bottom) Polysaccharide (example: amylose starch)

2.3. Types of Polysaccharides

Polysaccharide ordered structures are categorized into structural and storage polysaccharides as shown in FIGURE 3. Cellulose and chitin are examples of structural polysaccharides. They are formed of many glucose monomers that combine to form long fibers. While these polysaccharides have linear and long fibers that are deposited outside the cell membrane, storage polysaccharides like glycogen and starch are formed due to a spiral pattern [64, 65]. They form clusters with the help of a combination of proteins that attach to single polysaccharide and branch out in a complex spiral structure [65].

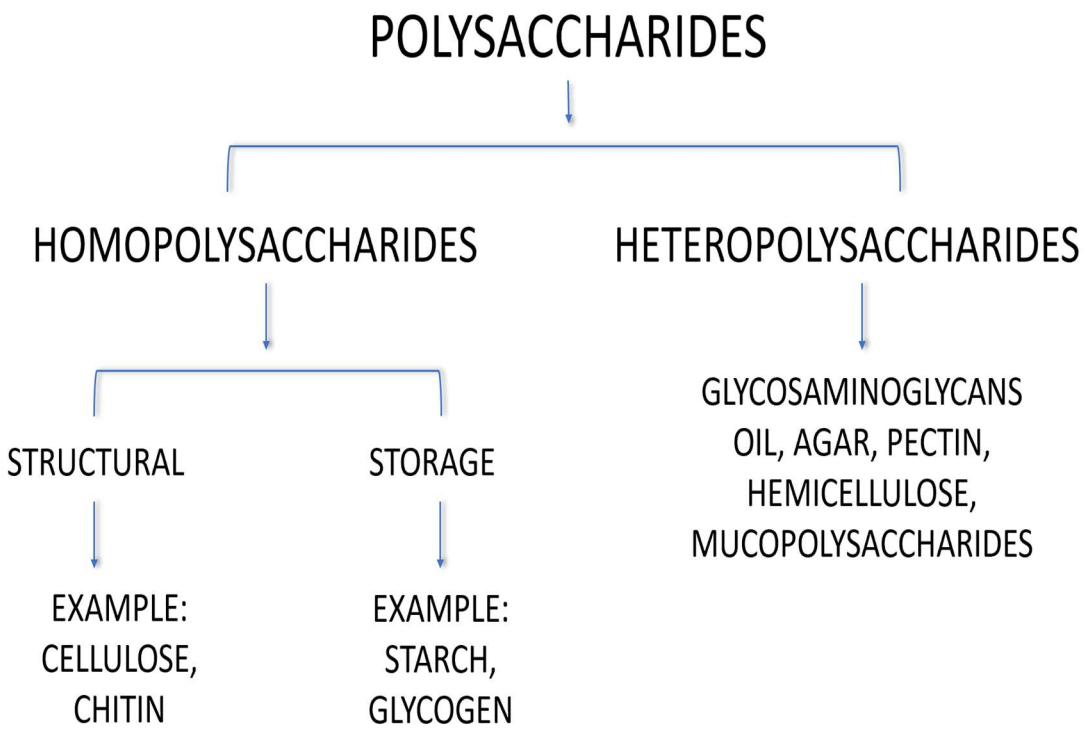

Figure 3. Types of Polysaccharides

2.4. Polysaccharides as Cellular Support

Tissue engineering and regenerative medicine needs attention in developing biomaterials for regeneration of damaged tissues as human body is a sensitive and complex biological framework. The need for biomaterials has risen in tissue engineering for cost-effective surgical procedures [66]. Some of the important properties that a biomaterial must deliver are biocompatibility, biodegradability and structural integrity. Polysaccharide polymers have been used to support these properties along with high porosity, increased surface area, low cost and moreover, polysaccharides support the cellular functions like adhesion, proliferation, migration and differentiation [62]. Polysaccharide polymers like chitosan, hyaluronic acid, alginates and cellulose are extremely versatile materials which can be formed into hydrogels to provide mechanical support for applications like drug delivery, stem cell differentiation and as a template for controlled tissue growth [67]. The different kind of polysaccharides used in the biomedical field are starch, fibrin, silk, hyaluronic acid, collagen, etc. that help mimic native tissue environment [66].

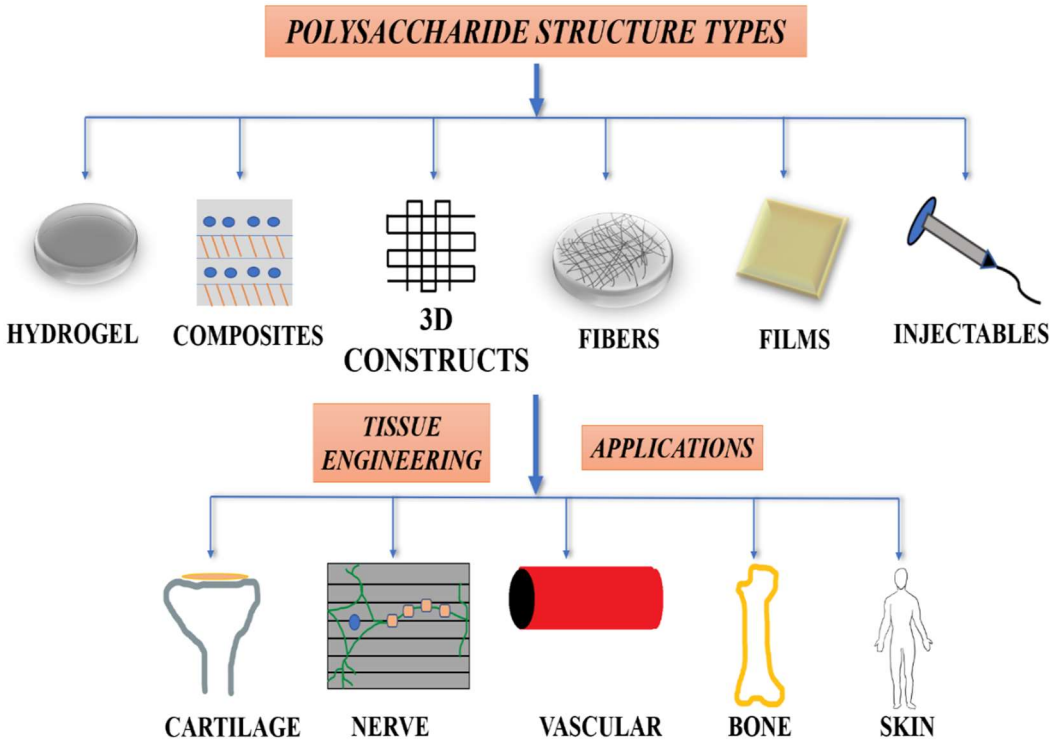

Figure 4. Fabrication of Polysaccharides into Different Structure Types and Its Applications in Tissue Engineering

2.4.1. Chitin and Chitosan

Chitin and it's alkaline deacetylated derivative chitosan are structural polysaccharides that comprise the exoskeletons of arthropods and cell walls of fungi [49, 62, 68, 69]. The annual production of chitin by living organism is estimated to be over a trillion tons/year [62, 70]. Chitin is a natural amino polysaccharide that consists of randomly arranged D-glucosamine and N-acetyl-D-glucosamine residues [49] as shown in FIGURE 5. The degree of deacetylation of chitosan varies between 75% and 95%. If the content of N-acetyl-D-glucosamine is higher, the polymer is chitin and if the content of glucosamine is higher, the polymer is chitosan [71]. Chitosan has unique properties like antimicrobial, anti-inflammatory, anti-fungal, antioxidant and mucoadhesiveness in addition to biocompatibility and biodegradability [72].

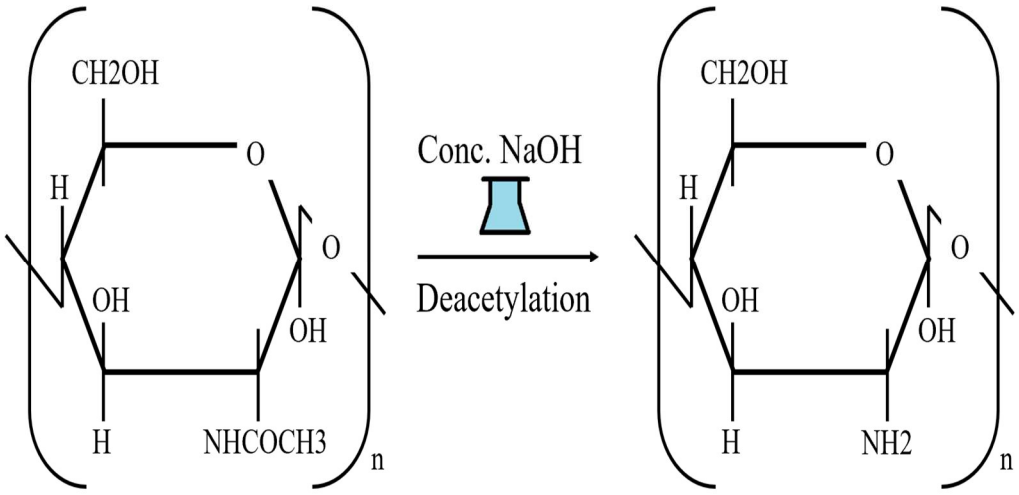

Figure 5. Chemical Structure of Chitin and Chitosan with Deacetylation Process

2.4.1.1. Tissue Engineering Applications

Many material properties of chitin that make it an attractive biomaterial for cell scaffolds are due to its chemical resemblance to naturally occurring substances in human body like glycosaminoglycans and amine groups in the polypeptides [72]. These properties are exhibited due to chemical resemblance to naturally occurring substances in human body like glycosaminoglycans and amine groups in the polymeric chain [72]. The chemical structure of chitin/chitosan also enhances its utility as a scaffold material. The free amine groups provide a simple means of functionalized this polysaccharide for many applications. For instance, nanoparticle functionalization of chitosan by the addition of nanoparticles have enhanced its materials properties, such as its mechanical durability and antimicrobial activity for its applications in burn wound regeneration [72]. Here, Chitosan scaffolds that had been doped with silver nanoparticles exhibit increased fibroblast cell adhesion and proliferation; interestingly, the rate of proliferation was a function of deacetylation which controls porosity and available surface. Chitosan and chitin have also been demonstrated to have inherent synthetic properties for the generation of silver nanoparticles and silver nanowires through the interactions of metal ions with these nitrogenous functional group, which seem to function in the nucleation and stabilization of the nascent materials [73]. However, chitosan and chitin have some challenges including low or no solubility in aqueous solutions and difficulty in controlling nanoscale and microscale organization, which is critical for controlling many of its mechanical properties [68, 69, 74, 75]. One way in which these issues have been overcome is through the applications of chitin/chitosan in polymer composites through

electrospinning processes [76-78]. Electrospinning is a process of creating long fibers when an electric field is applied between the collector and the polymer source. This electric potential forces the polymer solution to erupt, moving towards the collector and solidifying into fiber [79]. Polyglycerol sebacate/chitosan/gelatin nano-composite scaffolds have been used for nerve tissue engineering applications [77]. Once again, a mixture of other polymers, in this case, semi-crystalline polyglycerol sebacate and gelatin were used to enhance the electrospinning of chitosan under different electrospinning conditions. Chitosan as a component to composite hydrogels can also add desirable properties [78]. Chitosan was added to another nerve cell scaffold to enhance the hydrophilicity of poly(ε-caprolactone) and the electrically conductive polymer polypyrrole as well as increasing the adhesion and proliferation of the PC12 nerve cells [78].

2.4.1.2. Chitin and Chitosan for Bone Tissue Engineering

Chitin/chitosan have been considered as excellent materials for bone tissue engineering because of their mechanical properties as well as their functionalization that enables interactions with soluble metal ions [80]. In this context several groups have used these biopolymers as scaffolds usually as a component to composite material due to their structure like glycosaminoglycans; an important component of the extracellular matrix of bone [81].

For instance, a tricomponent bioactive nanocomposite made of nano-hydroxyapatite, chitosan and *Trigonella foenum graecum* Seed polysaccharide (TFSP) using co-precipitation method demonstrated improved mineralization [82]. This study used adenosine diphosphate (ADP) as a crosslinking agent for the fabrication of chitosan sponges. MC3T3 pre-osteoblasts differentiation on apatite-chitosan sponges showed improved biomineralization as compared to chitosan alone. Similarly, an injectable apatite-chitosan sponge construct showed improved biomineralization by MC3T3 pre-osteoblasts differentiation on apatite-chitosan sponges as compared to chitosan alone [81].

Chitosan has been used in bone tissue engineering due to its intrinsic antibacterial nature, ability to be molded into different shapes likes fibers, sponges, beads and films and formation of porous structures that support cell growth [83]. As chitosan lacks mechanical properties and itself is not osteoconductive, its application in the field of bone tissue engineering has improved by addition of ceramic materials that forms chitosan composite while mimicking the organic portion of the natural bone[83].

2.4.2. Hyaluronic Acid

Hyaluronic acid is a glycosaminoglycan polyssacharide that is comprised of repeating disaccharide units of N-acetyl-d-glucosamine and d-glucuronic acid as shown in FIGURE 6 and is synthesized by hyaluronan synthases and degraded by a family of enzymes called hyaluronidases [84]. Hyaluronic acid is a main component of the mammalian that is critical for the regulation of cell growth, cell migration and cell differentiation. It is also a major component of loose connective tissue, skin and the eye [85]. Hyaluronic acid has mechanical properties that enable it to function as a joint lubricant [86], shock absorber (in synovial fluid[85]), space filler, tissue damper, shear thinning ability (for vocal tissues), and flexibility. [44, 87].

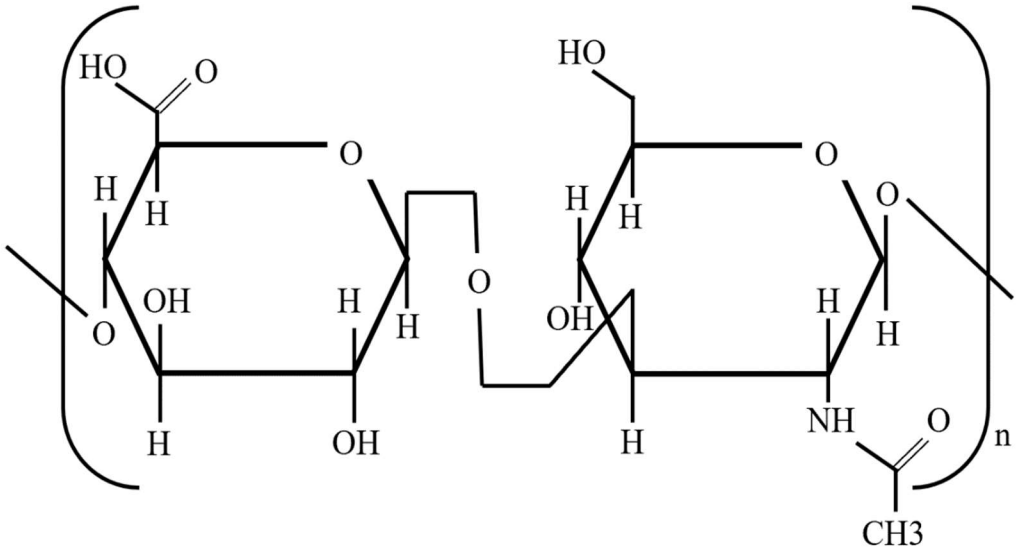

Figure 6. Chemical Structure of Hyaluronic Acid

2.4.2.1. Tissue Engineering Applications

Hyaluronic acid has been used in a few applications such as for soft tissues, bone regeneration, periodontal tissue, as an anti-cancer drug delivery as well as a protein delivery vehicle [88]. Hyaluronic acid has been used to stimulate angiogenesis; formation of a vascular network [89]. H. Kenar et al. fabricated collagen/hyaluronic acid-based poly(L-lactide-co-ε-caprolactone) (PLC/COL/HA) microfibrous scaffold using electrospinning. Adipose tissue-derived mesenchymal stem cell cultured on the scaffold showed improved adhesion and proliferation. Further, human umbilical vein endothelial cells were co-cultured for neovascularization. The study confirmed the formation of capillaries on PLC/COL/HA as compared to only PLC. E. Jooybar et al. studied HA for cartilage tissue engineering [90]. Injectable hyaluronic acid-tyramine (HATA) hydrogel was incorporated with plate-lysate (PL). PL is an inexpensive source of growth factors obtained from the peripheral blood of patients. The study concluded that the incorporation of PL did no significant effect on cell chondrogenesis, the scaffold HA-TA-PL did support the differentiation of human mesenchymal stem cells and can support as a cartilaginous construct. HA is also known as a skin's best friend. It provides hydration and promotes a healthy glow for the skin. To further study its effect on skin, A. Chanda et al. fabricated chitosan (CS)/ polycaprolactone (PCL) and hyaluronic acid (HA) using electrospinning [91]. Reduced bacterial adhesion was observed which demonstrates antimicrobial activity of the scaffolds along with proliferation, adhesion and viability of kidney epithelial cell in vitro.

The applications of HA has been limited due to its short residence time as well as lack of mechanical integrity, yet it exhibits many advantageous properties like biocompatibility, as a lubricant for joint tissues and it can maintain its hydrated state that allowed for cell infiltration [88].

2.4.2.2. Hyaluronic Acid for Bone Tissue Engineering

In the field of bone tissue engineering, hyaluronic acid has been used extensively as a composite material with other synthetic and natural polymers [49]. The use of hyaluronic acid in this capacity is natural as this polysaccharide has important role in the formation and development of bone during embryogenesis [92, 93]. A biomimetic scaffold that was composed of chitosan, chondroitin sulfate (CSA) and hyaluronic acid and which included nano hydroxyapatite demonstrated *in vitro* mineralization in simulated body fluid and supported the proliferation, adhesion and mineralization of osteoblasts [94]. Another composite of chitosan, Hyaluronic acid and graphene oxide enhanced the mechanical properties and functionality of the composite showed increased activity of mineralization and differentiation of MC3T3 cells as compared to scaffolds when stimulated by the osteogenic drug simvastatin [95].

The applications of hyaluronic acid in the field of bone tissue engineering has been used as a bone morphogenetic protein delivery vehicle for bone regrowth [88], supporting material for bone grafts to enhance physical and chemical properties of grafts materials to accelerate bone regeneration [96] and as a composite with beta-tricalcium phosphate for improved osteoconductive properties [96]. Since the mechanical properties of hyaluronic acid is weaker than the natural bone, it requires the use of other materials to

support the cell-scaffold construct for bone tissue engineering as described by some examples listed above [97].

2.4.3. Cellulose

Cellulose is a polysaccharide that consists of the linear arrangement of β-(1→4)-linked-D-glucose units as shown in FIGURE 7. Cellulose is the most abundant organic polymer found on the Earth as it is a structural component of plant cell walls and the primary structure component of wood, paper and cotton [49, 62]. Pure and crystalline nanoscale version of cellulose are also produced by a range of microorganisms including the Gram-negative and Gram-positive bacteria like *Acetobacter*, *Sarcina ventriculi*, and *Agrobecterium and* specific algae species such as *Gelidium elegans and Gelidium amansii* [62, 98].

The molecular formula of cellulose is $(C_6H_{10}O_5)_n$ in which *n* varies depending on the type of cellulose like native cellulose, oxycellulose, microcrystalline cellulose, etc. [99]. Cellulose has a flat ribbon-like conformation and engages in intramolecular hydrogen bonding with other cellulose polymers. The intramolecular interaction enables cellulose to crystallize, form fibrillary strands, possess high viscosity and alters its stiffness[62] . Cellulose is biocompatible polymer that chemically resembles the glycosaminoglycans (GAGs) in the extracellular matrix (ECM) of the human body [48]. Due to its low inflammatory response in its in vivo application, sustainability and easy availability it is an excellent choice as a biomedical material as well as in packaging and textiles [100].

Due to its crystalline and ordered structure, cellulose is insoluble in water and many solvents, which limits some of its applications. However, crystalline nanocellulose has extraordinary properties include high water-holding capacity, can be produced in different shapes and sizes, ability to form different compounds due to the presence of hydroxyl groups, highly crystalline, high tensile strength and has wide range of application in the field of tissue engineering. [49, 62].

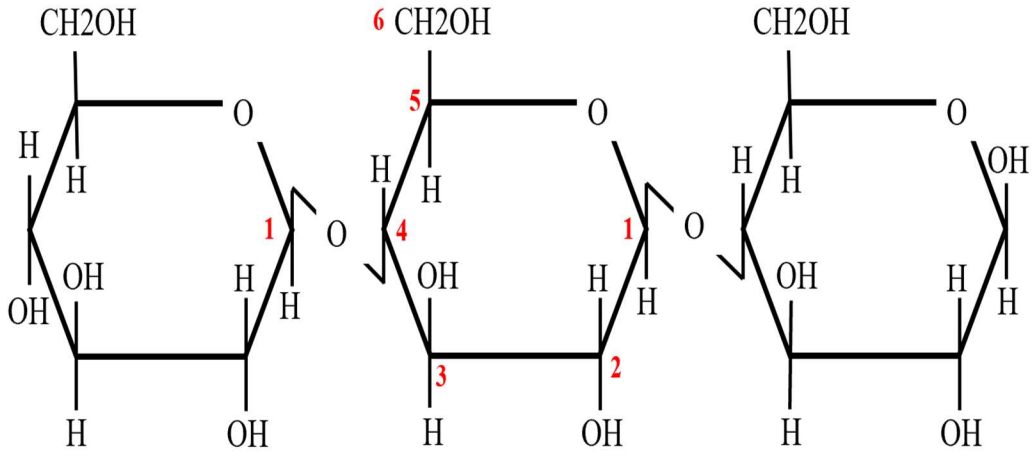

Figure 7. Chemical Structure of Cellulose

2.4.3.1. Tissue Engineering Applications

Different chemical modifications such as oxidation, esterification and micronization of cellulose are performed to produce cellulose derivatives for specific applications ranging from packaging to pharmaceuticals. A water-soluble derivative of cellulose ether was used as a scaffold for skin tissue engineering along with poly (vinyl) alcohol (PVA) for improved mechanical, chemical and physical properties [48]. Here, F.H. Zulkifli et al. showed human fibroblast growth on this composite scaffold along with improved degradation on hydroxyethyl cellulose/PVA with higher degradation observed on the composite scaffold with lowest percentage of PVA in the blend. J. Joy et al. fabricated gelatin-carboxymethyl cellulose using electrospinning for vascular tissue engineering [51]. Oxidized carboxymethyl cellulose was used to overcome the problems associated with other crosslinking agents like cell growth inhibition (glutaraldehyde) and increased cost of production (genipin). The scaffolds were non-toxic towards BALB/c 3T3 cells in vitro with complete resorption of the material in rats with no inflammation during the healing process. As porous cellulose is difficult to produce without electrospinning, J.W. Lee et al. produced porous film using cellulose and Poly (m-phenylene isophthalamide) (PMIA) using coagulation process with a peel-off method as a skin contruct [52]. Further, the scaffold supported the growth of human keratinocytes and showed no cytoxicity in vitro. Another study used cellulose acetate electrospun fibers for skin tissue engineering [101]. This study engineered the scaffold with the use of pullulan (produced by omnivorous fungi species *Aureobasidium pullulans*) to improve the height of the 3D construct, porosity and biostability. Further, pullulan acts as a stabilizer, an

adhesive and as a binder in various applications like wound healing and dentures. Mouse fibroblastic cell line (L929) showed cytocompatibility as they adhered and proliferated on the scaffold. Cellulose has also been studied for its application in cartilage tissue engineering. In order to demonstrate strong mechanical characteristics of three-dimensional scaffolds for application as a connective tissue, nano-reinforcement clay known as laponites were used to enable a strong gel structure [102]. Here, C. Boyer et al. fabricated injectable laponite nanoparticle-associated silated hydroxypropylmethyl cellulose and showed no side-effects with respect to cytocompatibility of human adipose stromal cells (hASC) cells due to laponite. The study also showed the formation of cartilaginous tissue post implantation in subcutaneous pockets of nude mice. Further, to combat neural disorders like Alzheimer's disease (AD), Parkinson's disease, and spinal cord injuries human and animal studies have limitations while conducting brain research. V. Kuzmenko et al. used cellulose nanofibril and carbon nanotubes as a conductive and composite ink to 3D print a neural construct [103]. This scaffold supported the growth and proliferation of the SH-SHY5Y human neuroblastoma cells in vitro and found cell communication via neurites.

A crystalline /nanoscale form of cellulose is synthesized by a variety of microbial species of bacteria like those of the genus *Acetobacter, Achromobacter, Alcaligenes, Aerobacter, Agrobacterium.* The chemically pure structure of these bacterial cellulose, along with the fibrous nanoscale morphology provides these cellulose materials with unique properties including high purity, increased surface reactivity and biocompatibility [47].

Furthermore, given the source of these cellulose along with simple production method, bacterial nanoscale cellulose has wide range of potential applications to the field of tissue engineering [47, 104]. Currently, bacterial nanoscale cellulose is used in a variety of applications including treatments of severe burns and cell scaffolds[47] .
A bacterial cellulose nanocomposite with the keratin protein for skin tissue engineering demonstrated enhanced binding of dermal fibroblasts and keratinocytes in vitro [50]. In this composite, keratin proteins specific cell adhesion binding motifs while the bacterial cellulose provided a mechanically stable platform. In the field of skin tissue engineering, bacterial cellulose/monmrillonite nanocomposite modified with Cu, Na and Ca not only improved tissue regeneration and wound healing in burnt mice but also also showed antimicrobial properties against pathogens associated with skin burns [105]. A porous bacterial cellulose/gelatin heparin hydrogel loaded vascular endothelial growth factor (VEGF)-loaded 3D (B/G) improved proliferation and migration of endothelial cells (PIECs) in vitro with angiogenesis observed by the application of the scaffold in an in vivo study [106].

BC is an extracellular polymer produced by many microorganisms using semi-synthetic or agricultural wastes media solution [107]. Though microorganisms like *Salmonella spp*. and *Escherichia coli* (E. coli) have the potential to produce cellulose, the amount of cellulose produced by *G.xylinus* is still higher [108]. The nanoporous structure along with free hydroxyl groups allows for many applications in the field of tissue engineering along with fabrication of nanocomposites [107].

The high surface area represents bacterial cellulose as an exciting class of nanomaterial to be used as a biopolymer for applications such as an artificial blood vessel, wound dressing, bone regeneration as well as for dental implants [109]. Further, the polysaccharide nature of bacterial cellulose makes it non-immunogenic; adding to its biocompatibility [109]. Some of the current limitations of bacterial cellulose despite its unique structure and excellent properties include high production cost on a large scale, low availability of an industrial fabrication line and inconsistency in quality [109]. With bacterial cellulose still being used as a dessert called 'nata de coco' to an ideal candidate as a scaffold in tissue engineering, this non-allergenic nanopolymer to be designed and used in the biomedical field [108].

2.4.3.2. Cellulose for Bone Tissue Engineering

Derivative of cellulose have been widely used to construct biodegradable scaffolds for bone tissue engineering [99, 110]. The use of natural polysaccharides came into effect when synthetic materials like polyesters did not offer uniform degradation rates, acidic by-products upon degradation and needed toxic solvents to dissolve these materials. To overcome these problems, researchers utilized the idea of blending natural and synthetic materials to offer good biocompatibility, biodegradability and better mechanical strength to be used as a scaffold for bone growth. Hydroxyethyl cellulose and polyvinyl alcohol composite with higher ratio of cellulose to polyvinyl alcohol supported human osteosarcoma cells in vitro and resulted greater proliferation of these cells that composts with lower ration, which suggests that the cells preferred higher content of cellulose which reflects that the cellulose closely mimics the native extracellular matrix

due to presence of β-glucose linkage and also shown to play an important role in the metabolism of the body. [111]. Another study fabricated a nanocomposite scaffold of cellulose-graft-polyacrylamide/nano-hydroxyapatite and showed mineralization on the scaffold when subjected to simulated body fluid study suggesting the formation of apatite layer [112].

To utilize the high purity of cellulose from bacteria as a property along with high hydrophilicity and mechanical strength, P.M. Favi et al. showed the osteogenic and chondrogenic ability of bacterial cellulose (BC). Equine-derived bone marrow mesenchymal stem cells were cultured on the scaffold and tested positive for alizarin red staining (Osteogenic differentiation) and alcian blue staining (Chondrogenic differentiation) in vitro [113]. Q. Shi et al. studied osteogenesis of bacterial cellulose scaffold with an aim to demonstrate the ability of BC to be used as a localized delivery system. This study showed that BC loaded with bone morphogenetic protein-2 caused better differentiation of mouse fibroblast-like C2C12 cells in vitro and better development of bone as well as calcium formation in Male Spraguee Dawley (SD) rats as compared to native BC [114].

Cellulose has a growing interest in the field of material science due to its availability in abundance, high purity, sustainability and biodegradability [115]. Bacterial cellulose has gained considerable interest due to its high purity as compared to plant cellulose and other modified forms of cellulose. The bacteria produce high amounts of cellulose with nano crystalline structure and possessing high water holding capacity. These properties make bacterial cellulose a potential candidate for tissue engineering applications. In this study, bacterial cellulose has been used with a detailed understanding of the material in its never-dried state following a key question: 'Can native never-dried bacterial cellulose be an ideal candidate for the osteogenic differentiation of human-derived placental stem cells for bone tissue engineering applications?

CHAPTER III

BACTERIAL CELLULOSE POLYSACCHAIRDE FOR TISSUE ENGINEERING

3.1. Introduction

Cellulose produced by bacteria was first discovered by A.J. Brown in 1886 from *Acetobacter xylinum [108].* The gelatinous and slippery bacterial cellulose is composed of pure form of cellulose with no lignin [116]. Bacterial cellulose (BC) has been long used by the Philippines as a raw material for its dessert food called *nata-de-coco* which is prepared by fermenting with coconut water and is immersed in a sugar syrup [116]. This product is now manufactured in Indonesia and even exported as a healthy diet [116]. The molecular formula of bacterial cellulose is $(C_6H_{10}O_5)^n$, having a β-1,4 linkage between two glucose molecules [117]. It is composed of nano and micro-sized fibrils arranged in random direction. Typical chain elongation rate is 2 μm/min. Inter- and intra-hydrogen bonding hold the glucan chains together in the bacterial cellulose structure as shown in FIGURE 8 [118].

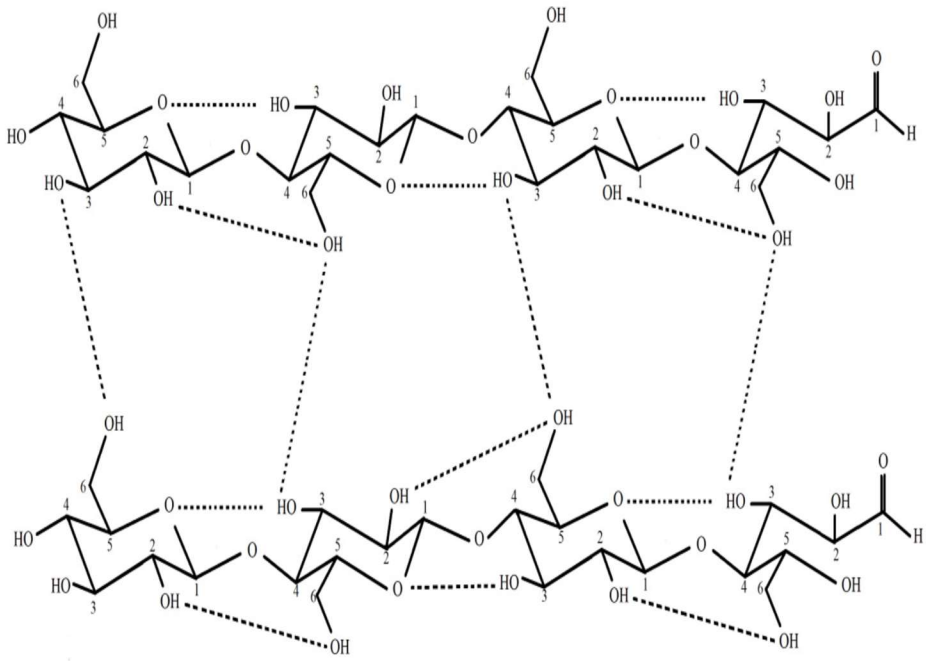

Figure 8. Bacterial Cellulose Structure with Inter- and Intra- Hydrogen Bonding

Cellulose producing bacteria synthesize nanoscale ribbon-like structure, of the dimension 40nmX60nm (width/height) with different crystallinity; either a cellulose-I structure or a thermally stable structure which is that of a cellulose-II structure [118]. This is because there are 50-80 pore-like sites on the surface of the cell which are presumed to be the sites of extrusion of precellulosic polymers which results in the association of glucan chains, aggregates, microfibrils, bundles and ribbons [119]. But when there is strong aeration and or there is presence of certain substances that can form hydrogen bonds with the β-1-4 glucan chains then cellulose II structure is formed instead of cellulose I [119]. These two allomorphs of cellulose have distinguishable properties. Cellulose-I has parallel glucan chains which consists of strong H-bonding patterns. This gives the structure high crystallinity but is less stable. Cellulose-II has low crystallinity as their H-bonding pattern is less ordered [120].

3.2. Bacterial Cellulose Synthesis

The bacterial cellulose synthesase complex is encoded by four genes (BCsA, BCsB, BCsC, BCsD), which are encoded by the bcs operon [120] [121]as shown in FIGURE 9. This enzyme was first characterized in the acetic acid bacteria, *Komagataeibacter xylinus* (*K. xylinus*) [120]. The bacterial cellulose biosynthesis pathway as proposed in *Acetobacter xylinum* contains seven distinct steps in which a monomer of glucose is assembled into a cellulose polymer which is then exported through the cell wall into the cell exterior to form a crystalline ribbon of nanocellulose [122].

To better understand the process of bacterial cellulose production it is important to study the biochemical synthesis pathway [122]. First, Glucokinase, phosphor-glucomutase and uridine triphosphate (UTP)-glucose1-phosphate uridylyltransferase transforms glucose to glucose-6-phosphate, glucose-1-phosphate, uridine diphosphate (UDP)-glucose. Further, in the presence of cellulase synthase UDP glucose transforms to bacterial cellulose which is unbranched β-1,4-D-glucan. Other sources of carbon which can be transformed to glucose are also used to improve the yield of bacterial cellulose. The bacterial cellulose synthase enzyme is a transmembrane complex that resides on the apical surface of the bacteria in a linear arrangement of 50-80 synthase complexes. BCsA encodes an integral inner membrane protein with a a small N-terminal domain and a large intracellular catalytic glycosyltransfersase domain. The C-terminal catalytic domain which contains a cyclic di-GMP/diguanylate PliZ domain, which is an activator of cellulose synthase enzymes, that control the synthesis of cellulose production. BCsB encodes a periplasmic polypeptide that binds to BCsA through a single C-teriminal helix. The BCsB protein contains two carbohydrate binding domains, CBD1 and CBD2, which stabilizes the transfer of the monosaccharide additions to the growing cellulose polymer chain. The growing cellulose polymer is fed and transported to the cell exterior/periplasmic space through a pore complex composted of proteins encoded by BCsC and the periplasmic polypetide encoded by BCsD.

Both protein products encoded by BCsC and BCsD are both involved in the maximization of BC production and crystallization by limiting the export of glucan chains and crystallization of the bacterial cellulose nanoribbon through the peptidoglycan layer found in the cell wall of gram-negative bacteria [122]. FIGURE 10 explains the biochemical pathway as proposed in *Acetobacter xylinum.* Further, the site of cellulose formation is on the upper side of the pellicle which is the air-pellicle interface [123]

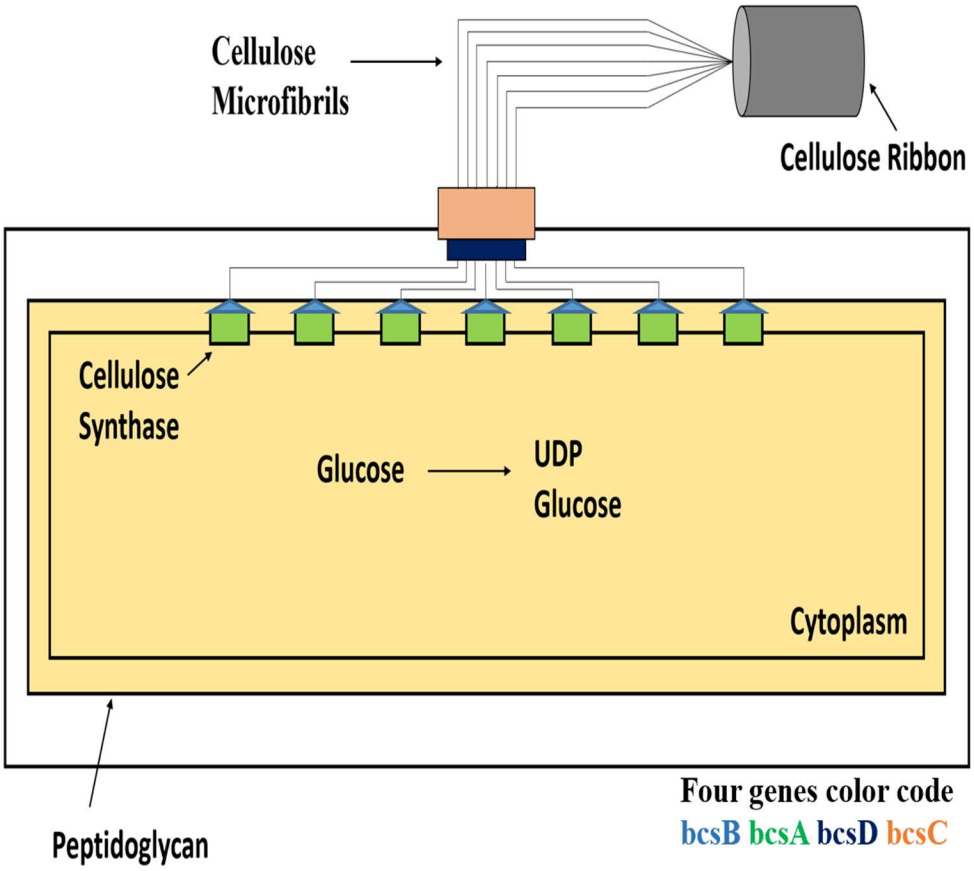

Figure 9. Bacterial Cellulose Synthesis Complex Organization

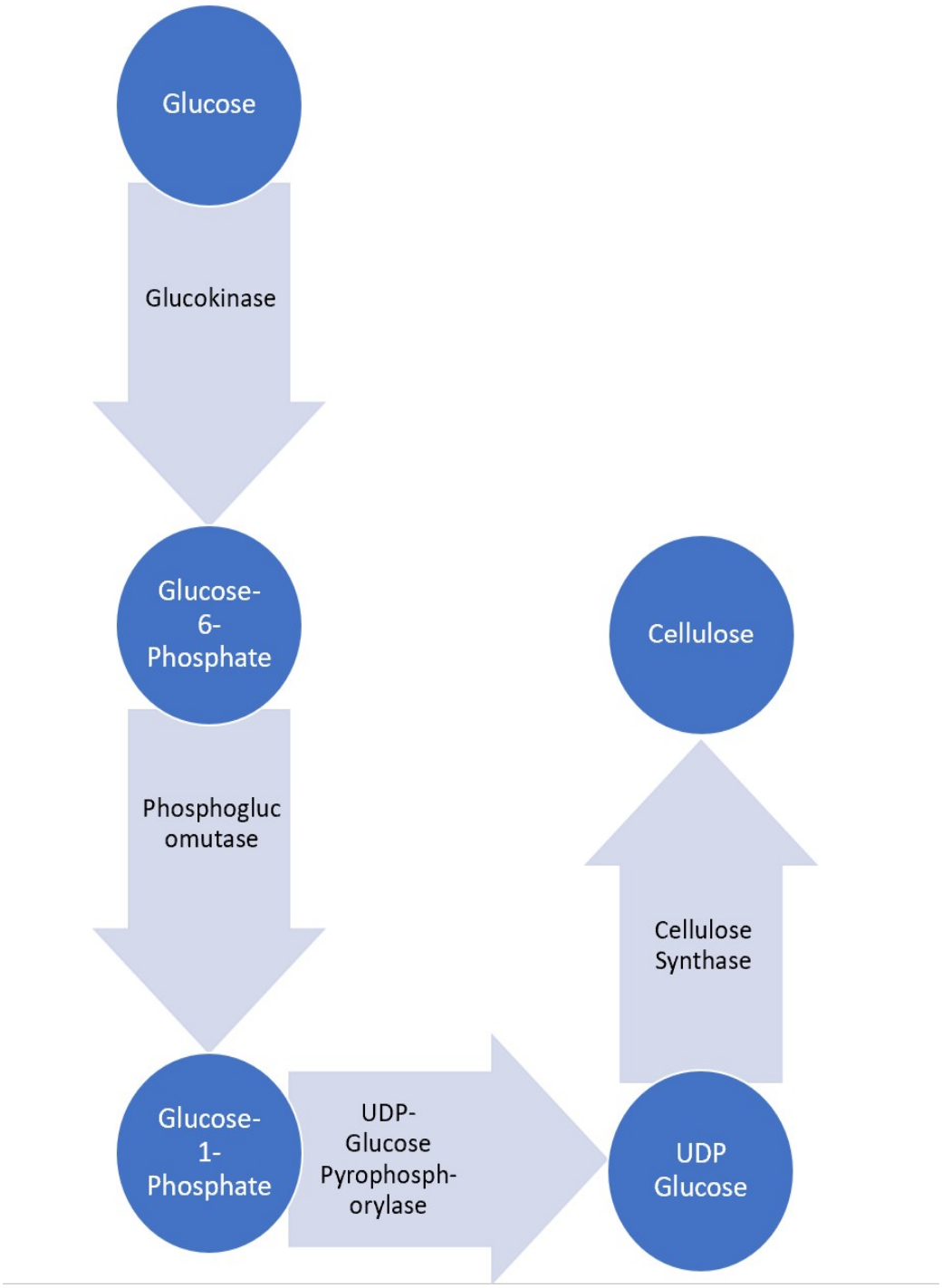

Figure 10. Bacterial Cellulose Biochemical Pathway

3.3. Parameters to Produce Bacterial Cellulose

Bacterial Cellulose has high crystallinity, purity and strength. It is necessary to optimize its production as it is a very important material in many industrial applications such as batteries, electronics and is gaining attention in the medical field too.

The factors that affect the production of cellulose include culture/growth medium, environmental conditions and the presence of any by-products formed during the process [119]. The different methods to improve the production of bacterial cellulose are described below [119, 124]:

- Culture Media: The three different types of media used to optimize yield of BC are Hestrinn-Schramm (H), Yamanaka (Y) and Zhou (Z) with each having optimum concentration of carbon and nitrogen sources [125]. Each of these media have different sources of carbon while maintaining a uniform pH of 5.5. Alternate methods to produce bacterial cellulose is by using feed stock like food processing effluents, molasses, fruit juice, rice bard and wheat straw as they are present in abundance, are low cost as well as impose no hazardous impact to the environment [104].
- Carbon and Nitrogen Sources: Date syrup, sucrose, mannitol, fructose, lactose, maltitol, sucralose, xylitol, glycerol and galactose are some of the alternate carbon sources to glucose. The need for alternate sources was important as using glucose causes the formation of gluconic acid which decreases the pH of the medium and leading to decrease in cellulose production [119]. Yeast extract, corn steep liquor

and peptone are some of the nitrogen sources used as nitrogen is necessary for cell metabolism[119].

- Other nutrients: phosphorus, sulfur, potassium and magnesium salts. Along with the carbon and nitrogen sources, the presence of ethanol, amino acids and vitamins also enhance the produce of cellulose [119]. The other factors that can help optimize bacterial cellulose production are pH and temperature [126]. The optimal temperature is around 28°C and 30°C and the pH is in the range of 4.0 to 6.0.

The most optimum methods for producing bacterial cellulose are static culture and agitated culture as they are affordable bench techniques.

- Static culture: When bacteria is immersed in the culture medium under static conditions, a cellulose biofilm of varying thickness is formed at the air-liquid interface [119]. The colonized bacteria at the air-liquid interface helps maintain the level of oxygen, protects the culture from drying while producing gelatinous pellicle with the doubling time of bacteria to be around 8-10 hours [119, 127].
- Agitated culture: Under agitated conditions, the oxygen is supplied by forced aeration as this improves bacterial respiration while producing cellulose with more fibrous morphology [119, 127]. The doubling time of bacteria is around 4-6 hours [119]. As compared to static culture, agitated culture produces cellulose with lower Young's modulus and crystallinity due to shear stress produced during agitation [127]. Further, the bacterial cellulose build-up under shaken conditions causes reduction in culture homogeneity which affects reduction in oxygen levels

[127]. Necessary modifications are being experimented to overcome these limitations like using airlift reactors, rotating disk reactors as well as trickling bed reactors for industrial applications [119, 128].

Komagataeibacter xylinus appears to be an interesting species from all the different types of acetic acid bacteria due to its ability to produce fibrils in the nano-micro scale [129]. Exploitation of bacterial cellulose gradually grew starting from the food industry to outperform currently used celluloses as food dressings, sauces and gravies and frozen dairy products [129]. But, because of the lack of fermentation tanks, the commercial development of bacterial cellulose was never achieved [129]. The added disadvantages of fermentation tanks also include high production and capital cost which has caused the process of producing cellulose at a larger scale relatively slower [129]. But, cellulose in the medical field came into effect when Johnson & Johnson tried to commercialize back in the 80s which lead to several industrial products by various companies like XCell for wound care, Biofill and Bioprocess for skin burns and ulcers and Gengiflex for periodontal diseases [129]. With bacterial cellulose entering intro drug delivery area the question that how bacterial cellulose will be produced on a larger scale stills needs to be answered.

3.4. Types of Cellulose Producing Bacteria

Bacterial cellulose is a renewable biomaterial that is produced by many species of bacteria including *Rhizobium leguminosarum, Burkholderia*, *Pseudomonas putida, Dickeya dadantii, Erwinia chrysanthemi, Agrobacterium tumefaciens, Escherichia coli, and Salmonella enterica,* however only three genera (*Gluconacetobacter, Acetobacter*,

and *Komagataeibacter)* produce this material in enough quantities and under standardized conditions to make them commercially important [119, 120]. TABLE 4 summarizes the different types of bacteria with varied cellulose morphology [122].

Table 4. Types of Cellulose Producing Bacteria

Organism (genus)	**Type of Cellulose Produced**
Acetobacter	Extracellular pellicle
Achromobacter	Cellulose ribbons
Aerobacter	Cellulose fibrils
Agrobacterium	Short fibrils
Alcaligenes	Cellulose fibrils
Pseudomonas	No distinct fibrils
Rhizobium	Short fibrils
Sarcina	Amorphous cellulose

3.5. Properties of Bacterial Cellulose

Unlike cellulose derived from plant sources, cellulose produced from bacteria is very pure lacking hemicellulose (a branch polysaccharide with 1-6 glucose linkages in addition to 1-3 linkages), lignin (a heterogeneous complex organic molecule which provides molecular structure to plant cellulose) and pectin (another branched polysaccharide). Furthermore, bacterial cellulose has higher degree of crystallinity and polymerization. It has a degree of polymerization between 2000-6000 [122, 130-132]. The most important property of bacterial cellulose for biological engineering is that it is highly biocompatible because the polysaccharide nature of bacterial cellulose makes it non-immunogenic and possess similarities with the extra cellular matrix structure in vivo [109] . Bacterial cellulose has many hydroxyl groups due to which the fibers demonstrate a property of self-assembly and production of cellulose sheets with high porosity and surface area [109]. BC has high water holding capacity, crystallinity, mechanical strength, purity and offers the advantage of forming other nanocomposites due to presence of -OH groups which offers sites for synthesis processes [133].

3.6. Applications of Bacterial Cellulose

Bacterial Cellulose is used a matrix material as well as a reinforcement material to form a nanocomposite. The unique properties of BC such as a high hydroscopic nature which makes the material highly hydrophilic, high tensile strength, the ability to produce different shapes, high crystallinity, sustainably sourced and substrates and the possibility of forming complex and novel composites due to the presence of -OH groups which offers sites for synthesis has offered potential applications. The table below (TABLE 5) provides various applications of bacterial cellulose [134].

Table 5. Applications of Bacterial Cellulose

Type	Description	Reference
Electronics	As acoustic films	[116]
Packaging	Edible nanocomposite films	[135]
Filtration Membrane	An adsorbent for heavy metal pollution	[136]
Drug Delivery	Localized cancer treatment, drug loading and release capabilities	[137], [138]
Blood Vessels	As a vascular graft	[139]
Wound Dressing	Third degree burn treatment, scar treatment	[140], [141]

Type	Description	Reference
Food Material	Dessert delicacy, frostings and icings, low-calorie additive	[142]
Biosensor	Biochemical and electrochemical devices	[143]

3.7. Bacterial Cellulose Immune Response

Biomaterials are required to be non-toxic and non-immunogenic [144]. Bacterial cellulose has gained attention in the biomedical field due to its unique properties like water absorption capacity, crystallinity and strength for its flexibility, nano and micro-scale structure and better biological affinity than plant cellulose [144]. However, there are concerns on the immunoreactivity of bacterial cellulose both *in vitro* and *in vivo*. This is because lipopolysaccharides (LPS) is an endotoxin that is present in the outer membrane of gram-negative bacteria which can induce the production of inflammatory cytokines [144].

Lipopolysaccharides are also termed as endotoxin that covers 90% of the cell surface that acts as a physical barrier from antibacterial agents [145]. The structure of lipopolysaccharide consists of a hydrophobic domain known as lipid A (endotoxin), a non-repeating core of oligosaccharide, and a distal polysaccharide (O-antigen) [146]. It is detected as a marker for the development of inflammatory response and bacterial pathogen invasion [145]. The lipid A component is responsible for the toxic effects from gram-negative bacteria [147].

This innovative biopolymer was studied for its immunoreactivity by seeding human umbilical vein endothelial cells in an *in vitro* study [144]. Bacterial cellulose did not increase inflammatory cytokine levels - Interleukin-4 and interferon(IFN)-γ as compared to lipopolysaccharide-treated cells used a control [144]. Further, lipopolysaccharides not only induce inflammatory response but also stimulates T cells (a lymphocyte participating in immune response) [144]. This study also confirmed that bacterial cellulose did not stimulate CD4+ and CD8+ T cells [144]. To evaluate the acute oral toxicity of bacterial cellulose, Kunming mice were fed with small portions of bacterial cellulose[148]. This study showed no abnormal symptoms or differences in the anatomy of the organs or even death [148]. Another study evaluated the genotoxicity of bacterial cellulose in presence of Chinese hamster ovaries *in vitro* and showed that bacterial cellulose did not cause any DNA damage and found that bacterial cellulose was not genotoxic [149]. Bacterial cellulose has also been commercially used for skin injury treatments like Biofill® for severe body burns [148]. Bacterial cellulose face masks and face scrubs are some of the applications in the dermal tissue engineering that have not shown to cause any skin irritation or inflammation [148]. Bacterial cellulose has also been biocompatible without invoking any foreign responses *in vivo*. The implantation of bacterial cellulose as an artificial blood vessel [150], as a subcutaneous implant [151] , for cartilage tissue engineering [152], as an artificial dura mater [153] and the application of Bionext® as a dressing to prevent scarring tissue formation are all examples wherein no immune reaction were observed, strongly suggesting that bacterial cellulose is not

carcinogenic and tumor generator and does not generate any inflammatory response or oxidative stress at the cellular level [148].

3.8. Experimental Section

3.8.1. Materials and Methods

3.8.1.1. Bacterial Cellulose Production

Gluconacetobacter hansenii was cultured in culture plate (6-well and 24-well) in a static culture at 30° C for a period of 4 days. The optimal culture medium consisted of (grams/liter): glucose 20, yeast extract 5, peptone 5, Na_2HPO_4 2.7 and citric acid 1.25. The BC pellicle obtained post culture was washed and soaked in sterile water for a period of 24 hours, boiled in 0.1N sodium hydroxide for 60 minutes and soaked in sterile water for 24 to 48 hours to a neutral pH. The pellicle was then autoclaved and stored in sterile water at 4° C until further use.

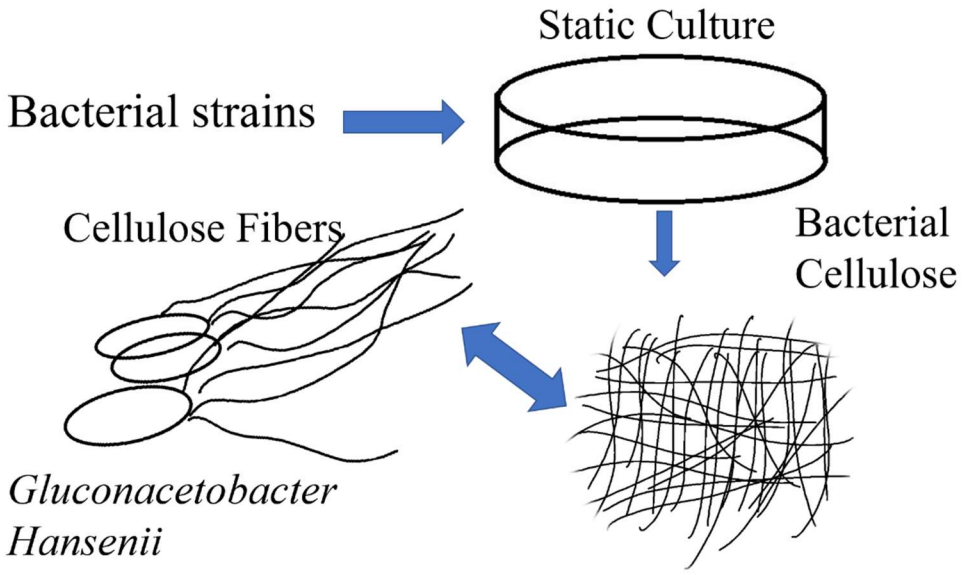

Figure 11. Schematic of Bacterial Cellulose Culture Using *Gluconacetobacter hansenii*

3.8.1.2. Morphology Characterization

Fiber diameter and morphology of BC were characterized using a Carl Zeiss Auriga-BU FIB FESEM Microscope (FESEM) (Carl Zeiss, Jena, Germany). Samples were first mounted on 1 cm_2 stubs using carbon tape sputter-coated with ~3nm gold-palladium using argon plasma Denton Vacuum Inc. Desk II Sputter Coater to avoid sample charging. Images were taken at a working distance of 5 mm and a gun accelerating voltage of 3 kV. The alignment of nanofibers was characterized using the fast Fourier transform method (FFT) using the FFT and orientation plug in for image j. The surface area and pore size were measures using Brunauer-Emmett-Teller (BET) Surface Analysis. Lyophilized bacterial cellulose were degassed at 120 ̊C for 3 hours followed by N2 adsorption at 77.144 K in a Micromeritics 3Flex 4.04.

3.8.1.3. Chemical and Structural Characterization

Attenuated total reflection Fourier transform infrared (ATR-FTIR) spectra was used to understand the chemical integrity of BC and BC-HA samples using Varian 670 IR (Paulo Alto, CA). All spectra were recorded in a wavenumber range of 4000–650 cm−1 with a resolution of 4 cm-1, accumulating 64 scans. The spectra of all samples were corrected for background.

The X-Ray diffraction pattern for BC was characterized using an X-ray diffractometer (Gemini A Since Crystal Diffractometer, from: Rigaku Oxford Diffraction having CrysAlisPro Software System, Version 3.8.43) with a 1.540598 angstrom K(alpha)1 copper X-ray source. The operating voltage and current used was 40kV and 40mA, respectively.

3.8.1.4. Thermal Characterization

Thermal behavior of BC was determined by Differential Scanning Calorimetry (DSC) and Thermo-gravimetric analysis (TGA). DSC tests were performed with a Q200 instrument (TA Instruments, New castle, DE, USA) under nitrogen atmosphere (nitrogen flowrate was 50 mL/min). The sample was heated from -20°C to 200 °C at the heating rate of 5 °C/min. The weight loss and the thermal stability of BC were measured by thermo-gravimetric analysis (TGA). TGA was performed by using Q500 thermogravimetric analyzer (TA instruments, New Castle, DE, USA) under nitrogen atmosphere. The sample (8-10 mg) was placed in the crucible and heated in the temperature range of 25–800 ◦C with a heating rate of 10 ◦C/mi.

3.8.1.5. Mechanical Characterization

The mechanical properties of BC were analyzed using MTS 858 Mini Bionix II. The BC sample were cut in a rectangular shape of the dimension 1cm X 6cm. They were cut in rectangular shape to enable fractures in the middle of the sample between the clamps. The thickness and the width of the BC sample was measured using a digital caliper. The distance between the clamps was maintained at 2cm and the sample was stretched at 5mm/min, until failure of the sample. The young's modulus was obtained using Testworks software.

3.8.1.6. Human-Derived Placental Mesenchymal Stem Cell (hPMSCs) Culture on Bacterial Cellulose Scaffold

Human PMSCs at passage 4 were additionally passaged 2-3 times in growth medium consisting of Minimum essential medium alpha modification 1X (HyClone, GE Healthcare Life Sciences, South Logan, Utah) supplemented with 17% AminoMax-C100 1X basal medium (gibco), 15% fetal bovine serum (FBS from SIGMA-ALDRICH), 2% AminoMax-C100 supplement (gibco), 1% glutamax-1 (100X: gibco) and 10ml of antibiotic/antimycotic solution (A/A from HyClone, GE Healthcare Life Sciences, South Logan, Utah). All cell culture reagents were used as received unless stated otherwise.

For all assays never-dried BC pellicles were seeded into wells of a 24-well tissue culture plates. BC samples were washed with 70 % ethanol followed by de- ionized (DI) water three times, sterilized under ultraviolet light for 2-4 hours and incubated in growth medium for 24 hours prior to seeding cells at 50k cells/well unless stated otherwise. Tissue culture plate (TCP) was used as control unless stated otherwise.

3.8.1.6.1. Adhesion Assay

hPMSCs were cultured on never-dried BC and tissue culture plate at cell seeding density of 50k cells/well and 10k cells/well respectively in complete growth medium. The cells were cultured for day 1 (post 24 hours) and day 5 and were fixed according to following protocol using the following protocol: each well was washed with 1X PBS and fixed with 4% paraformaldehyde in PBS for 15 minutes under incubation at 37◦C. The samples were washed 3 times with 1X PBS for two minute each followed by permeabilization using 0.2% Triton X-100 diluted with PBS for 15 minutes under incubation at 37◦C. Samples were rinsed again with 1X PBS three times for two minute each. 2% BSA was used as a blocking solution for 60 minutes under incubation at 37◦C. Nuclei were stained with DAPI and F-actin was detected using phalloidin. Laser scanning confocal microscopy was performed using a Carl Zeiss Axio Observer Z1, Spinning Disc Confocal Microscope (Carl Zeiss, Jena, Germany) and images were acquired at different magnifications. Confocal images were processed using the software and all quantitative images within a given experiment were captured using the same laser intensity and gain settings so that fluorescent intensities could be compared across sample.

3.8.1.6.2. Viability and Proliferation Assay

hPMSCs were cultured on native never-dried BC at cell seeding density of 50k cells/well in complete growth medium for live/dead cell assay. The cells were cultured for day 1 (post 24 hours), day 3 and day 5. The plate was incubated at 37̊ C and 5% CO2. Live/dead stain was prepared by adding 2 µmol/L acetomethoxy derivate of calcein (calcein-AM) and 2 µmol/L ethidium homodimer-1 per millilitre of media. The plate was then incubated for 20 min and images were obtained using Leica DMI4000B 487-4.

hPMSCs were cultured on never-dried BC at cell seeding density of 50k cells/well. The cells were cultured for day 1 (post 24 hours), day 3 and day 5 in complete growth medium for alamar blue assay. The plate was incubated at 37̊ C and 5% CO2. To measure viability, 10% (v/v) alamar blue was added to each well and the cultures were incubated at 37̊ C and 5% CO2. Viability was measured when the medium turned from blue to pink, typically at 4 h. Alamar blue fluorescence was measured using using a microplate reader (SpectraMax M5, Molecular Devices, Sunnyvale, CA, USA) with excitation at 560 nm and emission at 590 nm.

3.8.2. Results and Discussion

3.8.2.1. Morphology of Bacterial Cellulose

SEM analysis showed that a dried bacterial cellulose hydrogel is composed of a three-dimensional network of nanofibers. These nanofibers have an average diameter between 40-60nm and a helical twist due to the rotation of the bacteria during fibre foramtion [154]. In its native, ‘never dried state’, a bacterial cellulose hydrogel is a translucent and gelatinous film (FIGURE 12 A and B), with interwoven cellulose micro-

fibrils that are organized in random direction [117]. The material is flexible and resistant to tearing. Homogeneous pellicle of never-dried BC were obtained by maintaining the culture for a period of four days and incubating at 30℃ in a 24-well plate. The thickness of the pellicle was ~0.2mm with an average weight of 0.4 grams. Upon drying, bacterial cellulose becomes brittle as seen in FIGURE 12 D. FIGURE 13 shows the degree of fiber alignment using the fast Fourier transform method (FFT). A borad distribution of nanofibers was displayed which shows that the cellulose fibers produced by bacteria are in very random direction. The BET analysis of bacterial cellulose (TABLE 6) showed that the material had a pore size of 8.9nm with an average pore size of 11.51nm. The nanometer range of pore size also accounts for a high surface area of ~24 m2/g. Bacterial cellulose showed a random fiber alignment with nanoscale orientation and a high surface area . These parameters make bacterial cellulose an ideal candidate for its application in the field of tissue engineering.

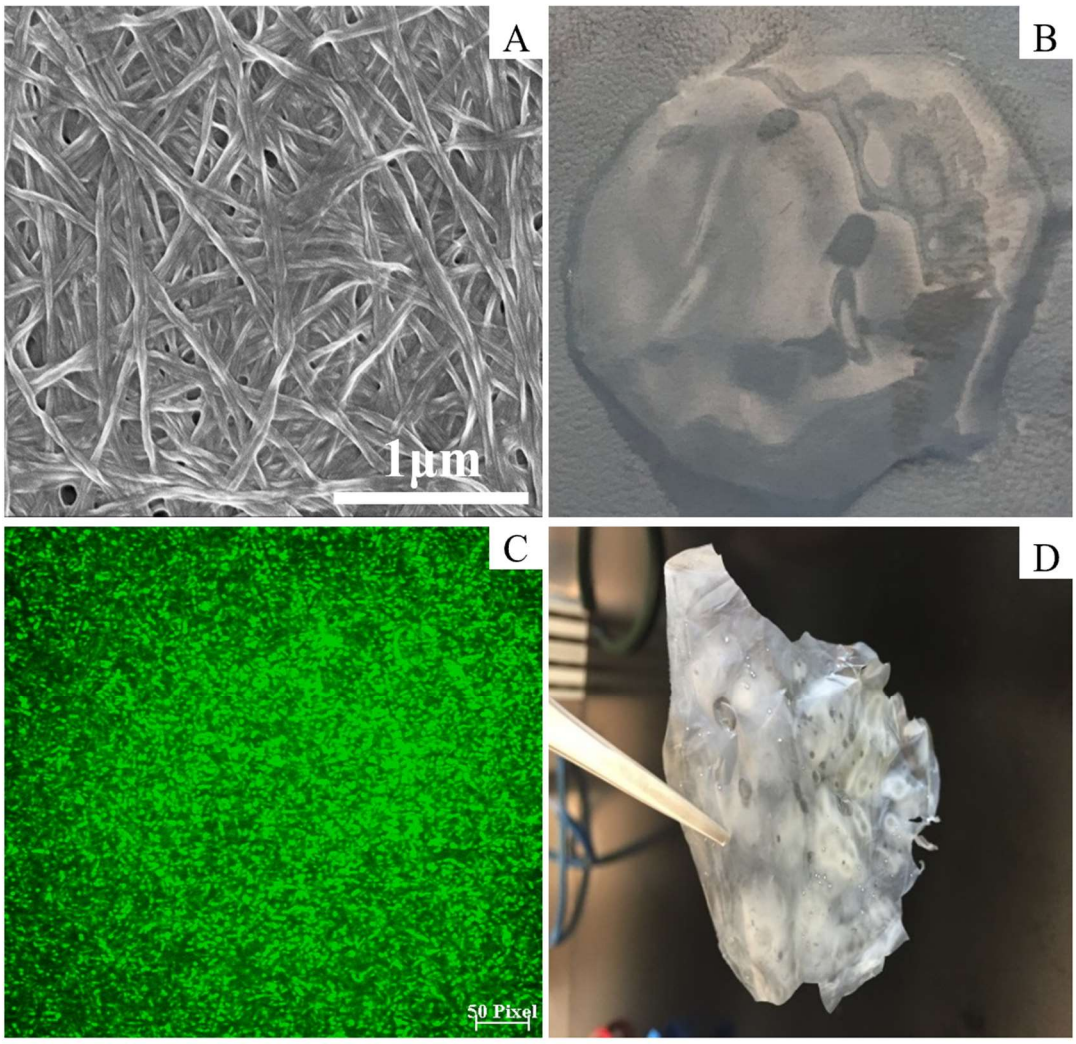

Figure 12. Morphology of Bacterial Cellulose: (A): Scanning Electron Microscope Image, (B): Never-Dried Bacterial Cellulose Post Cleaning, (C): Confocal Microscopy Image of Bacteria Stained Using Sox9, (D): Air-Dried Bacterial Cellulose

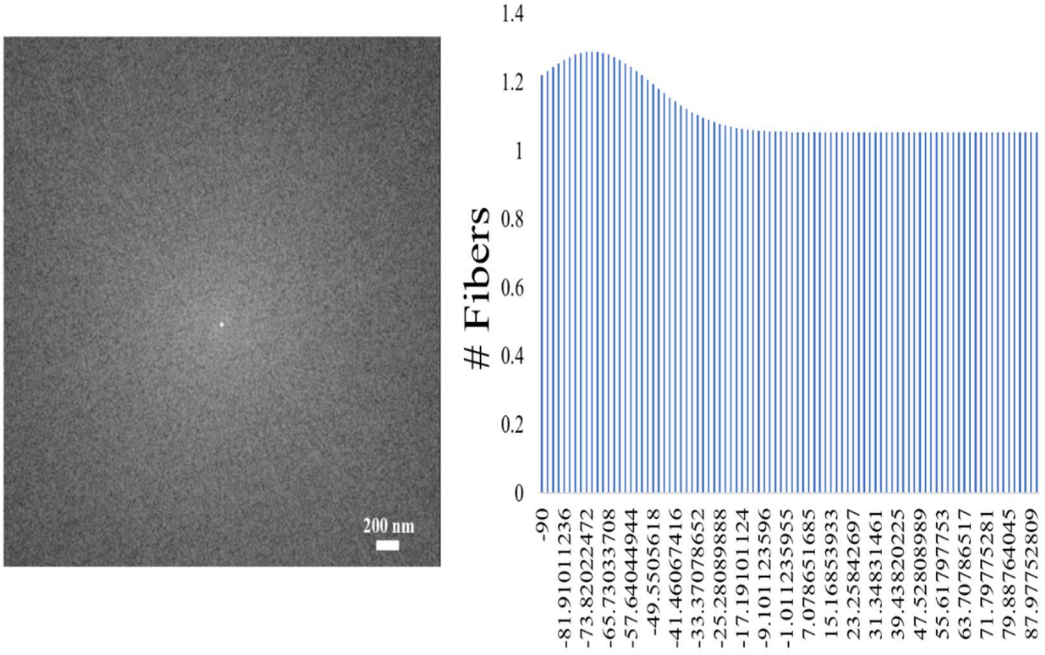

Figure 13. Alignment of Bacterial Cellulose Fibers Using Fast Fourier Transform (FFT) Method (left), Histogram Plot Against the Angle of Acquisition (right)

Table 6. BET Characterization of Bacterial Cellulose

BET Surface Area (m2/g)	**BET Pore Size (nm)**	**BJH Pore Size (nm)**	**Density (g/cm3)**
24.93	8.9	11.51	1.000

3.8.2.2. Chemical and Structural Characterization

The FTIR spectrum of neat bacterial cellulose (FIGURE 14) is summarized in TABLE 7 with individual peaks, respective chemical groups and bonds observed from the spectrum [155].

The x-ray diffraction of bacterial cellulose shown in FIGURE 15 demonstrates the characteristics peaks [156] for crystal plane (101), (10-1), (021), (002) and (040) which indicates the presence of both Iα and Iβ crystal cellulose and a typical crystalline form of cellulose I [155, 157, 158].

Table 7. FTIR Characteristic Peaks of Bacterial Cellulose

Frequency	**Assignment**	**Reference**
3340.14	OH Stretching: Intramolecular Hydrogen Bonding	[159]
2913.94	CH Stretching	[157]
2892.74	CH2 Symmetric Stretching	[157]
1643	Absorbed H2O	[160]
1427.08	CH2 Symmetric Bending	[157]
1160.95	Antisymmetric Bridge C-O-C Stretching	[157]
1052.95	C-O Stretching	[157]

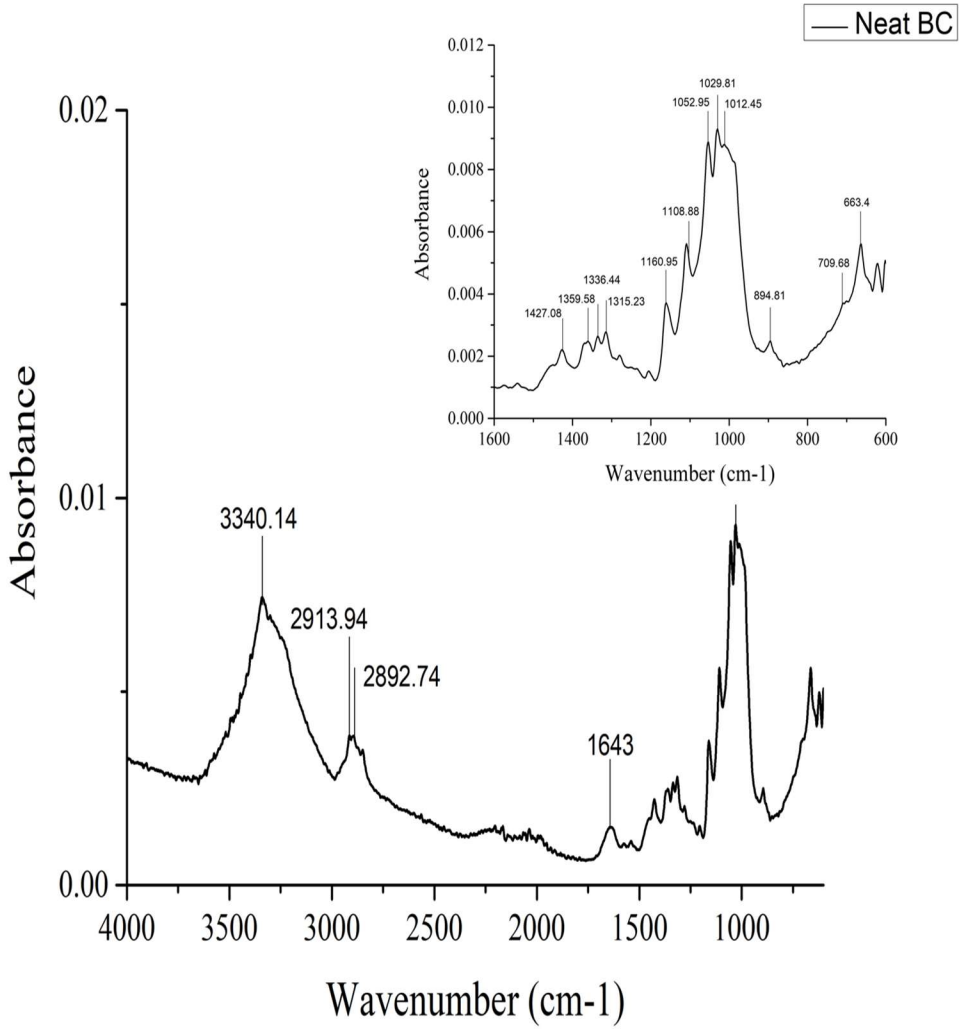

Figure 14. FTIR of Bacterial Cellulose

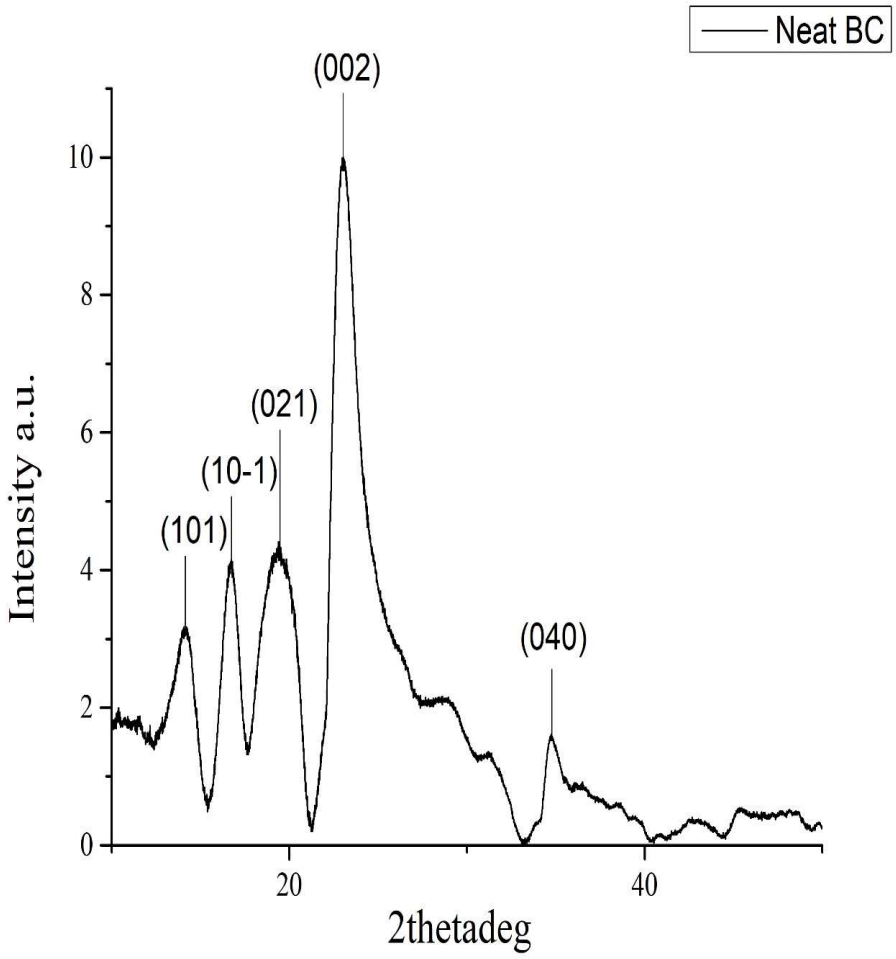

Figure 15. X-ray Diffraction of Bacterial Cellulose

3.8.2.3. Thermal Characterization

Thermogravimetric analysis of native bacterial cellulose allows us to understand the behavior of the material with temperature. As observed from the graph (FIGURE 16), the weight of the sample decreases with increasing temperature. The residual mass is negligible suggesting that there are no impurities in the bacterial cellulose sample. The thermal degradation of bacterial cellulose shows sequential dehydration, depolymerization, , and finally decomposition of glycosyl units, which is ultimately followed by the formation of charred residues [161]. The first weight loss for BC was between 5-6% which is attributed to desorption of water from the polysaccharide structure [162]. There is only one sharp peak observed at 311.73°C which is indicative of cellulose degradation in one step with an onset degradation temperature around 200°C for membrane dehydration. This also explains that the alkali treatment performed during BC cleaning as described earlier proved to effectively remove any impurities from the material. The maximum degradation of cellulose between 250°C and 320°C is when the glycosidic bonds within the fibers begin to break followed by decrease in fiber weight, degree of polymerization and crystallinity [160]. Our results prove that bacterial cellulose samples are highly stable at higher temperatures. This is an important property for sterilization of bacterial cellulose without changing its biophysical property as not many polymers can be sterilized above 100°C [107].

The Differential scanning calorimetry allows us to identify the changes in the thermodynamic variables during the physico-chemical transformations [163]. The Differential scanning calorimetry thermogram shows an endothermic event range from

30℃ to 160℃ which is indicative of the dehydration of surface water. The melting temperature is 111.91℃ and the enthalpy is 159.3J/g. Membrane dehydration observed in DSC compliments the data observed in TGA further suggesting that melting followed by degradation must occur [162].

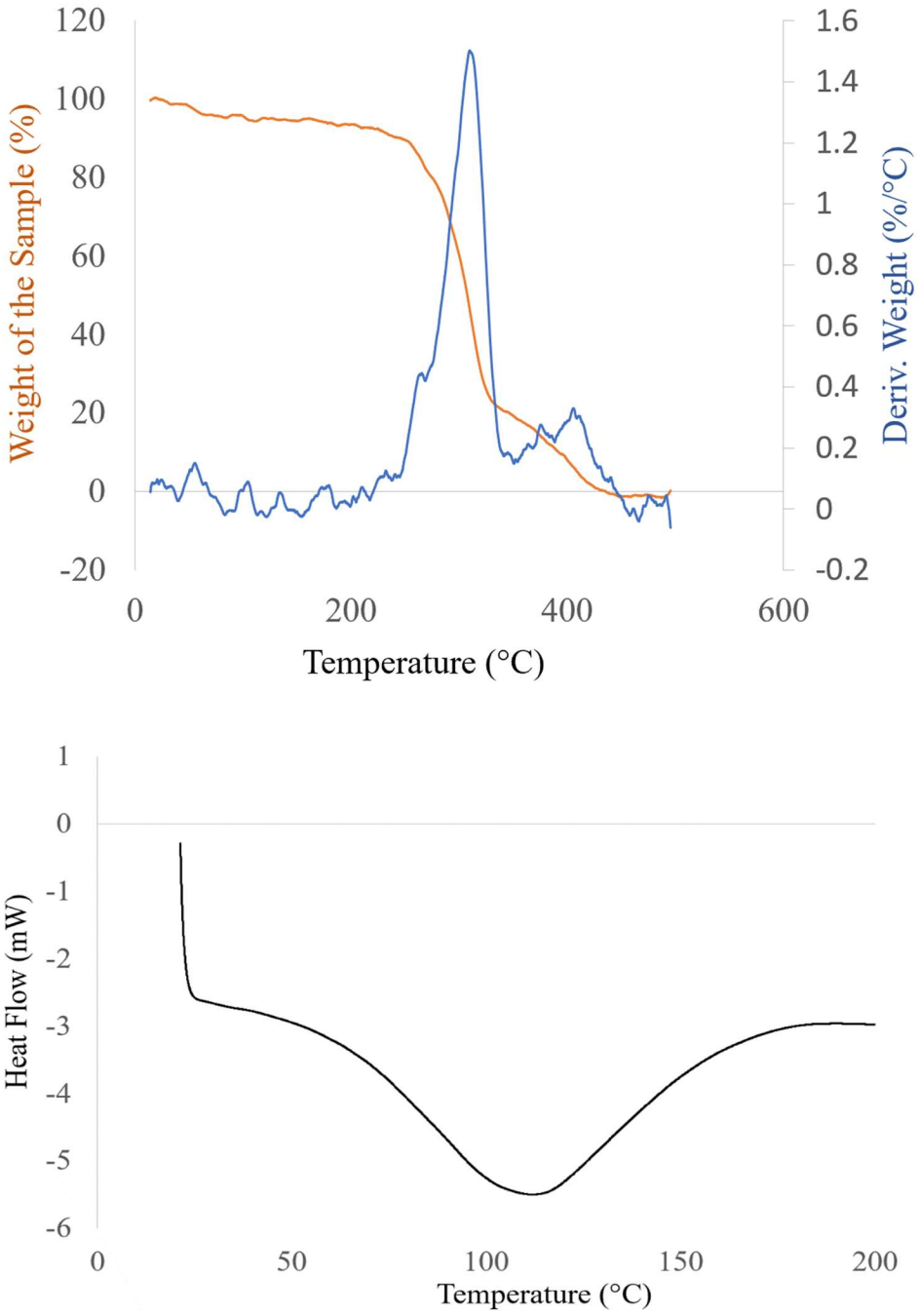

Figure 16. Thermal Analysis of Bacterial Cellulose: (top): Thermogravimetric Analysis, (bottom): Differential Scanning Calorimetry

3.8.2.4. Mechanical Characterization

Mechanical properties of bacterial cellulose were performed to evaluate its durability for its application in the field of bone tissue engineering. A typical stress-strain response of the BC material (FIGURE 17) in its never-dried state shows that this material has a linear elastic behavior followed by plastic behavior with an average young's modulus of 23.4 MPa. The average ultimate tensile stress and strain at break are listed in the TABLE 8. While bacterial cellulose has been reported with Young's modulus as high as 15GPa [164] (18 GPa of parietal bones of adult human skull [165]) depending on the cellulose content, the area of bacterial cellulose pellicle and material treatment (hot-pressed bacterial cellulose showed Young's modulus of ~6.86 GPa [166]), the material with ~23 MPa may be suitable for non-load bearing sites like plate bones of face and skull [165].

Table 8. Summary of Mechanical Properties of Bacterial Cellulose

Never-dried BC	**Young's Modulus (MPa)**	**Ultimate tensile stress (MPa)**	**Strain at break (mm/mm)**
Average values; N=3	23.4	1.67	0.38

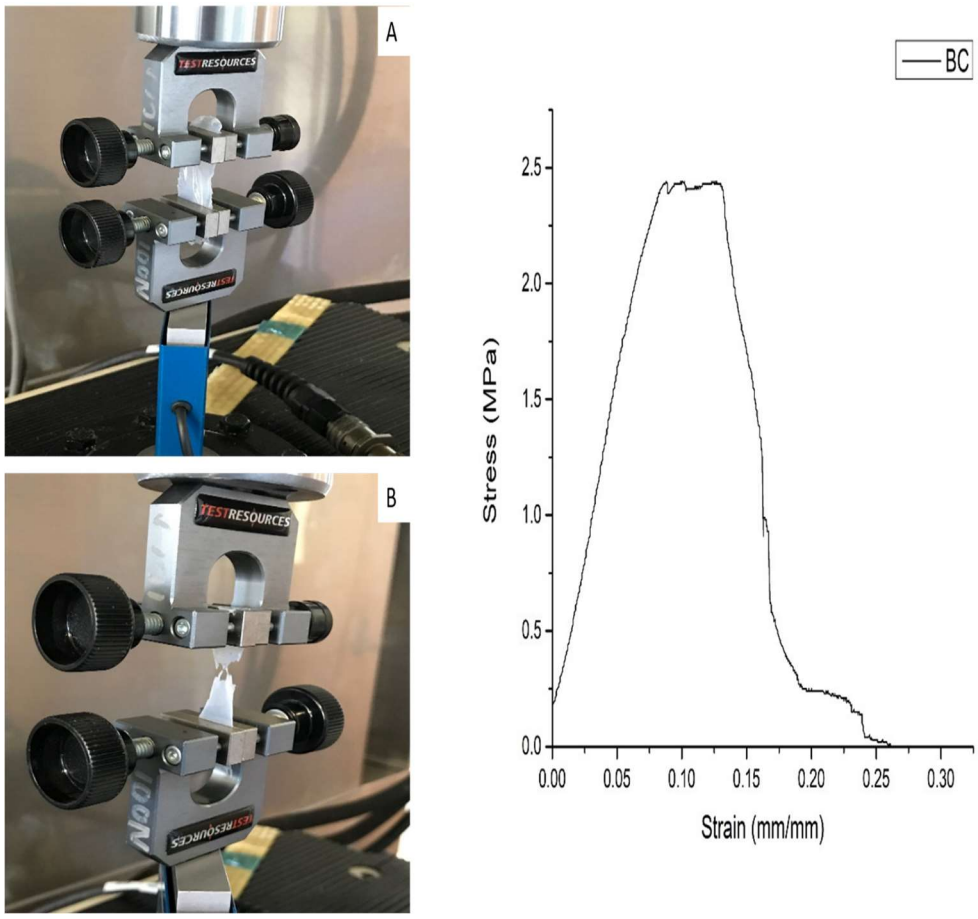

Figure 17. Mechanical Analysis of Bacterial Cellulose Showing: (A): Bacterial Cellulose During Application of Load, (B): Bacterial Cellulose After Application of Load, (right): Stress-Strain Curve of Never-Dried Bacterial Cellulose

3.8.2.5. Human-Derived Placental Mesenchymal Stem Cell Culture on Bacterial Cellulose Scaffold

3.8.2.5.1. Adhesion Assay

Although bacterial cellulose has been shown to be compatible with a broad range of cell types, to determine whether hPMSCs are compatible with bacterial cellulose we examine their proliferation and growth of these cells when cultured on these substrates. To do this, we cultured hPMSCs in a standard stem cell growth media on native never-dried BC and tissue culture plate (TCP as control). The ability of the cells to interact with the scaffolds were studied based on adhesion, proliferation and cytoskeleton development on Day 1 (after 24 hours), and Day 5 as seen in FIGURE 18 and 19. Both BC and TCP showed the development of distinctive actin filaments(green) surrounding the nucleus(blue). There is also an increase in number of cells per field of view which demonstrate that the hPMSCs are proliferating on the materials. At the start of the experiment, the morphology of the hPMSCs was a generally round-shaped; however, by day five on BC scaffolds the hPMSCs morphology was elongated as demonstrated by the increase in actin length. The small spots of actin (FIGURE 2 E and F) suggest that the cells might be migrating from one place to other leaving behind a part of the filament. Although there is a difference in the proliferation of hPMSCs on BC as compared to TCP, these experiments clearly demonstrate that bacterial cellulose supports the in-vitro growth on hPMSCs.

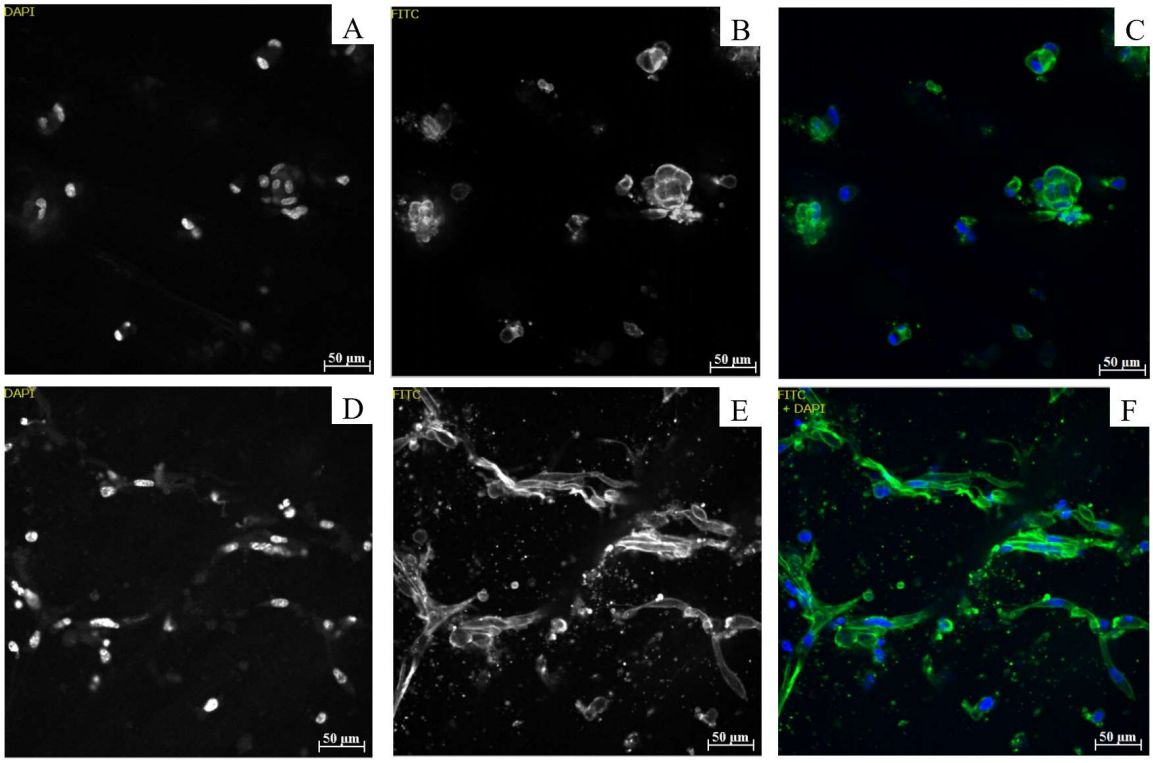

Figure 18. hPMSCs Culture on Bacterial Cellulose: (C): Day 1 Showing A: Nucleus, B: Actin Cytoskeleton; (F): Day 5 Showing D: Nucleus, E: Actin Cytoskeleton. Magnification: 20x, Green: Actin Cytoskeleton, Blue: Nucleus, Seeding Density: 50k cells/well in a 24-well plate

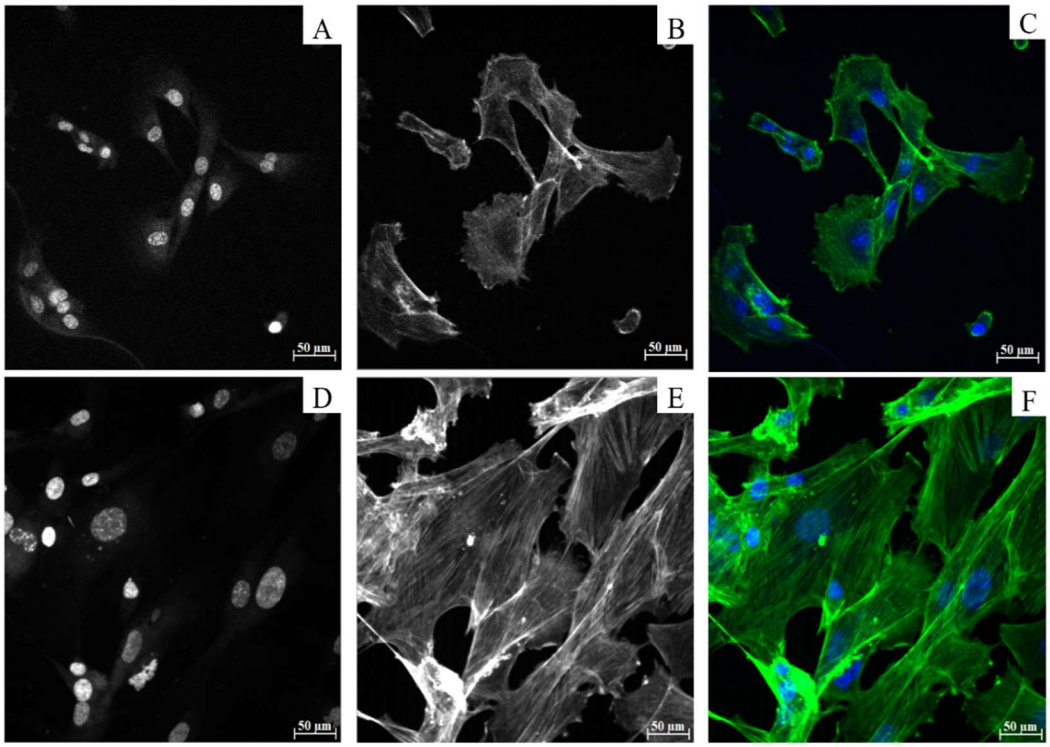

Figure 19. hPMSCs Culture on Tissue Culture Plate: (C): Day 1 Showing A: Nucleus, B: Actin Cytoskeleton; (F): Day 5 Showing D: Nucleus, E: Actin Cytoskeleton. Magnification: 20x, Green: Actin Cytoskeleton, Blue: Nucleus, Seeding Density: 10k cells/well in a 24-well plate

3.8.2.5.1.1. Mechanical Stress Analysis

We examined the mechanical environmental of hPMSC when in contact with the neat never-dried bacterial cellulose scaffold and a glass coverslip control. The formation of focal adhesions during cell-substrate adhesion is a mechanically induced event that controls cell morphology and gene expression. During the focal adhesion integrins bind specific extracellular targets, typically components of the extracellular matrix via interactions with the RGD moieties found in these molecules. Intracellularly, this interaction stimulates the local assembly of filamentous actin as well as the recruitment of actin binding proteins and proteins associated with the focal adhesion. Some of the proteins such as talin are found at these intracellular cites, while other proteins such as vinculin localize to these sites in a mechanical strain induced manner[167]. By determining the ratio of a vinculin to integrin signal using standard densitometric analysis of confocal images, we can measure the relative mechanical stress that a cell is experiencing in a bacterial cellulose scaffold when compared to a control.

Further, the structural signaling molecules that are crucial for cell adhesion and help define the cell-extracellular matrix expression are studied by vinculin and integrin respectively, on BC and TCP scaffolds as seen in FIGURE 20 on Day 5. hPMSCs on BC as seen in FIGURE 20 A has a distinctive expression of vinculin as compared to TCP. The arrows indicate the focal adhesion points marked in red. There was no significant difference in the expression of vinculin observed on BC and control although bacterial cellulose showed a higher number of focal adhesion site. The expression of integrin affects cell survival, cell differentiation as well as cell motility which is of key interest in

this study shows that there was no significant difference in the ratio of vinculin/integrin between bacterial cellulose and control. This concludes that BC promotes the survival of hPMSCs while being able to support cell-scaffold expression that can be applied towards studying osteogenic differentiation of HPMSCs. TABLE 9 summarizes the vinculin/integrin ratio on never-dried BC scaffold and control.

Table 9. Densitometric Analysis

Substrate	**Number of cells counted**	**Average number of focal adhesions with standard deviation**	**Average vinculin/ integrin with standard deviation**
Day 5 BC-HPMSCs	8	24±15.43	0.53±0.32
Day 5 TCP-HPMSCs	7	22.33±13.91	0.59±0.46

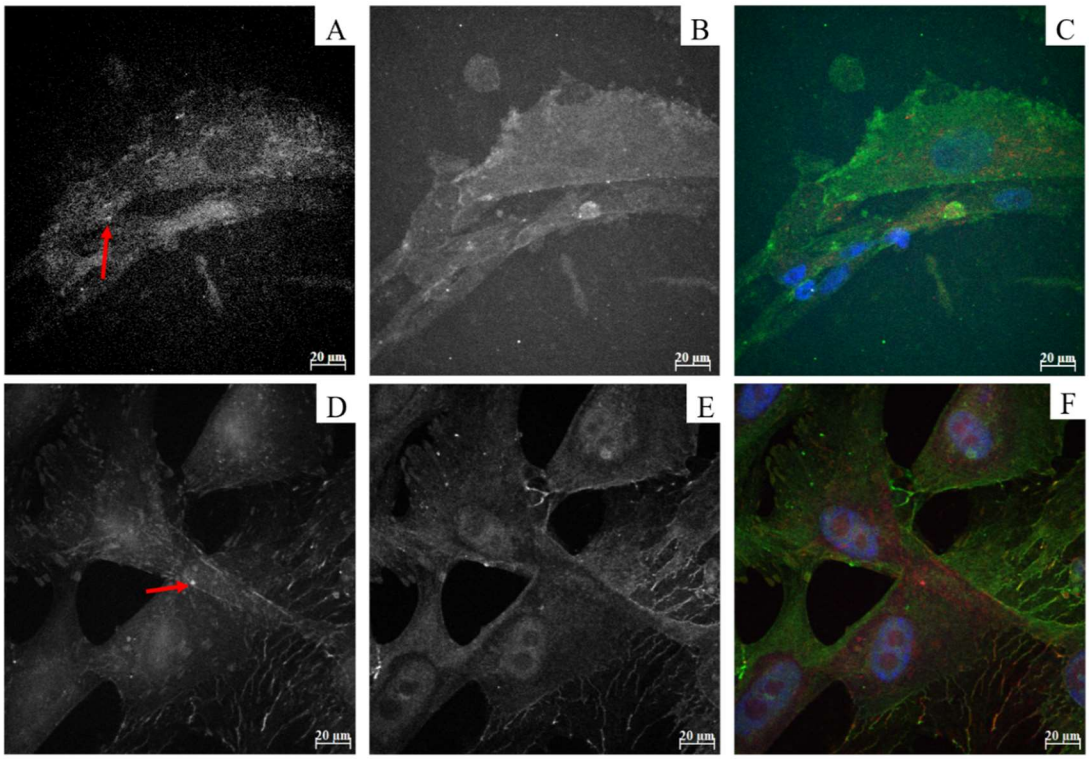

Figure 20. Analysis of Mechanical Stress During hPMSCs Culture on: (A-C): BC and (D-F): Tissue Culture Plate; Showing (A&D): Vinculin Expression, (B&E): Integrin Expression and (C&F): Merged Confocal Microscopy Image. Magnification: 40x, Green-Integrin, Red-Vinculin

3.8.2.5.2. Viability and Proliferation Assay

The toxicity of native never-dried BC was evaluated by culturing hPMSCs in-vitro using the Live/Dead cell assay kit. The cells were cultured for Day 1(after 24 hours), 3 and 5 as seen in FIGURE 21. The green color represents live cells and the red color represents dead cells. This study showed that BC is not only supporting the growth of hPMSCs but also is a viable scaffold for tissue engineering applications as compared to TCP. The material is non-toxic, biocompatible and supports the survival of hPMSCs in vitro.

FIGURE 22 shows cell viability and proliferation using alamar blue assay of hPMSCs on BC and TCP on Day 1 (post 24 hours), Day 3 and Day 5. The O.D. value increases over a period of 5 days on BC scaffold and TCP. TCP have a high proliferation rate with statistically significant difference between day 1 and day 3 and no significant difference between BC and TCP on day 1, 3 and 5. BC was not cytotoxic for hPMSCs culture and the proliferation and survival of the cells continued as compared to TCP were the confluency was achieved by the end of day 5 as supported by similar observations by live/dead cell assay.

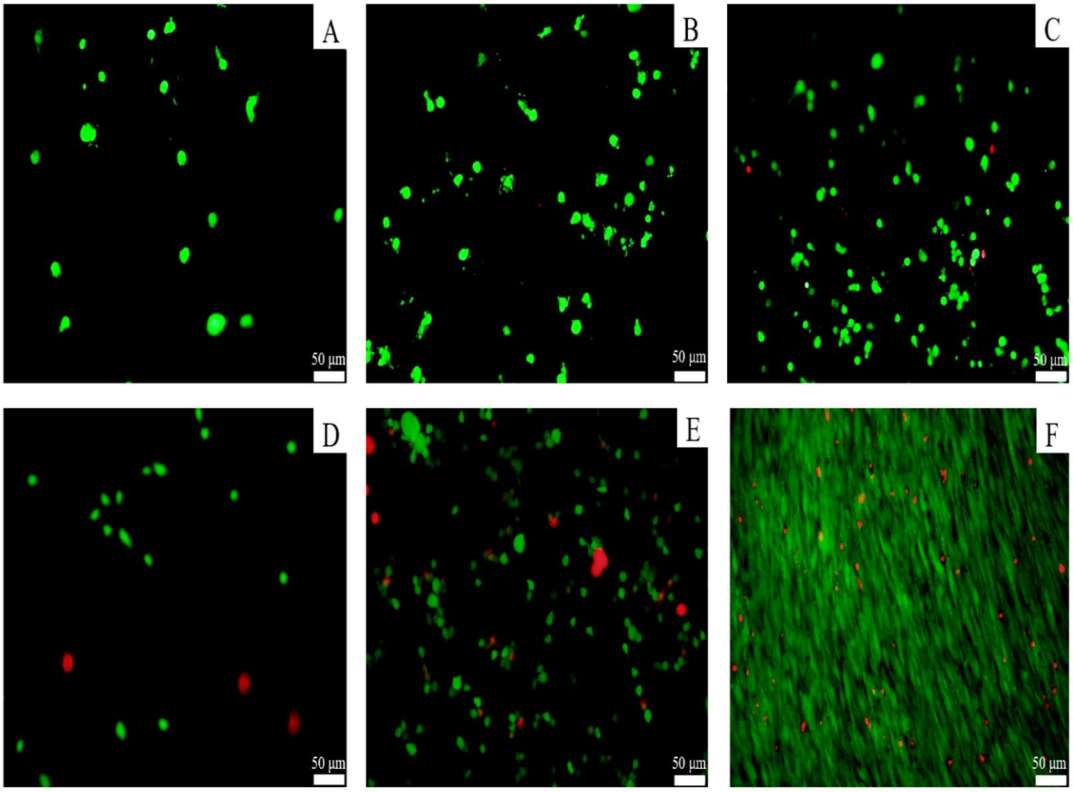

Figure 21. Live/Dead Image of hPMSCs on Bacterial Cellulose: (A): Day 1, (B): Day 3, (C): Day 5 and hPMSCs on Tissue Culture Plate: (D): Day1, (E): Day 3, (F): Day 5. Magnification: 20x, Green-Live, Red-Dead

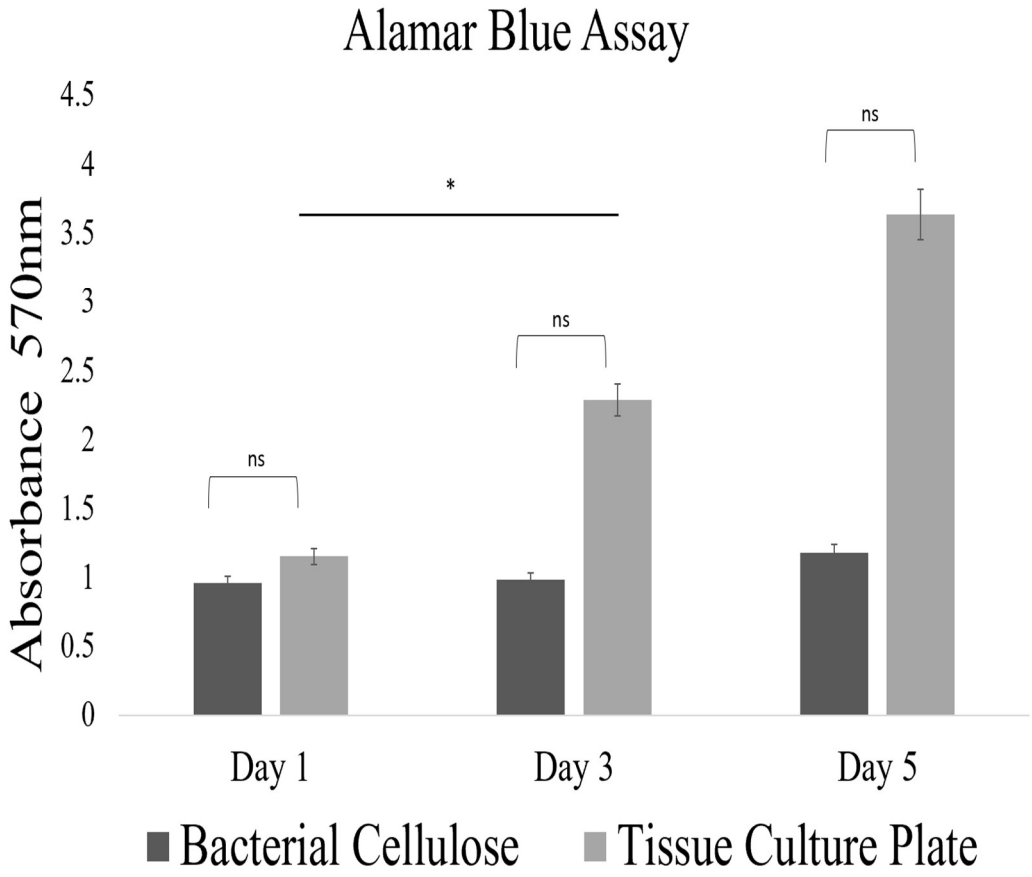

Figure 22. Viability and Proliferation Using Alamar Blue Staining

3.9. Conclusion

Bacterial cellulose pellicle was produced using *Gluconacetobacter Hansenii* under static conditions using mannitol as a source of carbon. The alignment of nanofibers occurs in random direction with an average diameter of 40-60nm and a thickness of 0.2 μm after four days of culture in an incubator at 30°C. The material obtained is hydrophilic in its never-dried state and becomes brittle upon drying. Characteristic peaks of neat bacterial cellulose were obtained using Fourier-transform infra-red spectroscopy showing intra molecular hydrogen bonding and glycosidic bonds. The thermal analysis showed that the material is stable up to 311.73°C with the maximum degradation occurring between 250-320°C. This allows for autoclaving as a sterilization method as the material can withstand higher temperature without causing change in material properties. The material also demonstrates good mechanical stability with an average modulus of 23 MPa in its never-dried state.

Since, bacterial cellulose offers biocompatibility with chemical and morphological controllability [168], it was studied for culturing human-derived placental mesenchymal stem cells in vitro towards osteogenic differentiation. The high surface area due to the nanoscale property of bacterial cellulose demonstrates native extracellular matrix behavior [169] which allows cells to express actin cytoskeleton and structural signaling molecules like vinculin and integrin. Further, the cells presented a more stacked morphology as compared to the tissue culture plate which shows enough cell spreading by the end of day 5. This could be either due to three-dimensional nature of bacterial cellulose (as the dense structure does not allow for cell migration [169]) which causes

slow cell spreading rate or lack of excellent bioactive molecules (like, collagen) that needs to be introduced along with bacterial cellulose to improve the formation of cell multilayer at an early stage of an in-vitro culture [168, 170]. Also, the pore size of bacterial cellulose as obtained by BET was 8.9094 nm. Since, the pore size of bacterial cellulose is below 100 μm it causes the formation of cell aggregates as observed by adhesion assay and low proliferation with no significant difference in cell viability as observed by alamar blue assay. However, the high surface area of 24.9 m^2/g as obtained by BET and material stiffness of 23 MPa makes bacterial cellulose a cell-supporting material while supporting the proliferation and adhesion of human-derived placental mesenchymal stem cells while presenting no toxicity towards the cells. In the next chapter, we will focus on how bacterial cellulose material properties supports osteogenic differentiation of human-derived placental mesenchymal stem cells.

CHAPTER IV

BACTERIAL CELLULOSE AS A SCAFFOLD FOR BONE TISSUE ENGINEERING

4.1. Introduction

The goal of tissue engineering is to overcome current limitations that are associated with the standard practice that autografts/allografts/ xenografts have in the restoration, maintenance, or improvement of tissue function due to an injury or disease [171]. The most notable are immune response complications, disease transmission associated with the implant, and increase morbidity that is associated prolonged operation hours [172]. The need for biocompatible materials that can be used as cell scaffolds which support and guide the formation of new tissue using an individual's own cells has gained enormous interest for treating bone defects that are inherently difficult to repair with being the second most transplanted tissue in the world [173, 174].

An ideal scaffold is used as a template to support neo-tissues, enhance cell interaction and support cellular activities without any toxic effects at the site of implantation [47, 175]. In addition, scaffolds should have specific properties like high surface area and high pore interconnectivity, while maintaining the mechanical properties required for the selected applications [176]. The advances in scaffolds for bone tissue engineering introduces us to different natural and synthetic biological materials.

Titanium-based scaffolds have been used to treat calvarial defects in patients and distal tibia and fibula fractures. These scaffolds have limited prospects due to their non-biodegradable nature and brittleness along with other scaffolds like hydroxyapatite and tantalum-based scaffolds [47, 176]. Ceramic scaffolds have been used for its osteoconductive properties due to similar composition to native bone mineral content but has limited applications due to its brittle structure and low mechanical properties. The application of bioactive glass has already been adapted in maxillofacial surgery, spinal fusion and clinical prosthesis, yet properties like brittleness, potential risk for release of toxic metal ions and a challenge to tune resorption rate limits its sue for clinical applications [172, 174, 177]. Since, the aim of native tissue is to resorb and replace implanted biological constructs that not only offer biodegradability but also allow regrowth of cells, natural polymers have been widely studied for bone tissue engineering. The scaffolds for bone tissue engineering must be gel-like/porous, osteoconductive and/or osteoinductive, biocompatible and support mineralization.

In this study, we have demonstrated the osteogenic differentiation of human placental mesenchymal stem cells in vitro (hPMSCs). hPMSCs have fibroblastic morphology and possess multilineage differentiation capacities which include osteogenesis, chondrogenesis, adipogenesis, neurogenesis, and endothelialization[178, 179]. hPMSCs are fetal-stage stem cells that have been extensively used for cartilage repair[180], neurogenesis[181], adipogenic differentiation[182], hepatogenic differentiation[183, 184], treating pancreatic disease[183, 185, 186], and treating bone disease and tumor growth[183, 187, 188].

In order to further enhance osteogenic property, I have developed Bacterial Cellulose (BC) scaffolds to promote cellular activities and support the differentiation of hPMSCs into the osteogenic lineage for bone tissue engineering applications. BC is a natural nanoscale polysaccharide material that is the secretion of the bacterium *Gluconacetobacter hansenii [133]* in this study. The molecular formula of BC is $(C_6H_{10}O_5)^n$, having a β-1,4 linkage between two glucose molecules [117]. BC has a fiber diameter of 20-40nm with interconnected pores and a high-water holding capacity[133]. BC serves as a competitive candidate in the field of bone tissue engineering due to its distinct chemical purity, ultrafine nanoscale structure and is an attractive alternative to collagen fibers due to its high tensile strength and moldability [104]. Further, high aspect ratio and reticulated structure has contributed to the excellent mechanical properties of BC. Depending on the source of carbon and method of production of BC it's Young's modulus can range from 3 MPa to 4 GPa [47]. For example, nanocomposites produced by Pickering emulsion method using BC showed a Young's modulus between 3.14 and 16.39 MPa [47, 189] while bacterial cellulose prepared from industrial wastes showed a Young's modulus between 1.84 to 2.02 MPa [47, 190].

Along with slow degradation rates due to the glycosidic linkage necessary for long term support in bone tissue engineering [47] and good mechanical integrity of BC, we hypothesize that the polysaccharide structure of BC offering resemblance to native ECM [191] will support the cellular activities of hPMSCs and the organization of functional groups in crystalline BC will offer sites for mineralization which is an important property in native bone tissues. The objectives in this work were to (1) evaluate

the structural and physical properties of BC, (2) examine the in vitro osteogenic differentiation of hPMSCs and (3) to evaluate the biological activity of hPMSCs-BC construct. Using osteogenic media supplements on pre-seeded hPMSCs on BC, osteogenic differentiation was studied, and the BC-cell culture were examined for the extent of in-vitro mineralization.

4.2. Osteogenesis: The Development of Bone

The process of bone formation either occurs by transformation of pre-existing mesenchymal cells to bone tissues via intramembranous ossification (flat bones in skull) or by differentiation of mesenchymal stem cells into cartilage that is later replaced by bone via endochondral ossification like in long bones, ribs and vertebrae [192, 193].

The process of bone formation is as follows [192, 193]: During embryonic skeleton development mesenchymal cells begin to differentiate into specialized cells that either form capillaries while others become osteogenic cells that mature into osteoblasts [192]. During early stages, osteoblasts are found in clusters and secrete osteoids in the ossification center [192]. Osteoids are uncalcified matrix of collagen and proteoglycan that calcifies after the deposition of mineral salts [192, 193]. The osteoblasts then get trapped in the calcified matrix that matures into osteocytes. Osteocytes can help detect any pressure or cracks in the bone which enables them to send signals to osteoclasts that help dissolve the bone. While the osteoblasts mature to osteocytes, old osteoblasts acquire a flat morphology and become lining cells as they align on the surface of the bone. These lining cells then control the passage of calcium ions.

The expression of osteogenic markers occurs as follows [194, 195]: The first stage of bone regeneration is proliferation that takes place after the cell seeding. The cells then start to differentiate into osteoprogenitor cells in the first two weeks of cell seeding with an increase in the expression of alkaline phosphatase and RUNX-2 which are early markers during differentiation. Followed by the expression of these markers, the next two week shows an increase in the expression of osteocalcin that is expressed by osteoblasts and marks the process of osteogenic differentiation. Lastly, biomineralization and presence of calcium is initiated within the collagen matrix.

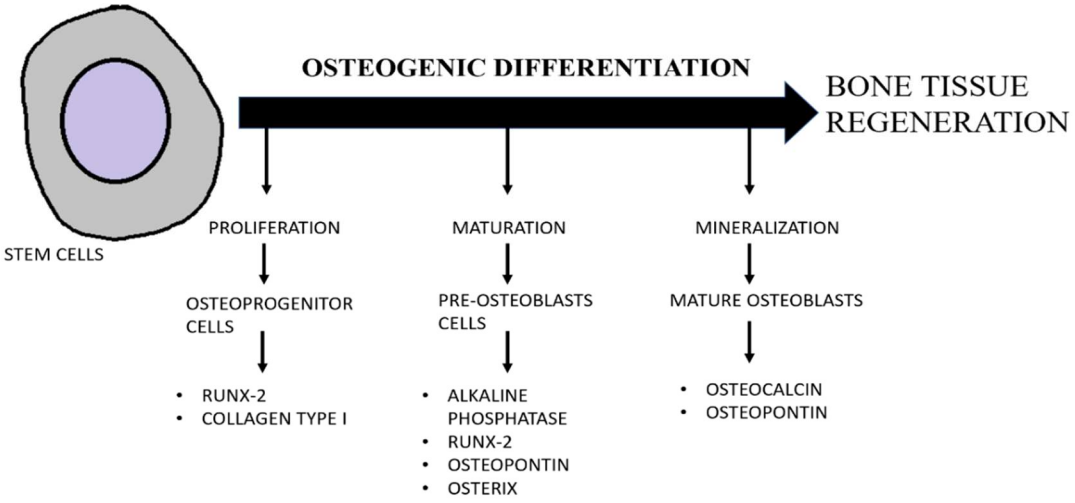

Figure 23. Expression of Osteogenic Markers During Bone Regeneration

4.3. Materials and Methods

4.3.1. Bacterial Cellulose Mineralization

The BC pellicle was soaked in 50mM calcium chloride solution for one hour, washed with sterile water and then soaked in 30mM phosphoric acid solution (pH 7.0) for 24 hours in a water bath maintained at 37° C to obtain a Calcium to phosphorus ratio of 1.67. The above procedure was followed to obtain calcium to phosphorus ratio of 1.33 by using 60mM calcium chloride solution and 45mM phosphoric acid solution. The BC pellicle was washed with ethanol and kept under UV for 15 min. The pellicle was then washed with sterile water and placed in hPMSCs medium for 24 hours prior to cell culture.

4.3.2. Characterization of Mineralized Bacterial Cellulose

Fiber diameter and morphology of mineralized BC were characterized using a Carl Zeiss Auriga-BU FIB FESEM Microscope (FESEM) (Carl Zeiss, Jena, Germany). Samples were first mounted on 1 cm2 stubs using carbon tape sputter-coated with ~3nm gold-palladium using argon plasma Denton Vacuum Inc. Desk II Sputter Coater to avoid sample charging. Images were taken at a working distance of 7 mm and a gun accelerating voltage of 3 kV.

Attenuated total reflection Fourier transform infrared (ATR-FTIR) spectra was used to understand the chemical integrity of mineralized BC using Varian 670 IR (Paulo Alto, CA). All spectra were recorded in a wavenumber range of 4000–650 cm−1 with a resolution of 4 cm-1, accumulating 64 scans. The spectra of all samples were corrected for background.

4.3.3. Osteogenic Differentiation of Human-Derived Placental Mesenchymal Stem Cells (hPMSCs) on Bacterial Cellulose Scaffolds

Human-derived PMSCs were cultured in osteogenic medium consisting of low-glucose Dulbecco's modified Eagle medium (DMEM) with 10% FBS, 1% Pen/Strep (HyClone, GE Healthcare Life Sciences, South Logan, Utah) and osteogenic supplements (Sigma Aldrich: 100 nM dexamethasone, 10 mM β-glycerophosphate and 50 mg mL−1 ascorbicacid-2-phosphate). Cells were cultured in growth medium as well as on tissue culture plate (TCP) as controls as stated in the experiments. The cells were cultured for a period of 28 days and the culture medium was changed every alternate day. The growth medium was replaced with differentiation medium after 48 hours for all in vitro osteogenic differentiation assays.

For all assays never-dried BC pellicles were seeded into wells of a 24-well tissue culture plates. BC samples were washed with 70 % ethanol followed by de- ionized (DI) water three times, sterilized under ultraviolet light for 2-4 hours and incubated in growth medium for 24 hours prior to seeding cells at 100k cells/well unless stated otherwise.

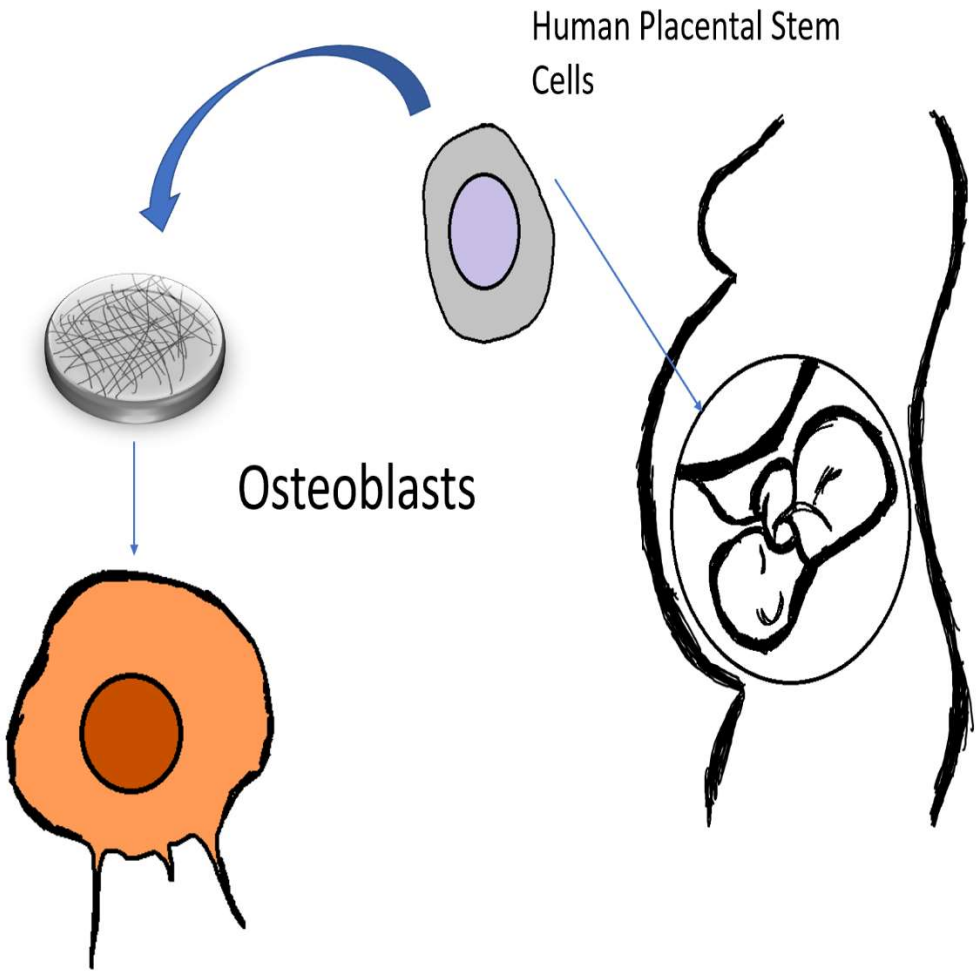

Figure 24. Schematic of *in vitro* Culture of Human-Derived Placental Mesenchymal Stem Cells on Bacterial Cellulose Scaffolds Towards Osteogenic Lineage

4.3.3.1. Alkaline Phosphatase Activity

Alkaline Phosphatase activity (ALP) was extracted from cell-BC construct and its activity was examined for the time points day 1 (post 24 hours), day 3 and day 14 using 1-Step™ PNPP (p-nitrophenyl phosphate disodium salt) Substrate Solution (37621-ThermoFisher Scientific) and used according to the manufacturer's guidance. Briefly, BC samples were homogenized in 0.2% Triton X-100, transferred to a 1 mL Eppendorf tube and incubated at 37˚C for 20 minutes. Similarly, cells seeded on TCP were lysed in 0.2% Triton X-100 and collected after 20 min of incubation. 50 µl of BC and TCP solution were added to 96-well plate and 100 µl of PNPP solution was added to each well. The plate was incubated for 15-30 minutes until the color in each well changed to a yellow-color product. 50 µl of 2N sodium hydroxide was added to each well to stop the reaction. The absorbance was read at 405nm using a microplate reader (SpectraMax M5, Molecular Devices, Sunnyvale, CA, USA).

4.3.3.2. Alizarin Red Assay

Bacterial cellulose-hPMSCs were cultured in 24 well plate and rinsed in PBS and fixed in 4% paraformaldehyde for 20 min. The samples were then rinsed in distilled water and 500 µl of 40mM alizarin red stain (pH 4.1) was added. The samples were incubated for 15-20 min with gentle shaking. The dye was removed, and samples were soaked in distilled water for 24 hours to remove any excess dye.

4.3.3.3. Energy-Dispersive X-ray Spectroscopy

hPMSCs were cultured on BC samples and TCP for Day 14, 21 and 28 for the calcium content in growth and differentiation medium. The samples for calcium analysis were examined using to SEM and Energy-Dispersive X-ray Spectroscopy (EDS). The samples are placed in the fixative solution for SEM and EDS analysis that consisted of 25% of 0.4M Cacodylate buffer, 12.5% of 16% formaldehyde, 10% of 25% glutaraldehyde and DI water. The samples are placed in this fix overnight, washed using autoclaved water (3X) and air-dried overnight before imaging. For imaging, the samples were mounted on 1 cm2 stubs using carbon tape sputter-coated with ~5nm gold-palladium using argon plasma Denton Vacuum Inc. Desk II Sputter Coater to avoid sample charging. Surface Characteristics of BC and TCP samples were observed using Carl Zeiss Auriga-BU FIB FESEM Microscope (FESEM) (Carl Zeiss, Jena, Germany). For each image obtained using SEM, calcium content was quantified using EDS. 5 different readings on the samples were obtained at varied locations and the average of these reading were plotted for individual sample. The analysis was performed using the HyperMap tool at 3000 x magnification and an accelerating voltage of 10kV.

4.3.3.4. Total Collagen Content

The total collagen content was measured using the colorimetric hydroxyproline quantification method (K218-100- BioVision Incorporated, Milpitas, California). Briefly, constructs were washed with deionized water three times for 5 min each and then homogenized with a deionized water in a 1 mL scintillation vials and equal amount of

concentrated HCl was added. The samples were hydrolyzed at 60°C overnight to extract collagen. 4 mg of charcoal was added to each vial and centrifuged at 10000 X g for 3 min to remove the precipitate and activated charcoal. 20 µl of each sample was added to a 96-well plate and evaporated to dryness at 60°C for 20-30 minutes. The reagents were prepared as per the manufacturer's instructions. Once the samples have been dried, 100µl of Chloramine T was added to each well and incubated for 5 min followed by 100 µl of DMAB reagent and incubated for 90 min at 60°C. The plate was then measured at absorbance at 560 nm in a microplate.

4.3.3.5. Gene Expression Study

hPMSCs for osteogenic differentiation were cultured on BC and TCP for Day 14, 21 and 28. The expression levels of osteogenic marker genes were determined by quantitative real-time PCR. Total RNA was isolated from differentiated cells using the TRIZOL reagent (Invitrogen, Carlsbad, CA). The RNA was subjected to a wash using RNeasy MinElute Cleanup Kit from Qiagen. An equivalent amount of each RNA sample was converted into cDNA using the QuantiTect Reverse Transcription Kit from Qiagen. Next the cDNA was subjected to gene-specific PCR for RUNX-2 and OCN (osteocalcin). Details of primers are listed in Table 1. PCR amplification was performed on a real-time PCR machine (ABI 7500, USA) using a kit (Power Syber Green master mix -Thermo Fisher Scientific) with GAPDH (glyceraldehyde-3-phosphate dehydrogenase) for normalization, and the data were analyzed using the $2^{-\Delta\Delta Ct}$ method [196].

Table 10. Osteogenic Gene Expression

Gene	Primer Sequence (Forward/Reverse), 5'-3'
RUNX-2	Runx2-F, TGGTTACTGTCATGGCGGGTA Runx2-R, TCTCAGATCGTTGAACCTTGCT A
OCN	Osteocalcin-F, GCCACCGAGACACCATGAGA Osteocalcin-R, AGCAGAGCGACACCCTAGACC
GAPDH	GAPDH-F, CATGAGAAGTATGACAACAGCC T GAPDH-R, AGTCCTTCCACGATACCAAAGT

4.3.4. Statistical Analysis

Student's *t* test was used to determine whether the differences within the same time point were significant. Two-way ANOVA were applied to all other comparisons. All values were reported as mean ± SD. A value of $P < 0.05$ was considered significant. Duplicates per group were used unless specified otherwise.

4.4. Results and Discussion

4.4.1. Characterization on Mineralized Bacterial Cellulose

We characterized the morphology and structure of our BC nanocomposites using SEM and FTIR spectroscopy shown in FIGURE 25 AND 26. SEM analysis of composites of mineralized BC resulted in a pellicle that is completely encased in hydroxyapatite crystals with little of the fibrous nanocellulose filaments observed (FIGURE 25 C and D). In the chemical precipitations procedure that we used, the HA crystals that deposited on the BC fibers formed in agglomerates and had a flake-like morphology (FIGURE 25 D, red arrow). We confirmed the presence of HA deposition on the BC nanofibers by FTIR analysis. The presence of HA on the BC was confirmed by the reduction in the intensity around 3340 cm-1, a band assigned to hydroxyl groups of the cellulose polymer demonstrated that the HA are interacting with this group. The FTIR bands further observed at 1024 and 960 cm-1 were attributed to vibrational modes of phosphate ions. the weak intensities around 871 and 1400 cm-1 suggests the absorption of CO_2 from air. Similar results in terms of morphology and chemical structure of hydroxyapatite have been obtained in the literature as well [157, 197].

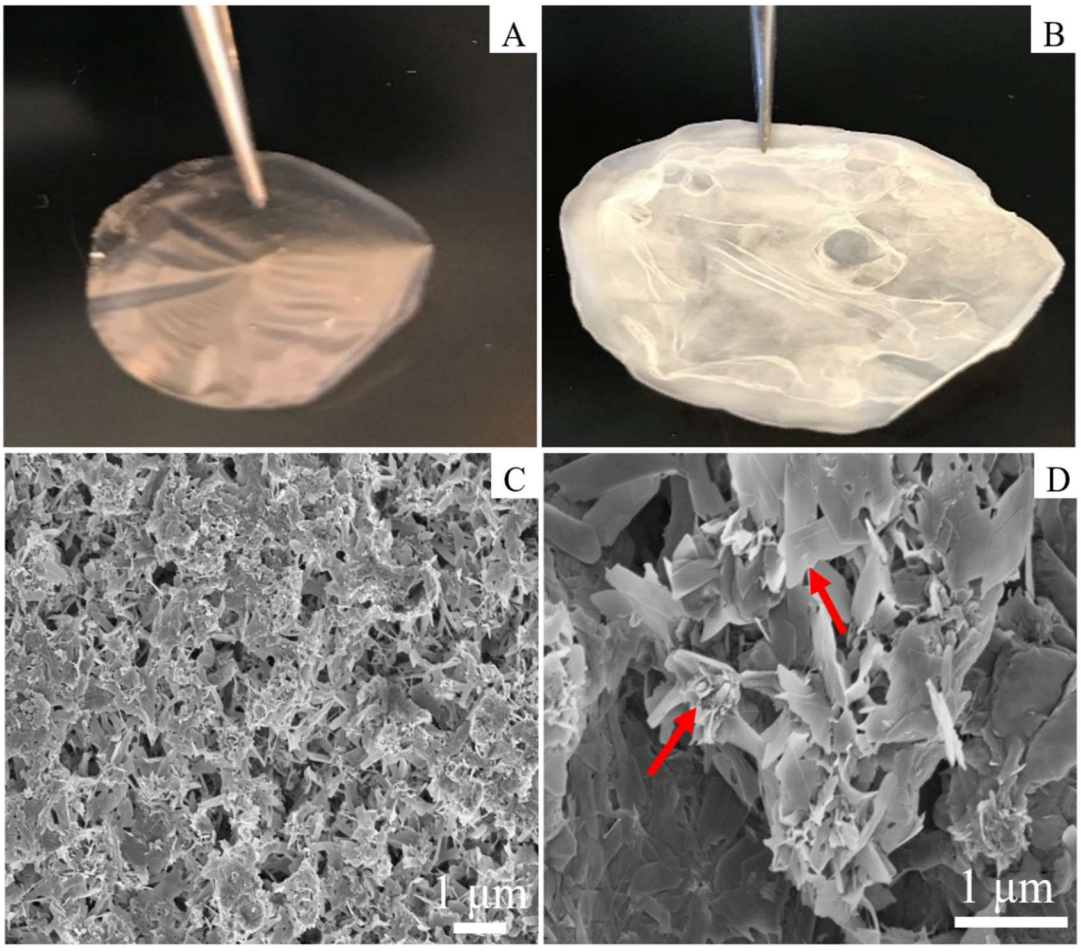

Figure 25. Bacterial Cellulose Characterization Showing (A): Dry Bacterial Cellulose Before Mineralization, (B): Dry Bacterial Cellulose After Mineralization, (C-D): Scanning Electron Microscope Image of Bacterial Cellulose After Mineralization

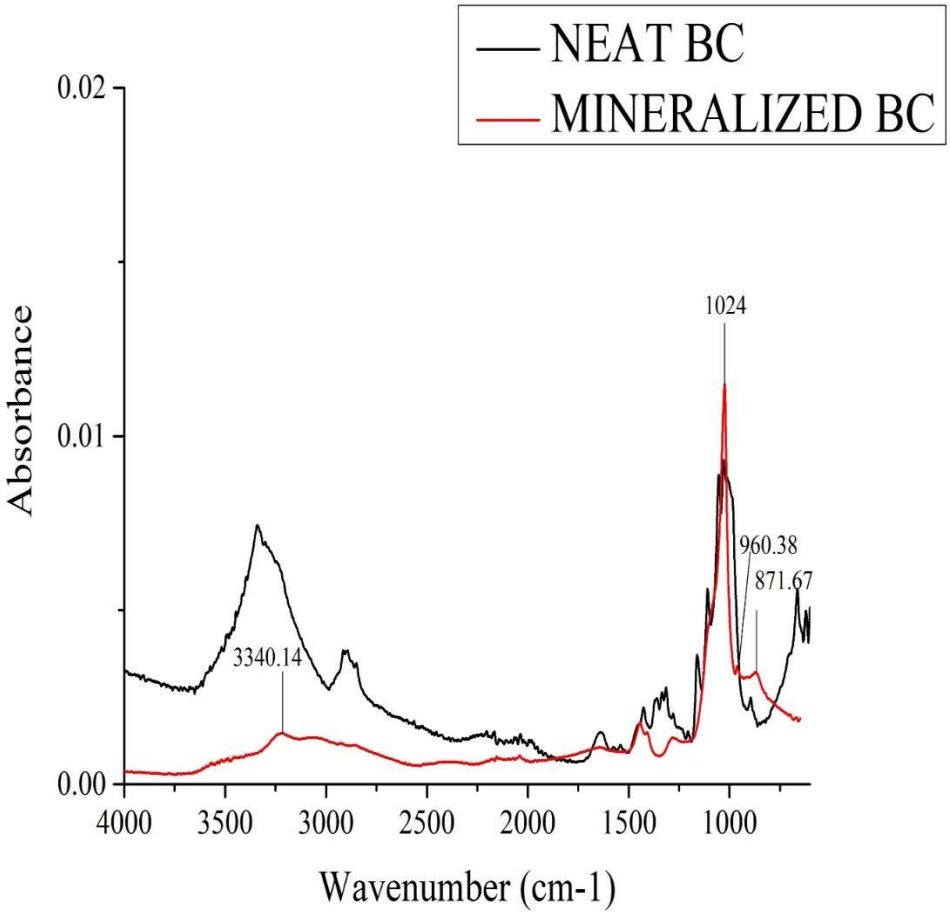

Figure 26. FTIR of Neat and Mineralized Bacterial Cellulose

4.4.2. Osteogenic Differentiation of Human-Derived Mesenchymal Stem Cells on Bacterial Cellulose Scaffolds

4.4.2.1. Alkaline Phosphatase Activity

ALP activity in hPMSCs on BC scaffolds and TCP was determined on day 1, day 3 and day 14 after induction in osteogenic medium and growth medium as shown in FIGURE 27. ALP activity on BC and TCP increased over a period of two weeks. The ALP activity in the cell/BC construct was significantly higher in differentiated cells as compared to growth medium. The ALP activity between the time points day 1 and day 14 ($p<0.05$) and day 3 and day 14 ($p<0.05$) in the cell/BC construct showed a significant difference. In the differentiated cells on BC and TCP, a significant difference was observed on day 14 with BC showing higher ALP activity as compared to TCP.

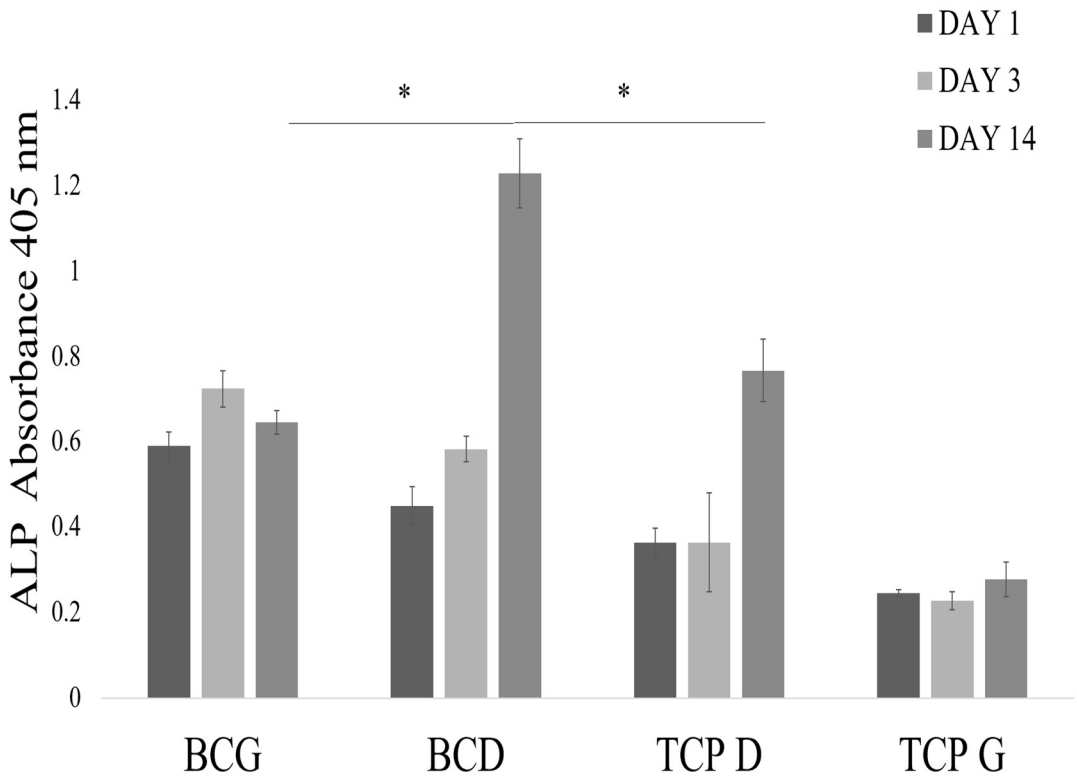

Figure 27. Alkaline Phosphatase Activity of hPMSCs Cultured Bacterial Cellulose (BC) and Tissue Culture Plate (TCP-control) In Growth (control) and Differentiation Media

4.4.2.2. Alizarin Red Assay

To study the deposition of calcium on bacterial cellulose alizarin red staining assay was performed. Never-dried BC in growth media did not show any red stain on Day 14, 21 and 28. Never-dried BC in differentiation media showed an increase in the red coloration with minimum on Day 14 (FIGURE 28D) to bright red on Day 28 (FIGURE 28F) suggesting complete differentiation of hPMSCs on bacterial cellulose.

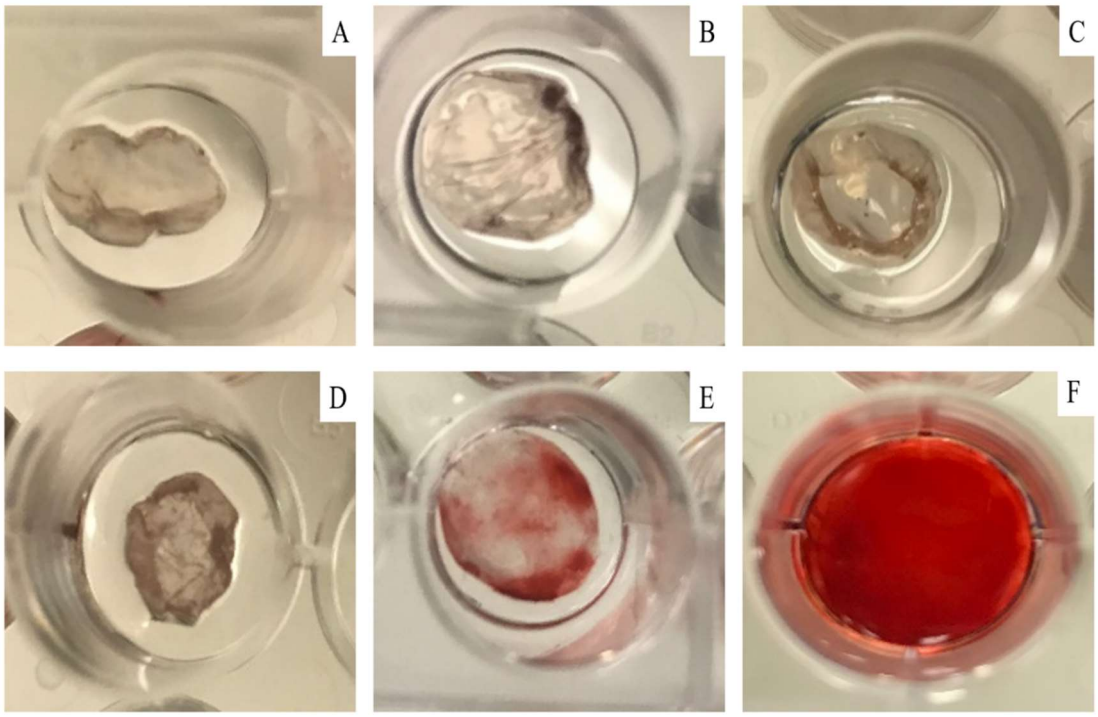

Figure 28. Alizarin Red Staining on hPMSCs Cultured Bacterial Cellulose Scaffold: (A-C): In Growth Media on Day 14, 21 and 28 Respectively; (D-F): In Differentiation Media on Day 14, 21 and 28 Respectively

4.4.2.3. Energy-Dispersive X-ray Spectroscopy

EDS was used to determine the calcium composition on BC scaffolds and TCP in osteogenic and growth medium. Graph shows that amount of calcium increased on both BC and TCP from day 14 through day 28 of the study (FIGURE 29 and 30). EDS of BC scaffolds shows significant difference over a period of 28 days in the amount of calcium as compared to cell/BC construct subjected to growth medium. A similar result is observed on TCP with high content of calcium in osteogenic medium as compared to growth medium. Further, BC scaffolds shows a significant increase in mineralization as compared to TCP (FIGURE 31). The electron microscope image of cell/BC (FIGURE 32 and 33) with and without mineralization with the amount of calcium as seen by EDS (FIGURE 32 and 33) over a period of 28 days confirmed that cells on bacterial cellulose utilized the entire surface to deposit mineralized layers of calcium.

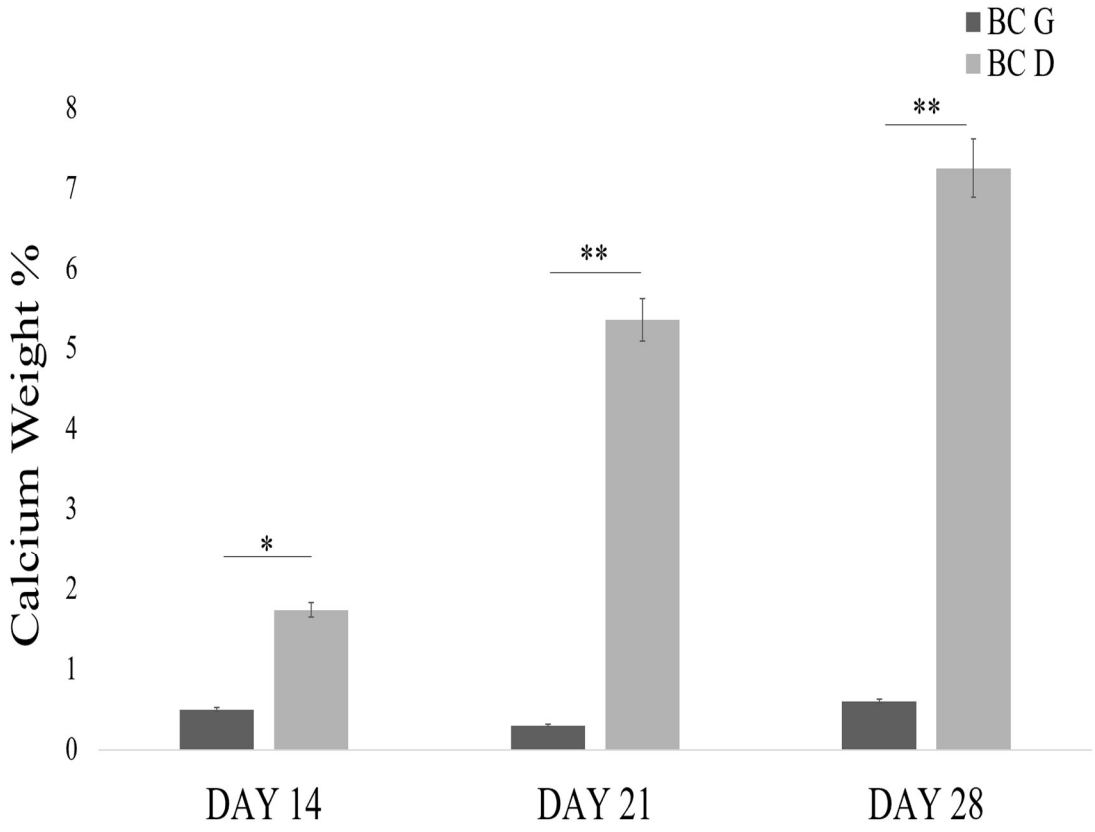

Figure 29. Energy-Dispersive X-ray Spectroscopy of hPMSCs on Bacterial Cellulose Towards Osteogenic Differentiation

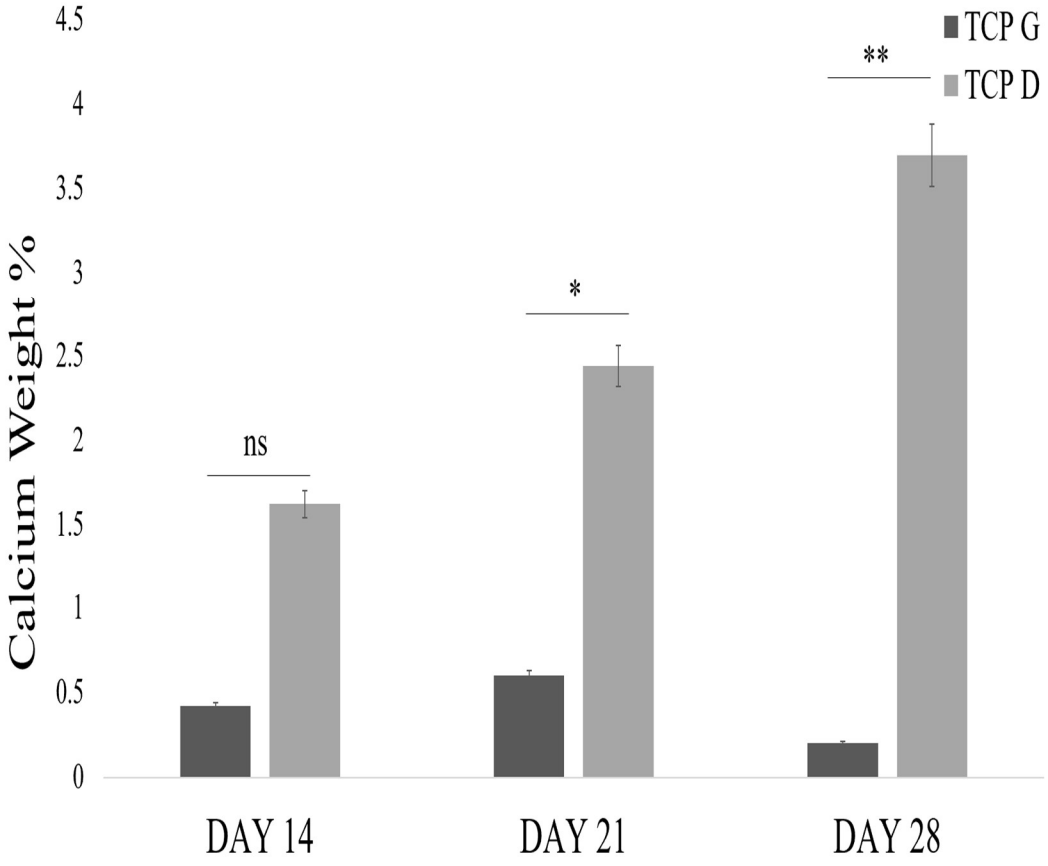

Figure 30. Energy-Dispersive X-ray Spectroscopy of hPMSCs on Tissue Culture Plate (control) Towards Osteogenic Differentiation

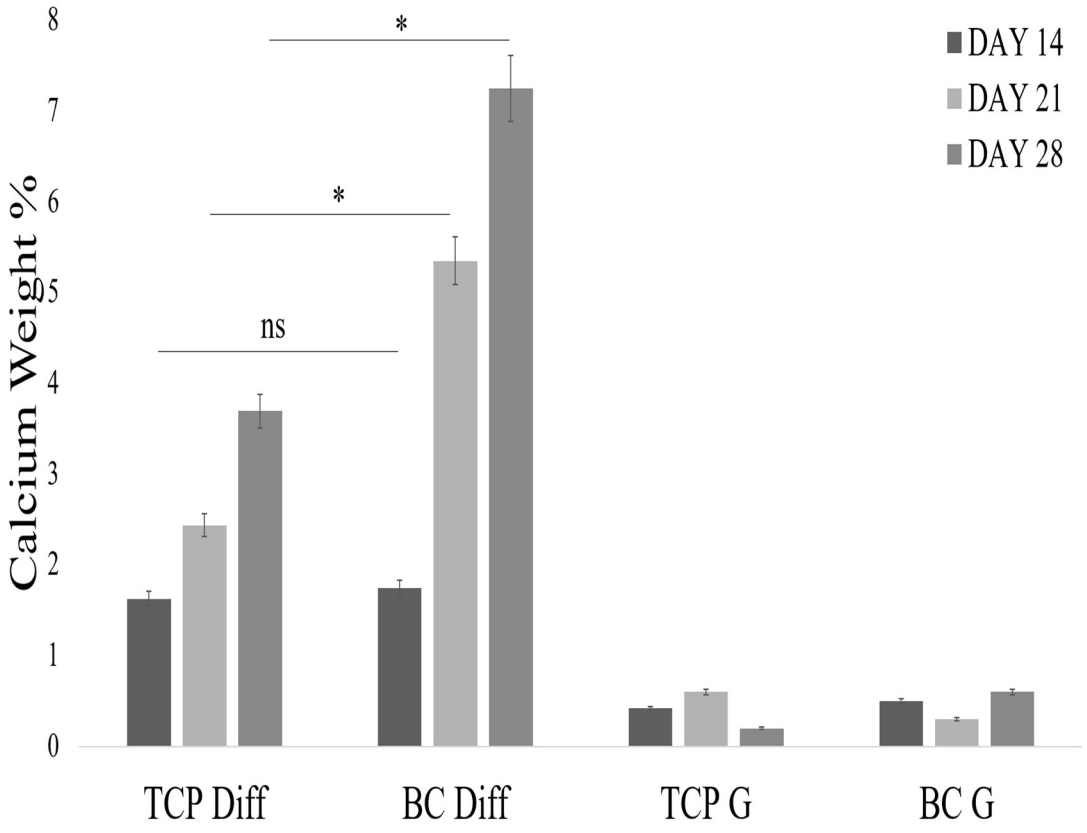

Figure 31. Energy-Dispersive X-ray Spectroscopy of hPMSCs on Bacterial Cellulose and Tissue Culture Plate (control) Towards Osteogenic Differentiation

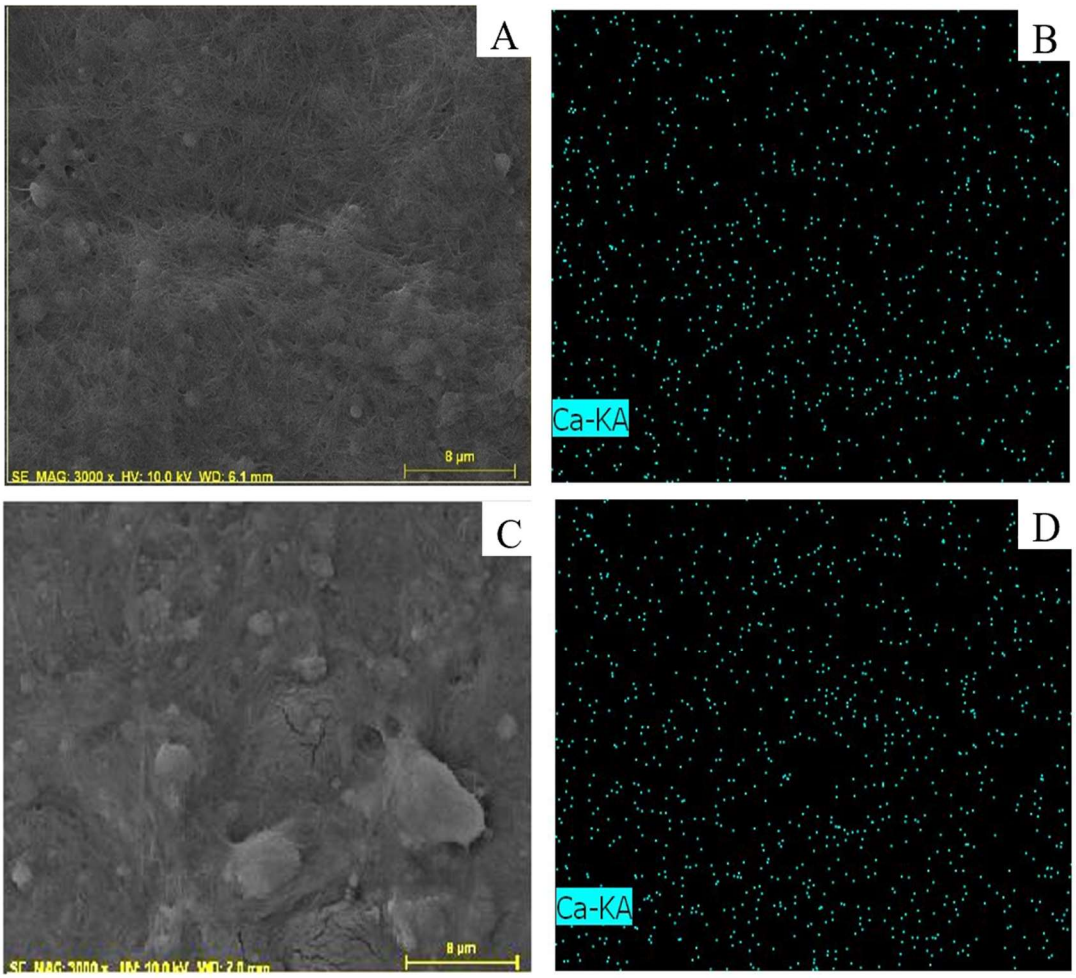

Figure 32. Scanning Electron Microscope Image and Energy-Dispersive X-ray Spectroscopy Showing Elemental Analysis of Calcium; (A-B): Day 14 hPMSCs Cultured on Bacterial Cellulose in Growth Media, (C-D): Day 28 hPMSCs Cultured on Bacterial Cellulose in Growth Media

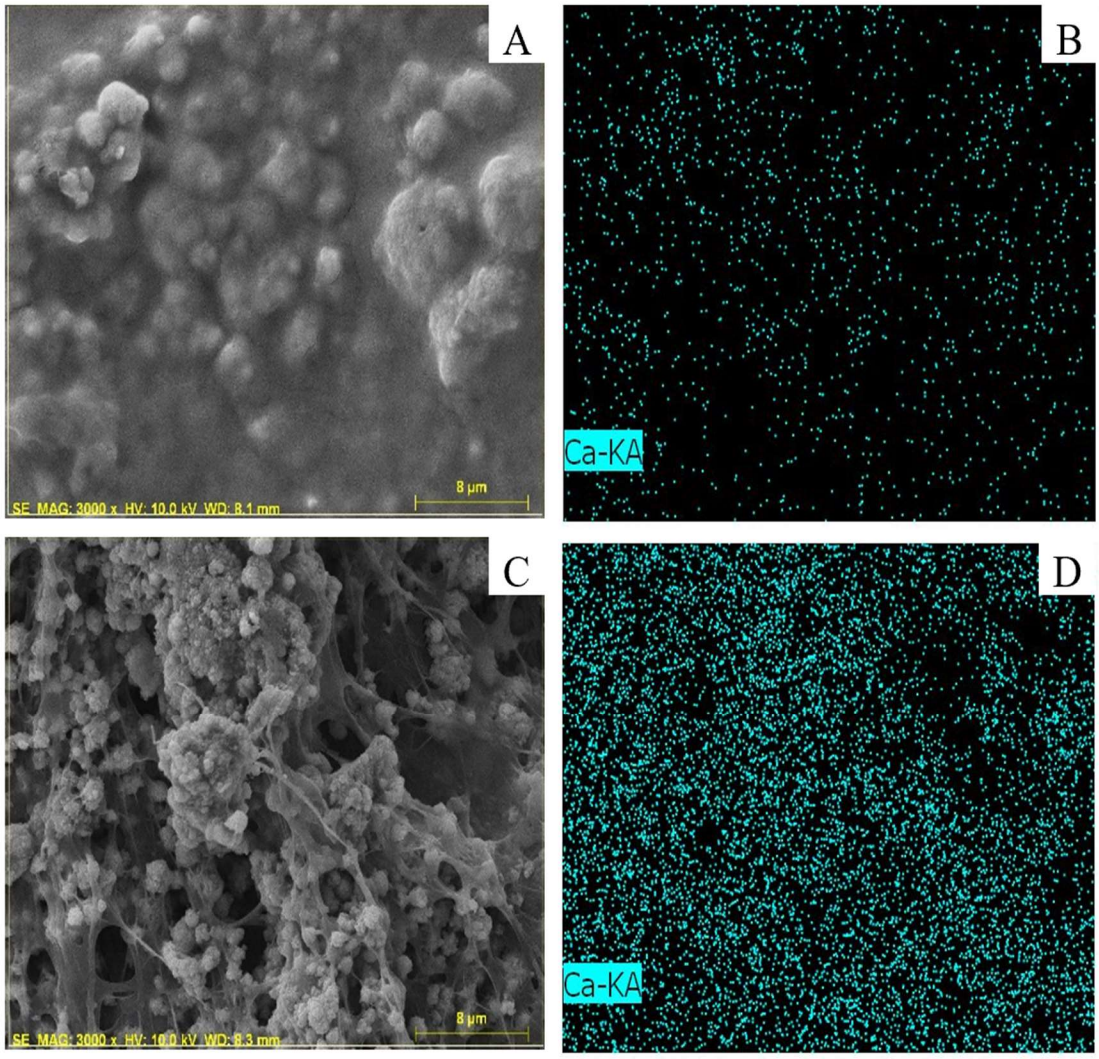

Figure 33. Scanning Electron Microscope Image and Energy-Dispersive X-ray Spectroscopy Showing Elemental Analysis of Calcium; (A-B): Day 14 hPMSCs Cultured on Bacterial Cellulose in Differentiation Media, (C-D): Day 28 hPMSCs Cultured on Bacterial Cellulose in Differentiation Media

4.4.2.4. Total Collagen Content

Total collagen content assay shows no difference between differentiated and non-differentiated group on neat never-dried BC scaffolds as observed in FIGURE 34. This suggests similar amount of collagen was produced in growth and differentiation medium. A significant difference was observed between the differentiated groups at 1- week and 4-week time points ($p<0.05$).

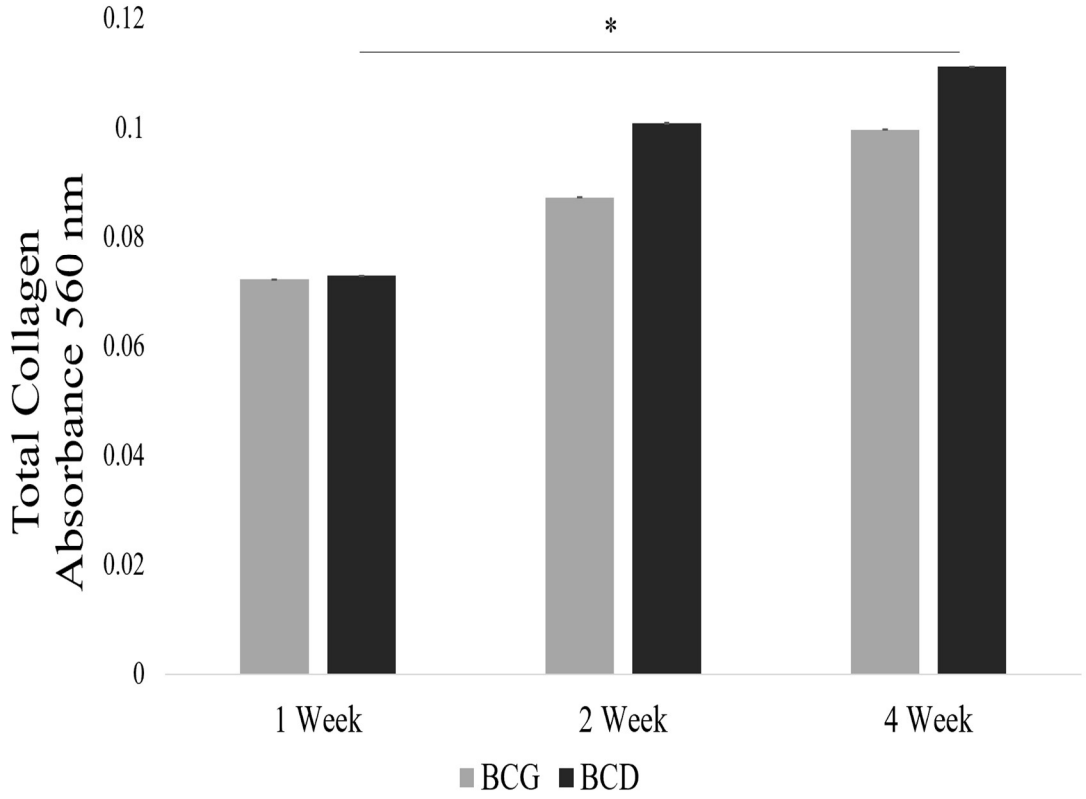

Figure 34. Total Collagen Content of hPMSCs Cultured on Bacterial Cellulose in Growth (control) and Differentiation Media

4.4.2.5. Gene Expression: Osteogenic Differentiation

Expression levels associated with osteogenic differentiation of mRNA levels were examined using PCR at day 14, 21 and 28 (FIGURE 35). Expression of two transcription factors related to osteogenic differentiation, osteocalcin (OCN) and RUNX2, were studied in the cells cultured on neat never-dried BC scaffolds. The expression of early marker RUNX2 was higher on day 14 as compared to day 28, yet there was no significant difference between time points for RUNX2. The high expression of RUNX2 in the early stages of differentiation have also been reported by several studies [198, 199]. The expression of non-collagenous bone ECM proteins OCN showed significant increase in its expression over a period of 28 days ($p<0.05$). This data suggests that the cell-BC construct can function as a tissue substitute for bone regeneration.

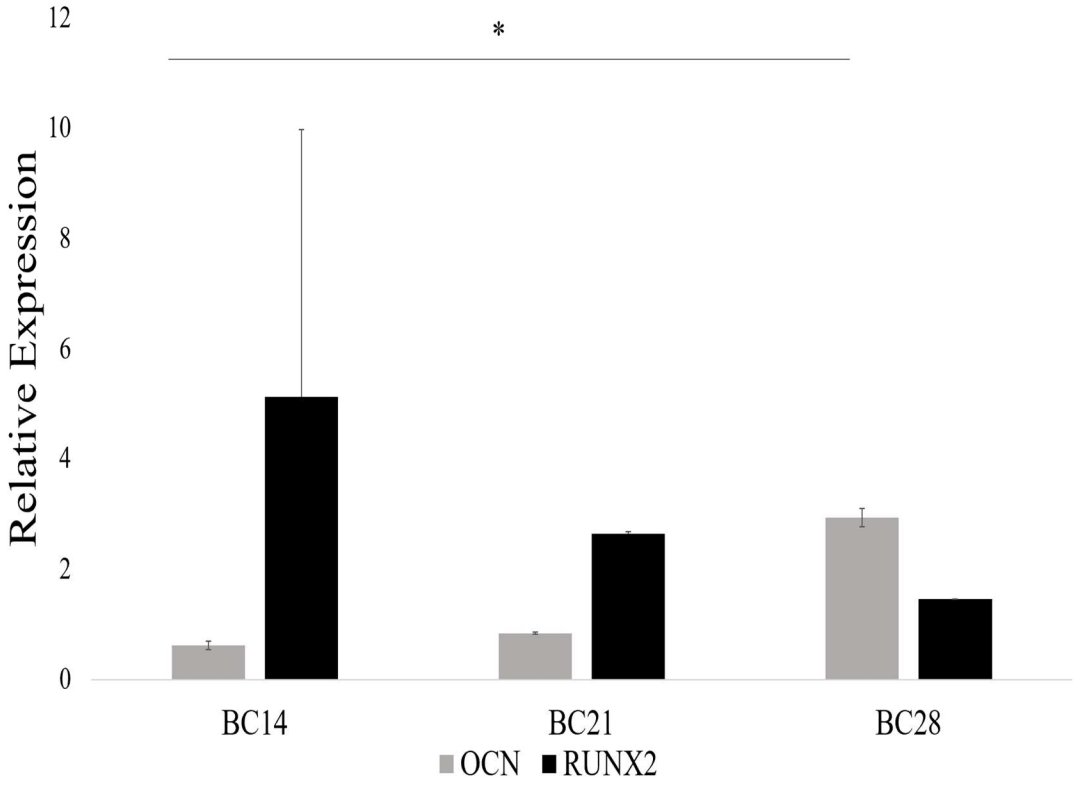

Figure 35. Gene Expression of hPMSCs on Bacterial Cellulose Towards Osteogenic Differentiation on Day 14, 21 and 28

4.5. Conclusion

In this study, we have explored the material properties of bacterial cellulose which enabled its application as a potential scaffold for bone tissue engineering. The free hydroxyl groups which is a characteristic of bacterial cellulose in its never-dried served as a site for the initiation of mineralization as shown by chemical precipitation of calcium chloride and phosphoric acid. The scanning electron microscope image and FTIR spectrum confirmed the presence of crystals formed due to the deposition of hydroxyapatite. The crystals formed as agglomerates while covering the entire surface of the never-dried bacterial cellulose pellicle. One important observation found in the FTIR spectrum was the reduction in the hydroxyl peaks of the hydroxyapatite spectrum as compared to neat never-dried bacterial cellulose. This reduction in hydroxyl peak formed the most important basis of this study as the functional groups in neat never-dried bacterial cellulose (hydroxyl groups -hydrophilic nature and neutral charge [200]) was able to support the mineralization process of hydroxyapatite. This was further applied to the process of bone regeneration by studying the differentiation of human-derived placental mesenchymal stem cells and the extent of *in vitro* mineralization. Alkaline phosphatase acitivity was studied as an early marker for osteogenic differentiation. An increase in the enzyme activity to measure alkaline phosphatase activity was observed over a period of 14 days in differentiation medium as compared to bacterial cellulose in growth medium and tissue culture plate in growth and differentiation medium. The deposition of calcium was analyzed by alizarin red assay which showed an increase in the deposition of calcium over a period of 28 days as seen by the increase in the intensity of

the red color which denotes the presence of calcium. There was no calcium present on hPMSCs-bacterial culture in differentiation medium. To quantify the amount of calcium present on the material, energy-dispersive x-ray spectroscopy was studied. A significant increase in the calcium weight percentage was observed in both hPMSCs-bacterial cellulose and hPMSCs-tissue culture plate culture in differentiation media over a period of 28 days and a significant increase in calcium weight percentage in hPMSCs-bacterial cellulose in differentiation medium on day 21 and 28 as compared to hPMSCs-tissue culture plate in differentiation medium. Further, bacterial cellulose morphological characterization shows random orientation of cellulose fibers which accounts for improved cell proliferation on day 5 as compared to day 1. This is because bacterial cellulose has a twisted fibrous morphology [154] which allows for efficient cell seeding of hPMSCs. Due to its random orientation which improves cellular functions, high osteogenic differentiation is observed as compared to tissue culture plate [194]. A significant difference in the total collagen content is observed over a period of 4 weeks in the differentiation media, although it is unclear how the collagen has deposited on the material based on the orientation of the fibers. Nevertheless, the deposition of collagen and cell differentiation on bacterial cellulose might be due to its fiber orientation as observed in the literature [194].

The pore size of bacterial cellulose as obtained by BET was 8.9094 nm. Since, the pore size of bacterial cellulose is below 100 μm it causes the formation of cell aggregates as observed by adhesion assay and low proliferation with no significant difference in cell viability as observed by alamar blue assay. The material was still able to support the

growth of cells due to its hydrophilicity and fibrous structure that is found in the native extracellular matrix. Further, it was observed that there was no significant difference in the alkaline phosphatase activity for a period of 14 days in differentiation media, but a significant difference between growth and differentiation media for bacterial cellulose scaffolds. Thus, low pore size causes delayed activity of alkaline phosphatase which is an early osteogenic marker. Another observation was obtained from the energy-dispersive x-ray spectroscopy which did show mineralization over a period of 28 days. This is due to the presence of hydroxyl groups (hydrophilic nature and neutral charge [200]) that allows as sites for the improved mineralization during the osteogenic differentiation with a significant difference over a period of 28 days. This further showed an upregulation of osteogenic gene expression. Low pore size is a limitation of bacterial cellulose, but its structural property and morphology benefits the growth of hPMSCs while supporting osteogenic differentiation.

In conclusion, bacterial cellulose is a promising biomaterial with simple fermentation protocol and ease of sterilization as it can with stand high temperatures without causing any change in morphological and structural properties. The chemical composition and physical structure of bacterial cellulose used in this study as a cell-supporting matrix meets the basic requirements of a tissue engineering scaffold like similar structure to native extracellular matrix [191], biocompatibility, high surface area and no toxicity. This is suitable for cell growth as well as differentiation. Further, properties like easy moldability, antimicrobial effect, hydrophilicity and nanoporosity makes bacterial cellulose a multidisciplinary material in the field of tissue engineering.

CHAPTER V

EXPERIMENTAL WORK AND FUTURE DIRECTIONS

5.1. Production of Bacterial Cellulose Foam

The tu´ngara frog of tropical America, *Engystomops pustulosus* (formerly *Physalaemus pustulosus*), release eggs along with foam precursor fluids which results in a foaming nest for their embryos to develop into tadpoles [201]. The foam formation is facilitated by the reduction in surface tension of the air-liquid interface[202]. These tropical and sub-tropical frogs produce their nests that are seen either floating on the surface of water, suspended in vegetation, on tree branches or found in enclosed spaces like underground burrows [201, 203]. These foam nests are composed of dilute solutions of proteins and carbohydrates that are one of the rare surfactants found in nature [203]. The foam nests are anti-bacterial and anti-fungal and can resist dehydration and microbial degradation [201, 203]. With the foam's natural ability to protect in its embryonic stages against harsh environmental conditions, its applications in the medical field can range from wound healing to surgical matrices for tissue engineering [204].

The túngara or mud-puddle frog form these nests that comprises of 90% air with 1-2mg/ml of proteins and complex carbohydrates in the aqueous phase [203]. The biochemical analysis shows that the foam is composed of a mixture of proteins called ranaspumins named from ranaspumins-1 to ranaspumins-6 in the 11-25 kDa size range.

Ranaspumin-3 to ranaspumin-6 are from the lectin family (carbohydrate-recognizing protein), ranaspumin-1 represents the cystatins (inhibits protein-degrading protease Enzymes) and ranaspumin-2 is a protein that is responsible for reducing surface tensions (at 1-10 μg/ml concentration [203]) and producing foams [204].

Ranaspumin-2 has an amino sequence with a highly-charged hydrophilic C-terminus coupled with a significantly non-polar N-terminal sequence that explains the amphiphilic (hydrophilic and hydrophobic) characteristics of common detergents [203]. A study explained that the natural foam showed an air-interface layer which can be applied towards producing bacterial cellulose foam as the synthesis of cellulose also takes place at the air-medium interface during bacterial culture [203, 205]. The advantages of ranaspumin-2 over other surfactants like lipopeptides and surfactin are that it causes no disruptive effect to the biological membranes when incorporated into surfaces and it can actively form foam when used at low concentrations [206]. The only disadvantage known about ranaspumin-2 is that unlike its ability to remain stable in its natural state (natural frog foam) it collapses in few minutes under laboratory conditions [206]. This suggests that the cocktail of proteins present in the natural foam is required for the foam to provide long term mechanical stability and resistance to dehydration [206]. In this work, we aim at producing foam structures of bacterial cellulose using the surfactant properties of ranaspumin-2 for improved morphology and achieving a three-dimensional structure of bacterial cellulose. This will enable us to control the porosity, structural arrangement of the cellulose fibers while improving its pellicle size as the bacterial cellulose fermented using static culture only produces a flat sheet up to a thickness of ~0.2μm.

5.1.1. Experimental Section

5.1.1.1. Plasmid Isolation Protocol:

1. Inoculate 5 ml LB medium with kanamycin culture overnight at 37 degree with shaking.
2. Harvest bacteria by centrifuge at 3000 rpm for 5 minutes, remove supernatant and keep the pellet.
3. Add one vial of RNase A to Solution A1 in the miniprep kit by Apex.
4. Resuspend the pellet in 250 µl Solution A1 by vortexing or pipetting and transfer the mixture to a clean microcentrifuge tube.
5. Add 250 µl Solution A2, mix gently by inverting 7-8 times at room temperature.
6. Add 350 µl Solution A3, mix immediately by inverting tube 7-8 times at room temperature.
7. Spin down at 12000 rpm for 10 min. transfer supernatant to a spin column and discard pellet.
8. Centrifuge spin column at 12000 rpm for 1 min. Discard flow through.
9. Wash spin column with DI water, centrifuge at 12000 rpm for 1 min. discard flow through.
10. Centrifuge at 12000 rpm for an additional 1 min to remove residual wash buffer.
11. Place spin column in a clean 1.5ml microcentrifuge tube. Add 50-100 µl Solution AE to the center of the membrane. Let stand for 2 min. Centrifuge at 12000 rpm for 1 min to collect eluted DNA.

12. Measure absorbance using Nanodrop. 260/280 ratio: less than 1.8 = protein and more than 2 = RNA.

5.1.1.2. Protein Expression in BL21 (DE3) Bacteria:

- Transform the expression rsn-2 plasmid collected in the PLASMID ISOLATION PROTOCOL into BL21 (DE3). Plate on LB-kanamycin selection plates and incubate at 25° C, 30° C and 37°C for 3-4 days and check the formation of colonies.
- Resuspend a single colony from each plate obtained at different temperatures in 10 ml LB culture with kanamycin antibiotic. Freeze the remaining colonies at -80° C for future use.
- Incubate at 37°C with shaking until OD600 reached 0.4-0.8.
- Induce with 4 or 40 µl of a 100 mM stock of IPTG (final concentration of 40 or 400 µM) and induce for 3 to 5 hours at 37°C or 1mM for 4 hours under agitation at 30 °C
- Check for expression under black light to observe a blue-green fluorescence. Compare with a control flask with only media.
- Proceed by spinning down the solution and freezing the cell paste only at -80° C. Before freezing the cell paste, wash the paste with DI water or PBS and centrifuge.

5.1.1.3. Lysis and Sonication of the Bacteria:

- Make lysis buffer 1/20 or 1/50 the volume of the bacterial culture: lysozyme 1mg/ml, (NaH2PO4+NaHPO4) 50nM, NaCl 300mM, Imidazole 10mM and water. Adjust pH to 8 using NaOH.
- Add the volume of lysis buffer to the frozen cell paste post IPTG induction.
- Incubate the suspension at room temperature for 20-30 minutes, or until the suspension becomes turbid and viscous due to the release of the bacteria's genomic DNA.
- Freeze-thaw 6 cycle in liquid nitrogen and water at 37°C to eliminate the extreme turbidity of the sample.
- Pass the solution through a 1ml syringe to help with the process of reducing turbidity. This step helps to shear the DNA.
- Spin the solution for 5 minutes at full speed. Proceed by collecting the supernatant. The protein collected in the supernatant can be frozen till further use.

5.1.1.4. Spin Purification of His-Tagged Proteins:

- After collecting the supernatant from the LYSIS and SONICATION of the BACTERIA steps, prepare a set of buffers needed to protein purification using nickel-charged nitriloacetic acid spin columns.
- Make the equilibration buffer (50mM (NaH2PO4+Na2HPO4), 300mM NaCl, 10mM Imidazole, pH 8 with NaOH), wash buffer (50mM (NaH2PO4+Na2HPO4), 300mM NaCl, 20mM Imidazole, pH 8 with NaOH) and

elution buffer (50mM (NaH2PO4+Na2HPO4), 300mM NaCl, 250mM Imidazole, pH 8 with NaOH).

- SAMPLE PREP: Mix equal volumes of both protein extract (supernatant: Lysis+cell paste) and equilibration buffer.
- First, remove the bottom tab from the spin column and place the column in a centrifuge tube. Centrifuge the column at 700 g for 2 minutes to remove storage buffer.
- Next, add the equilibration buffer to HisPur Ni-NTA spin column and adjust the volume to equal to 2 resin-bed volumes. Shake gently to allow the buffer to enter the resin bed.
- Centrifuge column at 700 g for 2 minutes to remove buffer.
- Place the bottom plug in the column and the prepared sample. Mix this set-up on an orbital shaker or end-over-end mixer for 24 hours at room temperature. Add 10-50µl of 0.1M sodium azide to avoid proteolytic cleavage of proteins.
- Remove the bottom plug and centrifuge the column at 700 g for 2 minutes. Collect the flow-through in a centrifuge tube.
- Wash the column with wash buffer with two resin-bed volumes and centrifuge at 700 g for 2 minutes and collect the flow-through. Repeat this process two more times.
- Elute the protein from the resin by adding on resin-bed volume of Elution buffer and centrifuge at 200 g for 2 minutes. Repeat this step two more times.

- Measure the protein absorbance at 280nm to calculate the yield. The protein can also be analyzed by SDS-PAGE analysis.

5.1.2. Results

Ranaspumin-2 plasmid were plated at different temperatures on LB-kanamycin plates at 25℃, 30℃ and 37℃ (from left to right indicated by yellow arrows) before resuspending the colony on LB-kanamycin media. The figure shows the expression of ranaspumin-2 post IPTG induction. A blue-green fluorescence was observed in the samples as compared to control (LB-kanamycin media-red arrow) as observed in FIGURE 36A. The protein was purified with HisPur Ni-NTA spin column and the foam was generated by blowing air through the purified protein column as seen in FIGURE 36B.

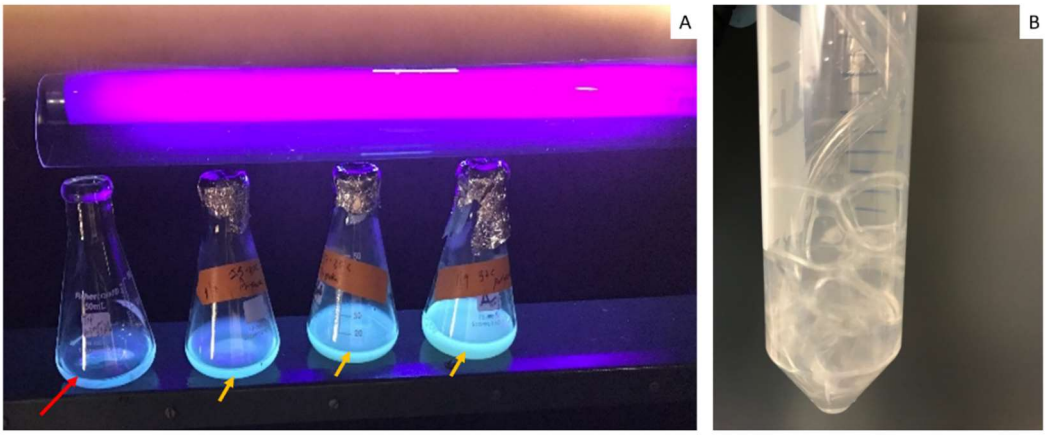

Figure 36. (A): Expression of Ranaspumin-2 After IPTG Induction; (B): Ranaspumin-2 Foam Post Purification from BL21(DE3) Bacteria

5.2. Importance of Hydrophilicity During Osteogenic Differentiation

5.2.1. Experimental Section

The difference in the extent of osteogenic differentiation and to assess the importance of hydrophilicity during the process of mineralization in bone regeneration two modified forms of bacterial cellulose were studied. The air-dried and lyophilized bacterial cellulose have been investigated for its biocompatibility as compared to neat never-dried bacterial cellulose.

5.2.1.1. Simulated Body Fluid Study

To evaluate the difference in bone bioactivity and the extent of osteogenic apatite formation, modified bacterial cellulose and neat never-dried bacterial cellulose were submerged in simulated body fluid. Simulated body fluid is an ionic solution composed of ion concentrations that are found in the human blood plasma. The solution was replaced every day for a period of 7 days. The materials were characterized using scanning electron microscope and energy-dispersive x-ray spectroscopy as explained in chapter 3.

5.2.1.2. Expression of Osteogenic Marker: Alkaline Phosphatase

hPMSCs were cultured on modified bacterial cellulose and neat never-dried bacterial cellulose to study the expression of alkaline phosphatase activity for a period of 14 days in growth and differentiation media as explained in chapter 4.

5.2.2. Results

The extent of mineralized layer on bacterial cellulose simulated body fluid study was performed. A high percentage of mineralized layer was found on neat never-dried bacterial cellulose with a significant increase in the calcium weight percentage as compared to dry bacterial cellulose and lyophilized bacterial cellulose (FIGURE 37 A-C). Further, an increase in alkaline phosphatase activity was observed on neat never-dried bacterial cellulose as compared to dry bacterial cellulose and lyophilized bacterial cellulose (FIGURE 37-top right). With the presence of functional groups in bacterial cellulose in its never-dried state the material offers sites for the formation of an apatite layer as compared to modified bacterial cellulose where there is less availability of hydroxyl groups. Similarly, bacterial cellulose with hydroxyl groups up-regulated the osteogenic expression of early marker alkaline phosphatase as compared to modified groups of bacterial cellulose.

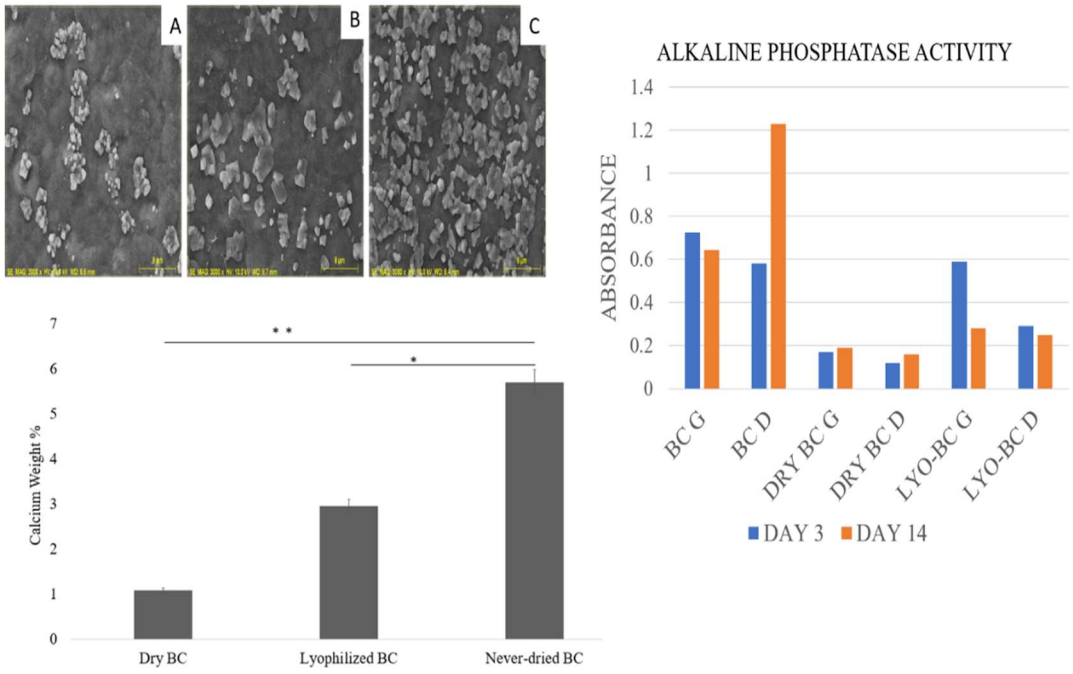

Figure 37. (A-C): Scanning Electron Microscope Image of Simulated Body Fluid Study on Dry BC, Lyophilized BC and Neat Never-Dried BC Respectively, Graph Showing the Calcium Weight Percentage Obtained by Energy-Dispersive X-ray Spectroscopy (bottom left), Graph Showing Alkaline Phosphatase Activity on Modified Bacterial Cellulose and Neat Never-Dried Bacterial Cellulose

5.3. Conclusion

In the biomedical field, bacterial cellulose has been applied to a wide range of applications for ideal structure and biocompatibility. In this work, we have presented unique properties of bacterial cellulose that facilitated its application to study bone tissue engineering.

Nanoscale morphology of bacterial cellulose presented with improved surface area which supported the growth of human-derived placental stem cells. The high surface area and nano pore structure can be applied in future to develop implants and prosthetic devices as it improves protein adsorption while reducing in bacterial infections and implant failure [207]. Further the hypothesis to present cells with nanoscale feature is that cells in its native state itself has many nanostructures like filipodia, cytoskeleton and membrane proteins [208]. Application of nanomaterials can help the cells proliferate in its more natural environment and enable scientists take a step closer to mimic complex human tissues [208].

The hydrophilicity of bacterial cellulose in its never-dried state also serves for many applications in tissue engineering as the presence of three accessible hydroxyl groups per repeat unit favors for modifications (like introducing ionic charge to facilitate cell attachment) and formation of composites [209]. It has been used to treat skin burns because an increase in re-epithelization was found when the wound healing process is supported in a moist environment [210]. We, therefore utilized this property of bacterial cellulose to study its feasibility to form hydroxyapatite crystals as a high concentration of hydroxyl groups promotes the precipitation formation of particles and the chemical

composition of hydroxyapatite are native to the natural bone which is the main objective of this study [211]. With never-dried bacterial cellulose able to form crystals of hydroxyapatite, human-derived placental stem cells (possess multilineage differentiation and is easy to isolate, expand without any ethical issues[212]) were cultured and differentiated towards osteogenic lineage on bacterial cellulose to examine if similar results are obtained. The calcium weight percentage increased over a period of 28 days and the material was found to be completely mineralized by the end of 28 days. The presence of hydroxyl groups served as a template for the cells to express its cellular functions in its most native state while expressing osteogenic markers. Further, low apatite layer was found when air-dried and lyophilized bacterial samples were studied as compared to never-dried bacterial cellulose.

Topographic guidance influences cell shape and cellular functions. The cells will further deposit extracellular matrix based on the material's morphological features. The use of bacteria in this study has a limitation in being able to control the topography as it can only produce cellulose at the air-liquid interface [123] in the form of a flat sheet. Since cells interact with the extracellular matrix, organize the matrix and generate patterns essential for tissue functions it is important to study different methods by which one can control the shape and size of bacterial cellulose that will help recreate tissue-specific geometry. In this study, we have shown a method to control the morphology and topography of bacterial cellulose using the frog surfactant protein- ranaspumin-2. We found that the foam was not stable for longer period as in nature there is a complex of 6 different types of materials that help stabilize the foam [204]. Foam stabilizers and

complex carbohydrates are therefore needed to mimic the native foam to achieve stability of the ranasmpumin-2 foam to allow for bacteria to deposit cellulose along the structure of foam.

In conclusion, bacterial cellulose has a three-dimensional nanoscale structure which presents as a biocompatible material for bone tissue engineering. Its ability to interact with different materials like polymers, metals and ceramics offers future improvements in mechanical properties and surface modifications while supporting the fabrication of bacterial cellulose-based composites for not only the biomedical field but also for its applications in areas like sensors, optics and food industry [123].

REFERENCES

1. Kwon, S.G., Recent advances in stem cell therapeutics and tissue engineering strategies. Biomaterials Research, 2018. **22**(1).

2. Agarwal, R. and A.J. García, Biomaterial strategies for engineering implants for enhanced osseointegration and bone repair. Advanced Drug Delivery Reviews, 2015. **94**: p. 53-62.

3. Roseti, L., et al., Scaffolds for Bone Tissue Engineering: State of the art and new perspectives. Materials Science and Engineering: C, 2017. **78**: p. 1246-1262.

4. Min, P.K., et al., Tissue Engineering and Regenerative Medicine 2017: A Year in Review. Tissue Engineering Part B: Reviews, 2018. **24**(5): p. 327-344.

5. Singh, A., et al., Stem cell niche: Dynamic neighbor of stem cells. European Journal of Cell Biology, 2018.

6. Mahla, R.S., Stem Cells Applications in Regenerative Medicine and Disease Therapeutics. International journal of cell biology, 2016. **2016**: p. 6940283-6940283.

7. Andreea Grosu-Bularda, E.-L.S. and A. Chiotoroiu, Future directions in tissue repair using biomaterials. industria textila, 2018. **69**.

8. Li, Y., et al., Senescence of mesenchymal stem cells (Review). Int J Mol Med, 2017. **39**(4): p. 775-782.

9. Pountos, I., Mesenchymal Stem Cells. 2016.

10. Sumer, H., J. Liu, and S. Roh, Mesenchymal Stem Cells and Regenerative Medicine. Stem Cells Int, 2018. **2018**: p. 9810972.

11. Song, L. and R.S. Tuan, Transdifferentiation potential of human mesenchymal stem cells derived from bone marrow. The FASEB Journal, 2004. **18**(9): p. 980-982.

12. Maged, A., et al., Mesenchymal stem cells associated with chitosan scaffolds loaded with rosuvastatin to improve wound healing. European Journal of Pharmaceutical Sciences, 2019. **127**: p. 185-198.

13. Lei, Z., et al., Bone marrow-derived mesenchymal stem cells laden novel thermo-sensitive hydrogel for the management of severe skin wound healing. Materials Science and Engineering: C, 2018. **90**: p. 159-167.

14. Li, F., et al., Cartilage tissue formation through assembly of microgels containing mesenchymal stem cells. Acta Biomaterialia, 2018. **77**: p. 48-62.

15. Pan, M., et al., Tissue engineering with peripheral blood-derived mesenchymal stem cells promotes the regeneration of injured peripheral nerves. Experimental Neurology, 2017. **292**: p. 92-101.

16. Zhang, T., et al., Photo-crosslinkable, bone marrow-derived mesenchymal stem cells-encapsulating hydrogel based on collagen for osteogenic differentiation. Colloids and Surfaces B: Biointerfaces, 2019. **174**: p. 528-535.

17. Keane, T.J. and S.F. Badylak, Biomaterials for tissue engineering applications. Seminars in Pediatric Surgery, 2014. **23**(3): p. 112-118.

18. Steffens, D., et al., Update on the main use of biomaterials and techniques associated with tissue engineering. Drug Discovery Today, 2018. **23**(8): p. 1474-1488.

19. Chen, F.-M. and X. Liu, Advancing biomaterials of human origin for tissue engineering. Progress in Polymer Science, 2016. **53**: p. 86-168.

20. Preethi Soundarya, S., et al., Bone tissue engineering: Scaffold preparation using chitosan and other biomaterials with different design and fabrication techniques. International Journal of Biological Macromolecules, 2018. **119**: p. 1228-1239.

21. Gabriel, L.P., et al., Bio-based polyurethane for tissue engineering applications: How hydroxyapatite nanoparticles influence the structure, thermal and biological behavior of polyurethane composites. Nanomedicine: Nanotechnology, Biology and Medicine, 2017. **13**(1): p. 201-208.

22. Farokhi, M., et al., Silk fibroin/hydroxyapatite composites for bone tissue engineering. Biotechnology Advances, 2018. **36**(1): p. 68-91.

23. He, X., et al., Incorporation of microfibrillated cellulose into collagen-hydroxyapatite scaffold for bone tissue engineering. International Journal of Biological Macromolecules, 2018. **115**: p. 385-392.

24. Lee, D.H., et al., Enhanced osteogenesis of β-tricalcium phosphate reinforced silk fibroin scaffold for bone tissue biofabrication. International Journal of Biological Macromolecules, 2017. **95**: p. 14-23.

25. Park, J., et al., Fabrication and characterization of 3D-printed bone-like β-tricalcium phosphate/polycaprolactone scaffolds for dental tissue engineering. Journal of Industrial and Engineering Chemistry, 2017. **46**: p. 175-181.

26. Ma, D., Y. Wang, and W. Dai, Silk fibroin-based biomaterials for musculoskeletal tissue engineering. Materials Science and Engineering: C, 2018. **89**: p. 456-469.

27. Diban, N., et al., Hollow fibers of poly(lactide-co-glycolide) and poly(ε-caprolactone) blends for vascular tissue engineering applications. Acta Biomaterialia, 2013. **9**(5): p. 6450-6458.

28. Haaparanta, A.-M., et al., Improved dimensional stability with bioactive glass fibre skeleton in poly(lactide-co-glycolide) porous scaffolds for tissue engineering. Materials Science and Engineering: C, 2015. **56**: p. 457-466.

29. Zhu, Y., et al., An injectable hydroxyapatite/poly(lactide-co-glycolide) composite reinforced by micro/nano-hybrid poly(glycolide) fibers for bone repair. Materials Science and Engineering: C, 2017. **80**: p. 326-334.

30. Rabionet, M., et al., 3D-printed Tubular Scaffolds for Vascular Tissue Engineering. Procedia CIRP, 2018. **68**: p. 352-357.

31. Sharifi, F., et al., Polycaprolactone/carboxymethyl chitosan nanofibrous scaffolds for bone tissue engineering application. International Journal of Biological Macromolecules, 2018. **115**: p. 243-248.

32. Gomes, S., et al., Evaluation of nanofibrous scaffolds obtained from blends of chitosan, gelatin and polycaprolactone for skin tissue engineering. International Journal of Biological Macromolecules, 2017. **102**: p. 1174-1185.

33. Melke, J., et al., Silk fibroin as biomaterial for bone tissue engineering. Acta Biomaterialia, 2016. **31**: p. 1-16.

34. Bhattacharjee, P., et al., Silk scaffolds in bone tissue engineering: An overview. Acta Biomaterialia, 2017. **63**: p. 1-17.

35. Singh, B.N. and K. Pramanik, Fabrication and evaluation of non-mulberry silk fibroin fiber reinforced chitosan based porous composite scaffold for cartilage tissue engineering. Tissue and Cell, 2018. **55**: p. 83-90.

36. Nune, M., et al., Melanin incorporated electroactive and antioxidant silk fibroin nanofibrous scaffolds for nerve tissue engineering. Materials Science and Engineering: C, 2019. **94**: p. 17-25.

37. Bombaldi de Souza, R.F., et al., Mechanically-enhanced polysaccharide-based scaffolds for tissue engineering of soft tissues. Materials Science and Engineering: C, 2019. **94**: p. 364-375.

38. Montalbano, G., et al., Synthesis of bioinspired collagen/alginate/fibrin based hydrogels for soft tissue engineering. Materials Science and Engineering: C, 2018. **91**: p. 236-246.

39. Goodarzi, H., et al., Preparation and in vitro characterization of cross-linked collagen–gelatin hydrogel using EDC/NHS for corneal tissue engineering applications. International Journal of Biological Macromolecules, 2019. **126**: p. 620-632.

40. Yang, X., et al., Collagen-alginate as bioink for three-dimensional (3D) cell printing based cartilage tissue engineering. Materials Science and Engineering: C, 2018. **83**: p. 195-201.

41. Zhou, J., et al., Dual layer collagen-GAG conduit that mimic vascular scaffold and promote blood vessel cells adhesion, proliferation and elongation. Materials Science and Engineering: C, 2018. **92**: p. 447-452.

42. Contessi Negrini, N., et al., Tissue-mimicking gelatin scaffolds by alginate sacrificial templates for adipose tissue engineering. Acta Biomaterialia, 2019.

43. S, G., et al., Development of 3D scaffolds using nanochitosan/silk-fibroin/hyaluronic acid biomaterials for tissue engineering applications. International Journal of Biological Macromolecules, 2018. **120**: p. 876-885.

44. Walimbe, T., A. Panitch, and P.M. Sivasankar, A Review of Hyaluronic Acid and Hyaluronic Acid-based Hydrogels for Vocal Fold Tissue Engineering. Journal of Voice, 2017. **31**(4): p. 416-423.

45. Chen, F., et al., Self-crosslinking and injectable hyaluronic acid/RGD-functionalized pectin hydrogel for cartilage tissue engineering. Carbohydrate Polymers, 2017. **166**: p. 31-44.

46. Fan, M., et al., Biodegradable hyaluronic acid hydrogels to control release of dexamethasone through aqueous Diels–Alder chemistry for adipose tissue engineering. Materials Science and Engineering: C, 2015. **56**: p. 311-317.

47. Torgbo, S. and P. Sukyai, Bacterial cellulose-based scaffold materials for bone tissue engineering. Applied Materials Today, 2018. **11**: p. 34-49.

48. Zulkifli, F.H., et al., Highly porous of hydroxyethyl cellulose biocomposite scaffolds for tissue engineering. International Journal of Biological Macromolecules, 2019. **122**: p. 562-571.

49. Tchobanian, A., H. Van Oosterwyck, and P. Fardim, Polysaccharides for tissue engineering: Current landscape and future prospects. Carbohydrate Polymers, 2019. **205**: p. 601-625.

50. Keskin, Z., A. Sendemir Urkmez, and E.E. Hames, Novel keratin modified bacterial cellulose nanocomposite production and characterization for skin tissue engineering. Materials Science and Engineering: C, 2017. **75**: p. 1144-1153.

51. Joy, J., et al., Gelatin — Oxidized carboxymethyl cellulose blend based tubular electrospun scaffold for vascular tissue engineering. International Journal of Biological Macromolecules, 2018. **107**: p. 1922-1935.

52. Lee, J.W., et al., Cellulose/poly-(m-phenylene isophthalamide) porous film as a tissue-engineered skin bioconstruct. Results in Physics, 2018. **9**: p. 113-120.

53. Pooyan, P., R. Tannenbaum, and H. Garmestani, Mechanical behavior of a cellulose-reinforced scaffold in vascular tissue engineering. Journal of the Mechanical Behavior of Biomedical Materials, 2012. **7**: p. 50-59.

54. Iozzo, R.V. and M.A. Gubbiotti, Extracellular matrix: The driving force of mammalian diseases. Matrix Biology, 2018. **71-72**: p. 1-9.

55. Patil, K.B. The Structure, Components, and Function of Extracellular Matrix. 2017; Available from: https://biologywise.com/extracellular-matrix-structure-components-function.

56. Bedian, L., et al., Bio-based materials with novel characteristics for tissue engineering applications – A review. International Journal of Biological Macromolecules, 2017. **98**: p. 837-846.

57. Wade, R.J. and J.A. Burdick, Engineering ECM signals into biomaterials. Materials Today, 2012. **15**(10): p. 454-459.

58. The Tissue Level of Organization, in Anatomy and Physiology

59. Organ Donation Statistics Available from: https://www.organdonor.gov/statistics-stories/statistics.html.

60. Nie, J., et al., Construction of ordered structure in polysaccharide hydrogel: A review. Carbohydrate Polymers, 2019. **205**: p. 225-235.

61. Pawar HA, K.S., Choudhary PD, An Overview of Natural Polysaccharides as Biological Macromolecules: Their Chemical Modifications and Pharmaceutical Applications. Biol Med, 2015. **7**(224).

62. Razak, I.F.W.a.S.I.A., Polysaccharides as Composite Biomaterials. Composites from Renewable and Sustainable Materials, 2016.

63. Ferreira, A.R.V., V.D. Alves, and I.M. Coelhoso, Polysaccharide-Based Membranes in Food Packaging Applications. Membranes, 2016. **6**(2): p. 22.

64. Prestegard JH, L.J., Widmalm G., Oligosaccharides and Polysaccharides, in Essentials of Glycobiology C.R. Varki A, Esko JD, Editor. 2017, Cold Spring Harbor Laboratory Press: Cold Spring Harbor (NY).

65. Polysaccharides, in Biologydictionary.net Editors, L. Li, Editor.

66. Khan, F. and M. Tanaka, Designing Smart Biomaterials for Tissue Engineering. International journal of molecular sciences, 2017. **19**(1): p. 17.

67. Oldenkamp, H.F., J.E. Vela Ramirez, and N.A. Peppas, Re-evaluating the importance of carbohydrates as regenerative biomaterials. Regenerative Biomaterials, 2018: p. rby023-rby023.

68. Hamed, I., Industrial applications of crustacean by-products (chitin, chitosan, and chitooligosaccharides): A review. Trends in food science & technology, 2016. **v. 48**: p. pp. 11-50-2016 v.48.

69. Younes, I. and M. Rinaudo, Chitin and chitosan preparation from marine sources. Structure, properties and applications. Marine drugs, 2015. **13**(3): p. 1133-1174.

70. Je, J.-Y. and S.-K. Kim, Antimicrobial action of novel chitin derivative. Biochimica et Biophysica Acta (BBA) - General Subjects, 2006. **1760**(1): p. 104-109.

71. Varun, T.K., et al., Extraction of chitosan and its oligomers from shrimp shell waste, their characterization and antimicrobial effect. Veterinary world, 2017. **10**(2): p. 170-175.

72. Piątkowski, M., et al., Microwave-assisted synthesis and characterization of chitosan aerogels doped with Au-NPs for skin regeneration. Polymer Testing, 2019. **73**: p. 366-376.

73. Marpu, S., Photochemical formation of chitosan-stabilized near-infrared-absorbing silver Nanoworms: A "Green" synthetic strategy and activity on Gram-negative pathogenic bacteria. Journal of Colloid and Interface Science, 2017. **507**: p. 437-452.

74. Chen, B., Fiber-continuous panel–pillar structure in insect cuticle and biomimetic research Materials and Design, 2015. **86**: p. 686-691.

75. Chandran, R., et al., SEM characterization of anatomical variation in chitin organization in insect and arthropod cuticles. Micron, 2016. **82**: p. 74-85.

76. Adeli, H., M.T. Khorasani, and M. Parvazinia, Wound dressing based on electrospun PVA/chitosan/starch nanofibrous mats: Fabrication, antibacterial and cytocompatibility evaluation and in vitro healing assay. International Journal of Biological Macromolecules, 2019. **122**: p. 238-254.

77. Saravani, S., M. Ebrahimian-Hosseinabadi, and D. Mohebbi-Kalhori, Polyglycerol sebacate/chitosan/gelatin nano-composite scaffolds for engineering neural construct. Materials Chemistry and Physics, 2019. **222**: p. 147-151.

78. Sadeghi, A., F. Moztarzadeh, and J. Aghazadeh Mohandesi, Investigating the effect of chitosan on hydrophilicity and bioactivity of conductive electrospun composite scaffold for neural tissue engineering. International Journal of Biological Macromolecules, 2019. **121**: p. 625-632.

79. Lannutti, J., et al., Electrospinning for tissue engineering scaffolds. Materials Science and Engineering: C, 2007. **27**(3): p. 504-509.

80. Kyzas, G.Z. and D.N. Bikiaris, Recent modifications of chitosan for adsorption applications: a critical and systematic review. Marine drugs, 2015. **13**(1): p. 312-337.

81. Jahan, K., M. Mekhail, and M. Tabrizian, One-step fabrication of apatite-chitosan scaffold as a potential injectable construct for bone tissue engineering. Carbohydrate Polymers, 2019. **203**: p. 60-70.

82. Zia, I., et al., Trigonella foenum graecum seed polysaccharide coupled nano hydroxyapatite-chitosan: A ternary nanocomposite for bone tissue engineering. International Journal of Biological Macromolecules, 2019. **124**: p. 88-101.

83. Venkatesan, J. and S.K. Kim, Chitosan composites for bone tissue engineering--an overview. Mar Drugs, 2010. **8**(8): p. 2252-66.

84. Upadhyay, R.K., Use of Polysaccharide Hydrogels in Drug Delivery and Tissue Engineering. Advances in Tissue Engineering & Regenerative Medicine: Open Access, 2017. **2**(2).

85. Sachin S. Kulkarni, S.D.P.a.D.G.C., Extraction, purification and characterization of hyaluronic acid from Rooster comb. Journal of Applied and Natural Science, 2018. **10**(1): p. 313-315.

86. Kutlusoy, T., et al., Chitosan-co-Hyaluronic acid porous cryogels and their application in tissue engineering. International Journal of Biological Macromolecules, 2017. **103**: p. 366-378.

87. Hemshekhar, M., et al., Emerging roles of hyaluronic acid bioscaffolds in tissue engineering and regenerative medicine. International Journal of Biological Macromolecules, 2016. **86**: p. 917-928.

88. Collins, M.N. and C. Birkinshaw, Hyaluronic acid based scaffolds for tissue engineering—A review. Carbohydrate Polymers, 2013. **92**(2): p. 1262-1279.

89. Kenar, H., et al., Microfibrous scaffolds from poly(l-lactide-co-ε-caprolactone) blended with xeno-free collagen/hyaluronic acid for improvement of vascularization in tissue engineering applications. Materials Science and Engineering: C, 2019. **97**: p. 31-44.

90. Jooybar, E., et al., An injectable platelet lysate-hyaluronic acid hydrogel supports cellular activities and induces chondrogenesis of encapsulated mesenchymal stem cells. Acta Biomaterialia, 2019. **83**: p. 233-244.

91. Chanda, A., et al., Electrospun chitosan/polycaprolactone-hyaluronic acid bilayered scaffold for potential wound healing applications. International Journal of Biological Macromolecules, 2018. **116**: p. 774-785.

92. Moradi, S.L., et al., Bone tissue engineering: Adult stem cells in combination with electrospun nanofibrous scaffolds. Journal of Cellular Physiology, 2018. **233**(10): p. 6509-6522.

93. Melrose, J., et al., The cartilage extracellular matrix as a transient developmental scaffold for growth plate maturation. Matrix Biology, 2016. **52-54**: p. 363-383.

94. Hu, Y., et al., Biomimetic mineralized hierarchical hybrid scaffolds based on in situ synthesis of nano-hydroxyapatite/chitosan/chondroitin sulfate/hyaluronic acid for bone tissue engineering. Colloids and Surfaces B: Biointerfaces, 2017. **157**: p. 93-100.

95. Rajan Unnithan, A., et al., A unique scaffold for bone tissue engineering: An osteogenic combination of graphene oxide–hyaluronic acid–chitosan with simvastatin. Journal of Industrial and Engineering Chemistry, 2017. **46**: p. 182-191.

96. Chang, Y.-L., et al., Bone Healing Improvements Using Hyaluronic Acid and Hydroxyapatite/Beta-Tricalcium Phosphate in Combination: An Animal Study. BioMed Research International, 2016. **2016**: p. 8.

97. Zhu, Z., et al., Hyaluronic acid: a versatile biomaterial in tissue engineering. Plastic and Aesthetic Research, 2017. **4**(12).

98. Chen, Y.W., et al., Production of new cellulose nanomaterial from red algae marine biomass Gelidium elegans. Carbohydrate Polymers, 2016. **151**: p. 1210-1219.

99. Lavanya, D., et al., Sources of cellulose and their applications- A review. Vol. 2. 2011. 19-38.

100. He, X., et al., Tissue engineering scaffolds electrospun from cotton cellulose. Carbohydrate Polymers, 2015. **115**: p. 485-493.

101. Atila, D., D. Keskin, and A. Tezcaner, Cellulose acetate based 3-dimensional electrospun scaffolds for skin tissue engineering applications. Carbohydrate Polymers, 2015. **133**: p. 251-261.

102. Boyer, C., et al., Laponite nanoparticle-associated silated hydroxypropylmethyl cellulose as an injectable reinforced interpenetrating network hydrogel for cartilage tissue engineering. Acta Biomaterialia, 2018. **65**: p. 112-122.

103. Kuzmenko, V., et al., Tailor-made conductive inks from cellulose nanofibrils for 3D printing of neural guidelines. Carbohydrate Polymers, 2018. **189**: p. 22-30.

104. Huang, Y., et al., Recent advances in bacterial cellulose. Vol. 21. 2014.

105. Sajjad, W., et al., Development of modified montmorillonite-bacterial cellulose nanocomposites as a novel substitute for burn skin and tissue regeneration. Carbohydrate Polymers, 2019. **206**: p. 548-556.

106. Wang, B., et al., Use of heparinized bacterial cellulose based scaffold for improving angiogenesis in tissue regeneration. Carbohydrate Polymers, 2018. **181**: p. 948-956.

107. Cacicedo, M.L., et al., Progress in bacterial cellulose matrices for biotechnological applications. Bioresour Technol, 2016. **213**: p. 172-180.

108. Ullah, H., et al., Advances in biomedical and pharmaceutical applications of functional bacterial cellulose-based nanocomposites. Carbohydr Polym, 2016. **150**: p. 330-52.

109. de Oliveira Barud, H.G., et al., A multipurpose natural and renewable polymer in medical applications: Bacterial cellulose. Carbohydr Polym, 2016. **153**: p. 406-420.

110. Courtenay, J.C., R.I. Sharma, and J.L. Scott, Recent Advances in Modified Cellulose for Tissue Culture Applications. Molecules, 2018. **23**(3): p. 654.

111. Chahal, S., Fabrication,characterizationandinvitrobiocompatibilityof electrospunhydroxyethylcellulose/poly(vinyl)alcoholnanofibrous compositebiomaterialforbonetissueengineering. Chemical Engineering Science, 2016. **144**: p. 17-29.

112. Saber-Samandari, S., et al., In vitro evaluation for apatite-forming ability of cellulose-based nanocomposite scaffolds for bone tissue engineering. International Journal of Biological Macromolecules, 2016. **86**: p. 434-442.

113. Favi, P.M., et al., Cell proliferation, viability, and in vitro differentiation of equine mesenchymal stem cells seeded on bacterial cellulose hydrogel scaffolds. Mater Sci Eng C Mater Biol Appl, 2013. **33**(4): p. 1935-44.

114. Shi, Q., et al., The osteogenesis of bacterial cellulose scaffold loaded with bone morphogenetic protein-2. Biomaterials, 2012. **33**(28): p. 6644-9.

115. Ruka, D.R., G.P. Simon, and K.M. Dean, Altering the growth conditions of Gluconacetobacter xylinus to maximize the yield of bacterial cellulose. Carbohydrate Polymers, 2012. **89**(2): p. 613-622.

116. IGUCHI, M., Bacterial Cellulose-a masterpiece of nature's arts.pdf. Journal of Materials Science, 2000. **35**: p. 261-270.

117. Picheth, G.F., et al., Bacterial cellulose in biomedical applications: A review. Int J Biol Macromol, 2017. **104**(Pt A): p. 97-106.

118. Esa, F., S.M. Tasirin, and N.A. Rahman, Overview of Bacterial Cellulose Production and Application. Agriculture and Agricultural Science Procedia, 2014. **2**: p. 113-119.

119. Chawla, P., et al., Microbial Cellulose: Fermentative Production and Applications. Vol. 47. 2009. 107-124.

120. Augimeri, R.V., A.J. Varley, and J.L. Strap, Establishing a Role for Bacterial Cellulose in Environmental Interactions: Lessons Learned from Diverse Biofilm-Producing Proteobacteria. Frontiers in Microbiology, 2015. **6**.

121. Ul-Islam, M., et al., Synthesis, Chemistry, and Medical Application of Bacterial Cellulose Nanocomposites, in Eco-friendly Polymer Nanocomposites. 2015. p. 399-437.

122. Rainer Jonas, L.F.F., Production and application of microbial cellulose. Polymer Degradation and Stability, 1998. **59**: p. 101-106.

123. Torres, F.G., J.J. Arroyo, and O.P. Troncoso, Bacterial cellulose nanocomposites: An all-nano type of material. Materials Science and Engineering: C, 2019.

124. Faranak Mohammadkazemi, M.A., Alireza Ashori, Production of bacterial cellulose using different carbon sources and culture media. Carbohydrate Polymers, 2015. **117**: p. 518-523.

125. Mohammadkazemi, F., M. Azin, and A. Ashori, Production of bacterial cellulose using different carbon sources and culture media. Carbohydrate Polymers, 2015. **117**: p. 518-523.

126. Evans, S.A.H.R.V.L.H.M.O.N.B.R., Statistical analysis of optimal culture conditions for Gluconacetobacter hansenii cellulose production 2007. **44**(2): p. 175-180.

127. Rajwade, J.M., K.M. Paknikar, and J.V. Kumbhar, Applications of bacterial cellulose and its composites in biomedicine. Appl Microbiol Biotechnol, 2015. **99**(6): p. 2491-511.

128. Keshk, S.M.A.S., Bacterial Cellulose Production and its Industrial Applications. Journal of Bioprocessing & Biotechniques, 2014. **04**(02).

129. Portela da Gama, F.M. and F. Dourado, Bacterial NanoCellulose: what future? Bioimpacts, 2018. **8**(1): p. 1-3.

130. Fiedler, S., Fiissel, M. and Sattler, K., Zentrulbl. , Micro- biol., 1989. **144**: p. 473.

131. Husemann, E.a.W., R., Makromol. , Chem., 1963. **59**: p. 43.

132. Purz, H.J.a.S., H. H., Faserforschung und Textiltechnik, 1976. **27**: p. 261.

133. Santos, S.M., et al., Characterization of purified bacterial cellulose focused on its use on paper restoration. Carbohydr Polym, 2015. **116**: p. 173-81.

134. Lin, S.-P., et al., Biosynthesis, production and applications of bacterial cellulose. Cellulose, 2013. **20**(5): p. 2191-2219.

135. Siddaramaiah, J.G.n., High performance edible nanocomposite films containing bacterial cellulose nanocrystals. Carbohydrate Polymers, 2012. **87**(3): p. 2031-2037.

136. Chen, S., et al., Kinetic and thermodynamic studies of adsorption of Cu2+ and Pb2+ onto amidoximated bacterial cellulose. Polymer Bulletin, 2009. **63**(2): p. 283-297.

137. Cacicedo, M.L., et al., Bacterial cellulose hydrogel loaded with lipid nanoparticles for localized cancer treatment. Colloids and Surfaces B: Biointerfaces, 2018. **170**: p. 596-608.

138. Badshah, M., et al., Surface modification and evaluation of bacterial cellulose for drug delivery. International Journal of Biological Macromolecules, 2018. **113**: p. 526-533.

139. Li, X., et al., Performance improvements of the BNC tubes from unique double-silicone-tube bioreactors by introducing chitosan and heparin for application as small-diameter artificial blood vessels. Carbohydrate Polymers, 2017. **178**: p. 394-405.

140. Jiji, S., et al., Thymol enriched bacterial cellulose hydrogel as effective material for third degree burn wound repair. International Journal of Biological Macromolecules, 2019. **122**: p. 452-460.

141. Jin, M., Patterned bacterial cellulose wound dressing for hypertrophic scar inhibition behavior. Cellulose, 2018. **25**(11): p. 6705-6717.

142. Khan, T., J.K. Park, and J.-H. Kwon, Functional biopolymers produced by biochemical technology considering applications in food engineering. Korean Journal of Chemical Engineering, 2007. **24**(5): p. 816-826.

143. Feng, Y., et al., A mechanically strong, flexible and conductive film based on bacterial cellulose/graphene nanocomposite. Carbohydrate Polymers, 2012. **87**(1): p. 644-649.

144. Kim, G.-D., et al., Evaluation of immunoreactivity of in vitro and in vivo models against bacterial synthesized cellulose to be used as a prosthetic biomaterial. Vol. 7. 2013. 201-209.

145. Rosenfeld, Y. and Y. Shai, Lipopolysaccharide (Endotoxin)-host defense antibacterial peptides interactions: Role in bacterial resistance and prevention of sepsis. Biochimica et Biophysica Acta (BBA) - Biomembranes, 2006. **1758**(9): p. 1513-1522.

146. Raetz, C.R.H. and C. Whitfield, Lipopolysaccharide endotoxins. Annual review of biochemistry, 2002. **71**: p. 635-700.

147. Wang, S.-S., et al., Insights into Bacterial Cellulose Biosynthesis from Different Carbon Sources and the Associated Biochemical Transformation Pathways in Komagataeibacter sp. W1. Polymers, 2018. **10**(9): p. 963.

148. Dourado, F., M. Gama, and A.C. Rodrigues, A Review on the toxicology and dietetic role of bacterial cellulose. Toxicology Reports, 2017. **4**: p. 543-553.

149. Moreira, S., et al., BC nanofibres: In vitro study of genotoxicity and cell proliferation. Toxicology Letters, 2009. **189**(3): p. 235-241.

150. Klemm, D., et al., Bacterial synthesized cellulose — artificial blood vessels for microsurgery. Progress in Polymer Science, 2001. **26**(9): p. 1561-1603.

151. Andrade, D.J., et al., Aspectos biológicos do ácaro Brevipalpus phoenicis vetor da leprose dos citros em plantas de buva (Conyza canadensis). Planta Daninha, 2012. **30**: p. 97-103.

152. Svensson, A., et al., Bacterial cellulose as a potential scaffold for tissue engineering of cartilage. Biomaterials, 2005. **26**(4): p. 419-431.

153. Xu, C., et al., Bacterial Cellulose Membranes Used as Artificial Substitutes for Dural Defection in Rabbits. International Journal of Molecular Sciences, 2014. **15**(6).

154. Reddy, N. and Y. Yang, Innovative Biofibers from Renewable Resources. 2014: Springer Berlin Heidelberg.

155. Du, R., et al., Production and characterization of bacterial cellulose produced by Gluconacetobacter xylinus isolated from Chinese persimmon vinegar. Carbohydr Polym, 2018. **194**: p. 200-207.

156. Cheng, K.C., J.M. Catchmark, and A. Demirci, Enhanced production of bacterial cellulose by using a biofilm reactor and its material property analysis. J Biol Eng, 2009. **3**: p. 12.

157. Saska, S., et al., Bacterial cellulose-hydroxyapatite nanocomposites for bone regeneration. Int J Biomater, 2011. **2011**: p. 175362.

158. Tsouko, E., et al., Bacterial Cellulose Production from Industrial Waste and by-Product Streams. Int J Mol Sci, 2015. **16**(7): p. 14832-49.

159. Cai, Z. and J. Kim, Bacterial cellulose/poly(ethylene glycol) composite: Characterization and first evaluation of biocompatibility. Vol. 17. 2010. 83-91.

160. Gao, W., Chen, K., Yang, R., Yang, F., & Han, W. , Properties of Bacterial Cellulose and Its Influence on the Physical Properties of Paper. BioResources, 2010. **6**(1): p. 144-153.

161. George, J., et al., Bacterial cellulose nanocrystals exhibiting high thermal stability and their polymer nanocomposites. International Journal of Biological Macromolecules, 2011. **48**(1): p. 50-57.

162. Oliveira, R., et al., Synthesis and Characterization of Methylcellulose Produced from Bacterial Cellulose under Heterogeneous Condition. Vol. 26. 2015.

163. León-Mancilla, B.H., et al., Physico-chemical characterization of collagen scaffolds for tissue engineering. Journal of Applied Research and Technology, 2016. **14**(1): p. 77-85.

164. Hsieh, Y.C., et al., An Estimation of the Young's Modulus of Bacterial Cellulose Filaments. Vol. 15. 2008. 507-513.

165. Zaborowska, M., et al., Microporous bacterial cellulose as a potential scaffold for bone regeneration. Acta Biomater, 2010. **6**(7): p. 2540-7.

166. Torres, F.G., S. Commeaux, and O.P. Troncoso, Biocompatibility of bacterial cellulose based biomaterials. J Funct Biomater, 2012. **3**(4): p. 864-78.

167. Boccafoschi, F., et al., Effects of mechanical stress on cell adhesion: a possible mechanism for morphological changes. Cell adhesion & migration, 2010. **4**(1): p. 19-25.

168. de Oliveira, C.R., Bacterial Cellulose Membranes Constitute Biocompatible Biomaterials for Mesenchymal and Induced Pluripotent Stem Cell Culture and Tissue Engineering. Journal of Tissue Science & Engineering, 2012. **S11**.

169. Oliveira Barud, H.G., et al., Preparation and characterization of a bacterial cellulose/silk fibroin sponge scaffold for tissue regeneration. Carbohydr Polym, 2015. **128**: p. 41-51.

170. Wang, J., et al., Novel Bacterial Cellulose/Gelatin Hydrogels as 3D Scaffolds for Tumor Cell Culture. Polymers, 2018. **10**(6).

171. Peltola, S.M., et al., A review of rapid prototyping techniques for tissue engineering purposes. Ann Med, 2008. **40**(4): p. 268-80.

172. Zhang, L., et al., Three-dimensional (3D) printed scaffold and material selection for bone repair. Acta Biomaterialia, 2019. **84**: p. 16-33.

173. Wubneh, A., et al., Current state of fabrication technologies and materials for bone tissue engineering. Acta Biomaterialia, 2018. **80**: p. 1-30.

174. Turnbull, G., et al., 3D bioactive composite scaffolds for bone tissue engineering. Bioactive Materials, 2018. **3**(3): p. 278-314.

175. Seok, J.M., et al., Fabrication and characterization of 3D scaffolds made from blends of sodium alginate and poly(vinyl alcohol). Materials Today Communications, 2019. **19**: p. 56-61.

176. Ao, C., et al., Fabrication and characterization of electrospun cellulose/nano-hydroxyapatite nanofibers for bone tissue engineering. International Journal of Biological Macromolecules, 2017. **97**: p. 568-573.

177. Kim, J., et al., In vitro osteogenic differentiation of human amniotic fluid-derived stem cells on a poly(lactide-co-glycolide) (PLGA)-bladder submucosa matrix (BSM) composite scaffold for bone tissue engineering. Biomed Mater, 2013. **8**(1): p. 014107.

178. Yeh, H.-Y., B.L. Yen, and S.-h. Hsu, Placental Stem Cells for Cartilage Tissue Engineering, in Perinatal Stem Cells. 2014. p. 183-189.

179. Talwadekar, M.D., V.P. Kale, and L.S. Limaye, Placenta-derived mesenchymal stem cells possess better immunoregulatory properties compared to their cord-derived counterparts-a paired sample study. Sci Rep, 2015. **5**: p. 15784.

180. Hsu SH, H.T., Cheng SJ, Weng SY, Tsai CL, Tseng CS, Chondrogenesis from human placenta-derived mesenchymal stem cells in three-dimensional scaffolds for cartilage tissue engineering. Tissue Eng Part A, 2011: p. 1549–60.

181. DARIA MARIA POP1), O.S., SERGIU ŞUŞMAN3), DAN RUS-CIUCĂ4), IOAN ŞTEFAN GROZA5), and D.M. RĂZVAN CIORTEA1), CARMEN MIHAELA MIHU6), Potential of placental-derived human mesenchymal stem cells for osteogenesis and neurogenesis. Rom J Morphol Embryol, 2015: p. 989–996.

182. Yumi Fukuchi, H.N., Daisuke Sugiyama, and T.K. Imiko Hirose, Kohichiro Tsuji, Human Placenta-Derived Cells Have Mesenchymal Stem/Progenitor Cell Potential. STEMCELLS, 2004. **22**: p. 649–658.

183. Oliveira, M.S. and J.B. Barreto-Filho, Placental-derived stem cells: Culture, differentiation and challenges. World J Stem Cells, 2015. **7**(4): p. 769-75.

184. Lee, H.J., et al., Comparison of in vitro hepatogenic differentiation potential between various placenta-derived stem cells and other adult stem cells as an alternative source of functional hepatocytes. Differentiation, 2012. **84**(3): p. 223-31.

185. Chang, C.M., et al., Placenta-derived multipotent stem cells induced to differentiate into insulin-positive cells. Biochem Biophys Res Commun, 2007. **357**(2): p. 414-20.

186. JI, N.S.A.H., In Vitro Differentiation of Human Placenta-derived Adherent Cells into Insulin-producing Cells. The Journal of International Medical Research, 2009. **37**: p. 400 – 406.

187. Jones, G.N., et al., Potential of human fetal chorionic stem cells for the treatment of osteogenesis imperfecta. Stem Cells Dev, 2014. **23**(3): p. 262-76.

188. Xin LI, a.W.L., a Angela Pennisi,a Yuping Wang,a Sharmin Khan,a Mohammad Heidaran,b Ajai Pal,b, b.S.H. Xiaokui Zhang, b Andy Zeitlin,b Stewart Abbot,b Herbert Faleck,b Robert Hariri,b, and J. John D. Shaughnessy, a Frits Van rhee,a Bijay Nair,a Bart Barlogie,a Joshua Epstein,a Shmuel Yaccoby, Human Placenta-Derived Adherent Cells Prevent Bone loss, Stimulate Bone formation, and Suppress Growth of Multiple Myeloma in Bone. Stem Cells Dev, 2011. **29**: p. 263–273.

189. Sousa, A.F., et al., Thermosetting AESO-bacterial cellulose nanocomposite foams with tailored mechanical properties obtained by Pickering emulsion templating. Polymer, 2017. **118**: p. 127-134.

190. Khattak, W.A., et al., Production, Characterization and Physico-mechanical Properties of Bacterial Cellulose from Industrial Wastes. Journal of Polymers and the Environment, 2014. **23**(1): p. 45-53.

191. Frantz, C., K.M. Stewart, and V.M. Weaver, The extracellular matrix at a glance. Journal of cell science, 2010. **123**(Pt 24): p. 4195-4200.

192. Bone Tissue and the Skeletal System. Available from: https://opentextbc.ca/anatomyandphysiology/chapter/6-4-bone-formation-and-development/.

193. SF, G., Osteogenesis: The Development of Bones. 6th ed. 2000.

194. Bobbert, F.S.L. and A.A. Zadpoor, Effects of bone substitute architecture and surface properties on cell response, angiogenesis, and structure of new bone. Journal of Materials Chemistry B, 2017. **5**(31): p. 6175-6192.

195. A, C., D. D, and C. H, Gene Therapy Applications for Fracture Repair, in Gene Therapy Applications. 2011.

196. Huang, Y., et al., Modification and evaluation of micro-nano structured porous bacterial cellulose scaffold for bone tissue engineering. Mater Sci Eng C Mater Biol Appl, 2017. **75**: p. 1034-1041.

197. Zimmermann, K.A., et al., Biomimetic design of a bacterial cellulose/hydroxyapatite nanocomposite for bone healing applications. Materials Science and Engineering: C, 2011. **31**(1): p. 43-49.

198. Granéli, C., et al., Novel markers of osteogenic and adipogenic differentiation of human bone marrow stromal cells identified using a quantitative proteomics approach. Stem Cell Research, 2014. **12**(1): p. 153-165.

199. Marupanthorn, K., et al., Bone morphogenetic protein-2 enhances the osteogenic differentiation capacity of mesenchymal stromal cells derived from human bone marrow and umbilical cord. Vol. 39. 2017.

200. Hsin-I Chang, Y.W., Cell Responses to Surface and Architecture of Tissue Engineering Scaffolds, in Regenerative Medicine and Tissue Engineering. 2011.

201. Fleming, R.I., et al., Foam nest components of the tungara frog: a cocktail of proteins conferring physical and biological resilience. Proc Biol Sci, 2009. **276**(1663): p. 1787-95.

202. Schor, M., et al., The Diverse Structures and Functions of Surfactant Proteins. Trends Biochem Sci, 2016. **41**(7): p. 610-620.

203. Cooper, A., et al., Frog foams and natural protein surfactants. Colloids and Surfaces A: Physicochemical and Engineering Aspects, 2017. **534**: p. 120-129.

204. Biofoams. 2009; Available from: www.chemistryworld.org.

205. Żywicka, A., et al., Bacterial cellulose yield increased over 500% by supplementation of medium with vegetable oil. Carbohydrate Polymers, 2018. **199**: p. 294-303.

206. Mackenzie, C.D., et al., Ranaspumin-2: structure and function of a surfactant protein from the foam nests of a tropical frog. Biophys J, 2009. **96**(12): p. 4984-92.

207. Singh, A.V., et al., Quantitative characterization of the influence of the nanoscale morphology of nanostructured surfaces on bacterial adhesion and biofilm formation. PLoS One, 2011. **6**(9): p. e25029.

208. Norman, J.J. and T.A. Desai, Methods for fabrication of nanoscale topography for tissue engineering scaffolds. Ann Biomed Eng, 2006. **34**(1): p. 89-101.

209. Courtenay, J.C., et al., Surface modified cellulose scaffolds for tissue engineering. Cellulose, 2016. **24**(1): p. 253-267.

210. Moniri, M., et al., Production and Status of Bacterial Cellulose in Biomedical Engineering. Nanomaterials, 2017. **7**(9).

211. Zhu, J., et al., The Influence of Conditions on Synthesis Hydroxyapatite By Chemical Precipitation Method. IOP Conference Series: Materials Science and Engineering, 2011. **18**(6).

212. Kim, H.J. and J.S. Park, Usage of Human Mesenchymal Stem Cells in Cell-based Therapy: Advantages and Disadvantages. Dev Reprod, 2017. **21**(1): p. 1-10.